

Eigenprojectors, Bloch vectors and quantum geometry of N -band systems

Ansgar Graf^{*}, Frédéric Piéchon[†]

Université Paris-Saclay, CNRS, Laboratoire de Physique des Solides, 91405, Orsay, France

^{*}ansgar.graf@universite-paris-saclay.fr

[†]frédéric.piechon@universite-paris-saclay.fr

December 23, 2024

Abstract

The eigenvalues of a parameter-dependent $N \times N$ Hamiltonian matrix form a band structure in parameter space. Quantum geometric properties (Berry curvature, quantum metric, etc.) of such N -band systems are usually computed from parameter-dependent eigenstates. This approach faces several difficulties, including gauge ambiguities and singularities in the multicomponent eigenfunctions. In order to circumvent this problem, this work exposes an alternative approach based on eigenprojectors and (generalized) Bloch vectors. First, an expansion of each eigenprojector as a matrix polynomial in the Hamiltonian is deduced, and using $SU(N)$ Gell-Mann matrices an equivalent expansion of each Bloch vector is found. In a second step, expressions for the N -band Berry curvature and quantum metric in terms of Bloch vectors are obtained. This leads to new explicit Berry curvature formulas in terms of the Hamiltonian vector, generalizing the well-known two-band formula to arbitrary N . Moreover, a detailed treatment is given for the case of a particle-hole symmetric energy spectrum, which occurs in systems with a chiral or charge conjugation symmetry. For illustrating the formalism, several model Hamiltonians featuring a multifold linear band crossing are discussed; they have identical energy spectra but completely different geometric and topological properties. The methodology used in this work is more broadly applicable to compute any physical quantity, or to study the quantum dynamics of any observable without the explicit construction of energy eigenstates.

Contents

| | | |
|----------|--|-----------|
| 1 | Introduction | 2 |
| 2 | Review of two-band systems | 5 |
| 3 | Eigenprojectors and Bloch vectors for N-band systems | 10 |
| 3.1 | Eigenprojectors as polynomials in the Hamiltonian: $P_\alpha(H, E_\alpha)$ | 10 |
| 3.2 | Generalized Bloch vectors: $\mathbf{b}_\alpha(\mathbf{h}, E_\alpha)$ | 12 |

| | | |
|-------------------|---|-----------|
| 4 | Quantum geometric tensor without eigenstates | 16 |
| 4.1 | From eigenstate to projector picture | 16 |
| 4.2 | Two alternative Bloch vector pictures | 17 |
| 4.3 | N -band Berry curvature from the Hamiltonian vector | 18 |
| 5 | N-band systems with particle-hole symmetric energy spectrum | 19 |
| 5.1 | Definition of a particle-hole symmetric spectrum | 19 |
| 5.2 | Eigenprojectors, Bloch vectors and quantum geometric tensor | 20 |
| 6 | Application to multifold linear band crossings with distinct topology | 21 |
| 6.1 | Particle-hole symmetric isotropic multifold fermions in 3D | 23 |
| 6.2 | Pseudospin- S multifold fermions and beyond | 24 |
| 6.2.1 | Pseudospin- S multifold fermions | 25 |
| 6.2.2 | Beyond spin- S multifold fermions | 27 |
| 7 | Summary and conclusions | 32 |
| Appendices | | 34 |

1 Introduction

In a quantum mechanical system characterized by an N -dimensional Hilbert space, a particularly frequent scenario is the one where the $N \times N$ Hamiltonian matrix $H(\mathbf{x})$ depends on a set of parameters \mathbf{x} , say the crystal momentum in solid state physics, the intensity of an external field, an applied strain or any mean-field order parameter. A Hamiltonian of this kind has a set of eigenvalues $E_\alpha(\mathbf{x})$ that form a band structure, and may therefore be referred to as an *N -band system*, or equivalently a *(parametric) $SU(N)$ system*¹ – these designations will be used synonymously during this work.

In this paper, we will be mainly concerned with the *(quantum) geometric properties* of N -band systems. The concept of quantum geometry can be viewed as originating from the overlap of energy eigenstates $|\psi_\alpha(\mathbf{x})\rangle$ (assumed to be non-degenerate and labeled by $\alpha \in \{1, \dots, N\}$) that are infinitesimally close in parameter space: $\langle\psi_\alpha(\mathbf{x})|\psi_\alpha(\mathbf{x} + d\mathbf{x})\rangle$. Obviously, a Taylor expansion of this overlap will produce terms determined by derivatives $\partial/\partial x_i$ acting on energy eigenstates $|\psi_\alpha(\mathbf{x})\rangle$. Hence arises the conventional point of view on quantum geometry, which regards quantum geometric information as being

(i) encoded in *rates of changes of energy eigenstates* $|\psi_\alpha(\mathbf{x})\rangle$ upon variation of \mathbf{x} .

This perspective is of considerable conceptual value, but leads to several issues in practical computations (see Section 2). An equivalent point of view, which is adopted more rarely, consists in saying that quantum geometry is

(ii) encoded in *rates of changes of eigenprojectors* $P_\alpha(\mathbf{x}) = |\psi_\alpha(\mathbf{x})\rangle\langle\psi_\alpha(\mathbf{x})|$.

¹This is due to the mathematical fact that the Hermitian matrix $H(\mathbf{x})$ is an element of the Lie algebra $\mathfrak{su}(N)$, closely related to the Lie group $SU(N)$, and therefore $H(\mathbf{x})$ may be called a *(parametric) $SU(N)$ Hamiltonian*.

This is the starting point for our work. More precisely, considering the Hamiltonian's spectral decomposition $H(\mathbf{x}) = \sum_{\alpha=1}^N E_\alpha(\mathbf{x}) P_\alpha(\mathbf{x})$, a third point of view may be predicted: If we can invert the spectral decomposition to find a unique function $P_\alpha(\mathbf{x}) = P_\alpha(E_\alpha(\mathbf{x}), H(\mathbf{x}))$, it is clear from point of view (ii) that quantum geometry can also be regarded as being

(iii) encoded in *rates of changes of the Hamiltonian $H(\mathbf{x})$ and its eigenvalues $E_\alpha(\mathbf{x})$* .

In fact, for $N = 2$, the relation $P_\alpha = \frac{1}{2}(1_2 + H/E_\alpha)$, with 1_2 the 2×2 identity matrix, is well known and accordingly point of view (iii) is widely used. The main contribution of this paper is to clarify and quantify the generalization to arbitrary N .

It should be stressed that no information is lost when replacing point of view (i) by (ii) or (iii); when necessary, any eigenstate can easily be recovered as $|\psi_\alpha(\mathbf{x})\rangle = P_\alpha(\mathbf{x})|\psi\rangle$ from the projectors, where $|\psi\rangle$ can be chosen at convenience for each α and \mathbf{x} . In other words, the overlap $\langle\psi_\alpha(\mathbf{x})|\psi_\alpha(\mathbf{x} + d\mathbf{x})\rangle$ and more generally the full quantum geometric information about a given $SU(N)$ Hamiltonian is encoded in the eigenprojectors $P_\alpha(\mathbf{x})$. In contrast to point of view (i), however, point of view (iii) is extremely convenient for practical computations, since the only ingredients required are the Hamiltonian $H(\mathbf{x})$ (known at the very outset) and its set $\{E_\alpha(\mathbf{x}), \alpha = 1, \dots, N\}$ of eigenvalues (easy to find in many cases).

Let us state more precisely what we have in mind, quantitatively, when speaking of *quantum geometric properties*. Historically, their fundamental importance was first revealed in the context of geometric phases which can have striking effects on physical observables. While apparently distinct notions of geometric phase were initially introduced, such as the Aharonov-Bohm [1, 2], Pancharatnam [3] and Stone-Longuet-Higgins [4] phases, the discovery of Berry's phase [5, 6] then formalized the notion of a geometric phase in a very general way. Berry phases and their extensions [7–11] are now omnipresent in the physics literature.

More fundamental than Berry's phase is the underlying gauge field, known as the (Abelian) Berry connection $\mathcal{A}_{\alpha,i}(\mathbf{x}) \equiv i \langle\psi_\alpha(\mathbf{x})|\partial_i\psi_\alpha(\mathbf{x})\rangle$, where $\partial_i \equiv \partial/\partial x_i$. Before its formalization [5, 6], this concept popped up in some noteworthy early works, most explicitly in Blount's *Formalisms of Band Theory* [12]. The origin of the Berry connection lies in the above-mentioned overlap $\langle\psi_\alpha(\mathbf{x})|\psi_\alpha(\mathbf{x} + d\mathbf{x})\rangle$; the phase of this complex number gives rise to the Berry connection gauge field whose curvature field $\Omega_{\alpha,ij}(\mathbf{x}) = \partial_i\mathcal{A}_{\alpha,j}(\mathbf{x}) - \partial_j\mathcal{A}_{\alpha,i}(\mathbf{x})$, the *Berry curvature*, plays the role of a pseudo-magnetic field in parameter space. However, also the modulus is of importance; it defines a metric tensor $g_{\alpha,ij}(\mathbf{x})$ of Riemannian type on the manifold of quantum states [13], known as *quantum metric*. Both quantum metric and Berry curvature $\Omega_{\alpha,ij}(\mathbf{x})$ can be summarized in terms of a single complex tensor, called the *quantum geometric tensor (QGT)* [14–16]:

$$T_{\alpha,ij}(\mathbf{x}) \equiv g_{\alpha,ij}(\mathbf{x}) - \frac{i}{2}\Omega_{\alpha,ij}(\mathbf{x}). \quad (1)$$

This object vanishes identically in the case of a one-dimensional Hilbert space, but is potentially non-zero for any N -band system with $N \geq 2$.

The importance of the Berry curvature is well established, as it is recognized to be essential for explaining many fundamental physical phenomena [15, 17–21]. In contrast, the influence of the quantum metric on physical effects is more subtle and has started to attract growing attention only in recent years. On the theory side, many measurable effects influenced by it were identified [22–31], several measurement protocols were developed [32–36], and very recently the full QGT of a two-level system was measured directly, using a nitrogen vacancy center in diamond [37] and a planar microcavity [38]. It is now well established that the *entire QGT*, not only the Berry curvature part, are essential for understanding the geometric contributions to observables in N -band systems. While higher-order geometric quantities

exist, we will, in this paper, typically have in mind the QGT when speaking about *quantum geometric properties*.

In accordance with point of view (i) on quantum geometry, the QGT is formulated in terms of energy eigenstates $|\psi_\alpha(\mathbf{x})\rangle$ in the large majority of the afore-mentioned references. However, as we mentioned above, practical computations of the QGT via the $|\psi_\alpha(\mathbf{x})\rangle$ face several problems. First, closed-form expressions for energy eigenstates, *i.e.* expressions that can be used independently of the Hamiltonian of interest, are very hard to construct. Second, the gauge arbitrariness in the parameter-dependent global phase is problematic, especially if derivatives with respect to these parameters are to be carried out. Third, it may be that singularities in some of the components of multicomponent states occur at certain points in parameter space, which cannot be excluded *a priori*. These issues are of particular relevance when addressing geometric information encoded in the eigenstates. Already for two-band systems, the task of finding the QGT from energy eigenstates (in a basis of practical interest) is not trivial; for three-band systems, it can pose serious difficulties, see for instance Ref. [39]. For higher N – aside from special cases that allow for simple analytical treatment – it is usual to resort to (not always well-controlled) numerical methods or to employ approximate perturbative analytical approaches that decouple the $SU(N)$ Hamiltonian into effective $SU(2)$ sub-Hamiltonians valid locally in parameter space.

In the present work, we therefore reformulate geometrical properties of N -band systems avoiding energy eigenstates. The transition from point of view (i) to points of view (ii) & (iii) is demonstrated. The latter provide closed-form analytical formulas for the QGT that can be used, in principle, for arbitrary N . Over the last few years, some efforts in this spirit have been made for the $N = 3$ case [40–42]. Very recently, Pozo and de Juan [43] published a paper of much more general scope. They point out that, quite generally, any observable of an N -band system can be computed without energy eigenstates if the eigenenergies are known, and also briefly apply this idea to the QGT. While similar in spirit, our work is less ambitious in scope. Indeed, we feel that the topic of computing observables and physical quantities more complex than the QGT without using eigenstates requires a much more detailed treatment, and therefore defer it to future work [44]. In the present study, we essentially concentrate on the eigenprojectors and the quantum geometric tensor. In particular, we emphasize the role of generalized Bloch vectors, an important concept in the quantum information community, and establish links between different strategies that can be used to obtain the QGT.

The setup of this paper is as follows. In Section 2, the familiar two-band case involving a simple $SU(2)$ Hamiltonian is reviewed, in order to motivate the eigenprojector approach and outline the strategy for the N -band generalization.

Then, in a first step, we derive a generic formula $P_\alpha(\mathbf{x}) = P_\alpha(E_\alpha(\mathbf{x}), H(\mathbf{x}))$ for the eigenprojectors of $SU(N)$ Hamiltonians, cf. Section 3.1. This formula expresses $P_\alpha(\mathbf{x})$ as a matrix polynomial of degree $N - 1$ in the Hamiltonian, with coefficients that are elementary symmetric polynomials in the corresponding eigenvalue E_α . Besides its utility for quantum geometry, this formula can be used (a) to expand any function of the Hamiltonian in powers of $H(\mathbf{x})$ and (b) to analytically construct energy eigenstates of any $SU(N)$ Hamiltonian. In Section 3.2, these results are translated to an equivalent but more convenient vectorial language. In particular, expanding the Hamiltonian and the eigenprojectors in $SU(N)$ Gell-Mann matrices (the generalization of Pauli matrices), one is led to a formalism involving two kinds of $SU(N)$ vectors: the Hamiltonian vector $\mathbf{h}(\mathbf{x})$ and the (*generalized*) *Bloch vector* $\mathbf{b}_\alpha(\mathbf{x})$, the $SU(N)$ analog of the familiar $SU(2)$ Bloch vector on the unit sphere. In this vectorial language, the eigenprojector polynomial formula translates into a function $\mathbf{b}_\alpha(\mathbf{x}) = \mathbf{b}_\alpha(E_\alpha(\mathbf{x}), \mathbf{h}(\mathbf{x}))$ that expresses the generalized Bloch vectors in terms of the Hamiltonian vector and the energy eigenvalues.

In a second step, in Section 4.1, we review how to make the transition between eigenstate- and eigenprojector-based expressions of the QGT; this further allows to obtain two different $SU(N)$ invariant formulae for the QGT in terms of Bloch vectors, cf. Section 4.2. Section 4.3 shows how this may be used for computing the QGT of N -band systems only from the knowledge of $\mathbf{h}(\mathbf{x})$ and the energy eigenvalues. For the Berry curvature, a closed form formula for arbitrary N is obtained; applying it to cases of low N , we recover the familiar $SU(2)$ result, observe that the $SU(3)$ formula found in Ref. [40] can be considerably simplified, and write down new explicit formulas for the $SU(4)$ and $SU(5)$ Berry curvature. It will also become clear that computing the quantum metric is more cumbersome (though equally straightforward in methodology) than computing the Berry curvature.

In Section 5, we consider in depth the special case of a particle-hole symmetric (PHS) spectrum, meaning an energy spectrum that is symmetric about zero energy. This applies to a plethora of physical systems, in particular those with a chiral and/or charge conjugation symmetry. In this scenario, the eigenprojectors and Bloch vectors are considerably simplified, and so are the geometrical quantities constructed from them.

Section 6 serves to illustrate the formalism by means of explicit examples. Several three-dimensional (3D) models in the class of (linear) multifold fermions are presented, for both $N = 3$ and $N = 4$, and compared to the simplest kind of multifold fermion, *i.e.* a pseudospin S , where $S = (N - 1)/2$. In particular, these models are designed in such a way as to exhibit geometrical and topological properties completely different from a pseudospin S , even though they have exactly the same energy spectrum. This emphasizes the fact that, for any given pair of Hamiltonians, the indistinguishability of their band structures does not in the least establish their equivalence. Most strikingly, for some of the models, characterized by a global chiral symmetry, quantum metric and Berry curvature can be continuously tuned while maintaining a completely unchanged band structure. This is somewhat reminiscent of 2D models with tunable quantum geometry, first discovered in the $\alpha - \mathcal{T}_3$ lattice [45].

Finally, we sum up and conclude in Section 7.

2 Review of two-band systems

The properties of two-level/two-band systems are well known, and widely applied in the study of qubits, in the band theory of graphene, Chern insulators, and countless other systems in atomic and condensed matter physics. The reason why such systems are rather easy to describe is the very simple structure of the underlying $\mathfrak{su}(2)$ algebra. In the following, we compile various key facts that will serve for comparison when we treat the $N > 2$ case below.

Consider a (parametric) $SU(2)$ Hamiltonian, *i.e.* a 2×2 Hermitian matrix $H(\mathbf{x})$ with a set of energy eigenvalues $\{E_\alpha(\mathbf{x}) | \alpha = \pm\}$ and (orthonormal) eigenstates $\{|\psi_\alpha(\mathbf{x})\rangle | \alpha = \pm\}$, and where the vector \mathbf{x} represents a set of parameters. Note that, here and in the following, the \mathbf{x} -dependence of quantities of interest is stated explicitly in their definition, but often understood as implicit afterwards.

Without loss of generality, the trivial part of H (proportional to the identity matrix 1_2) is set equal to zero such that $\text{Tr } H = 0$. A Hamiltonian of this type can be expanded in the Pauli matrices $\boldsymbol{\sigma} = (\sigma_x, \sigma_y, \sigma_z)$:

$$H(\mathbf{x}) = \mathbf{h}(\mathbf{x}) \cdot \boldsymbol{\sigma}. \quad (2)$$

The Hamiltonian vector can be written as $\mathbf{h} = (h_x, h_y, h_z) = |\mathbf{h}|\mathbf{u}_h$. Here, the unit vector $\mathbf{u}_h(\mathbf{x}) \equiv (\sin \theta_h \cos \phi_h, \sin \theta_h \sin \phi_h, \cos \theta_h)$ is characterized by two *Hamiltonian's angles* $(\theta_h(\mathbf{x}), \phi_h(\mathbf{x}))$ whose expressions in terms of the components $h_{x,y,z}$ read $\cos \theta_h = h_z/|\mathbf{h}|$ and

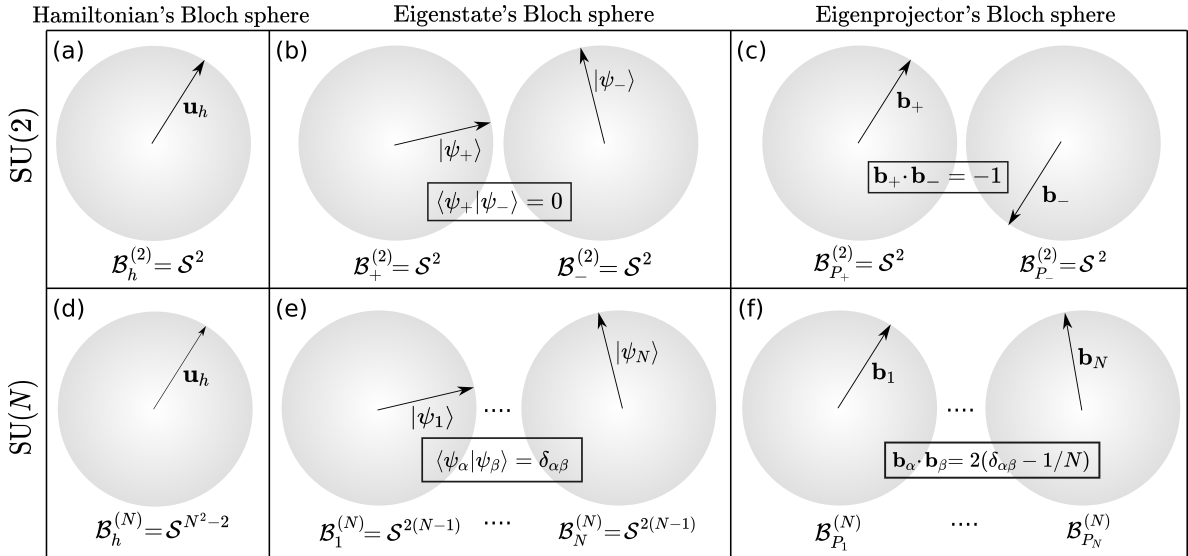


Figure 1: Schematic visualization of the different Bloch sphere's appearing in the treatment of $SU(N)$ Hamiltonians. The familiar $SU(2)$ case is illustrated in the first row, while the second row treats the general case of arbitrary N . The *Hamiltonian's Bloch sphere* $\mathcal{B}_h^{(2)}$ is the relevant space for the mapping $\mathbf{u}_h(\mathbf{x})$, and corresponds to a proper unit sphere for all values of N . The *eigenstate's Bloch sphere* $\mathcal{B}_\alpha^{(N)}$ associated to the mapping $|\psi_\alpha(\mathbf{x})\rangle$ is also a proper unit sphere for all N , but of different dimension than the Hamiltonian's Bloch sphere if $N > 2$. The *eigenprojector's Bloch sphere* $\mathcal{B}_{P_\alpha}^{(N)}$ associated to the mapping $P_\alpha(\mathbf{x})$ is only a proper sphere for $N = 2$. In the $N > 2$ case, where it is often called *generalized Bloch sphere*, it is of very complicated shape, see Appendix E.

$\tan \phi_h = h_y/h_x$. The vector $\mathbf{u}_h(\mathbf{x})$ defines a map from the parameter space to a *Hamiltonian's Bloch sphere* $\mathcal{B}_h^{(2)}$, which is simply a unit two-sphere, $\mathcal{B}_h^{(2)} = S^2$, see Fig. 1(a). The eigenspectrum of the Hamiltonian introduced in Eq. (2) is simply

$$E_\alpha(\mathbf{x}) = \alpha \sqrt{\text{Tr}(H^2(\mathbf{x}))/2} = \alpha |\mathbf{h}(\mathbf{x})|, \quad (3)$$

with $\alpha = \pm$. The variation $E_\alpha(\mathbf{x})$ defines a two-band spectrum in parameter space. It is *particle-hole symmetric*, *i.e.* energy levels occur in pairs of opposite sign.

Eigenstates vs. eigenprojectors

Since one major focus of this paper is how the N -band eigenstates can be replaced by eigen-projectors, a somewhat detailed discussion of the two-band eigenstates and the complications that arise already in this simple $N = 2$ case is now in order. This will make clear why it is favorable to work with eigen-projectors.

The eigenstate for $\alpha = +$, *i.e.* the state $|\psi_+(\mathbf{x})\rangle$, can be written in either of the forms

$$\begin{aligned} |\psi_+\rangle &= e^{i\Gamma_+} \begin{pmatrix} \cos \theta_+ \\ \sin \theta_+ e^{i\phi_+} \end{pmatrix} \\ &= \frac{1}{\sqrt{2\left(1 + \frac{h_z}{E_+}\right)}} \begin{pmatrix} 1 + \frac{h_z}{E_+} \\ \frac{h_x + ih_y}{E_+} \end{pmatrix} = \frac{1}{\sqrt{2(1 + \cos \theta_h)}} \begin{pmatrix} 1 + \cos \theta_h \\ \sin \theta_h e^{i\phi_h} \end{pmatrix}, \end{aligned} \quad (4)$$

and similarly for $|\psi_-(\mathbf{x})\rangle$. The first equality simply corresponds to the formal parametrization of a complex-valued two-component unit vector. It expresses the fact that, at each point \mathbf{x} in the parameter space, the eigenstate $|\psi_+\rangle$ is minimally encoded by a global phase $\Gamma_+(\mathbf{x})$ and two *eigenstate's angles* $(\theta_+(\mathbf{x}), \phi_+(\mathbf{x}))$. These angles can be viewed as defining a map from parameter space to an *eigenstate's Bloch sphere* $\mathcal{B}_+^{(2)}$. Since the angles θ_+ and ϕ_+ can be interpreted as spherical coordinates, the eigenstate's Bloch sphere, just like the Hamiltonian's Bloch sphere, is a unit two-sphere: $\mathcal{B}_+^{(2)} = \mathcal{S}^2$, as visualized in Fig. 1(b). Similarly, for $|\psi_-\rangle$, one has two eigenstate's angles $(\theta_-(\mathbf{x}), \phi_-(\mathbf{x}))$ defining a corresponding Bloch sphere $\mathcal{B}_-^{(2)} = \mathcal{S}^2$, see Fig. 1(b). The second line in Eq. (4) illustrates the possible singular behavior of eigenstates. If the eigenstate components are written directly in terms of the corresponding energy eigenvalue and the components of the Hamiltonian vector \mathbf{h} , a singularity is evidently to be expected when $h_z(\mathbf{x}_0)/E_+(\mathbf{x}_0) = -1$ for some point $\mathbf{x} = \mathbf{x}_0$ in parameter space. Similarly, if the eigenstate components are written in terms of the angles (θ_h, ϕ_h) , the explicit relation $\tan \phi_h = h_y/h_x$ points towards further possible singular behavior in parameter space when $h_x(\mathbf{x}_0) = 0$. As a final subtlety, note that the previous expressions in Eq. (4) reflect a peculiar gauge choice.

In contrast to the eigenstate $|\psi_\alpha\rangle$, the corresponding eigenprojector $P_\alpha(\mathbf{x}) \equiv |\psi_\alpha\rangle \langle \psi_\alpha|$ is an explicitly gauge-independent quantity, and it generically exhibits a less singular behavior in parameter space. In the $N = 2$ case, it simply writes as

$$P_\alpha(\mathbf{x}) = \frac{1}{2} \mathbf{1}_2 + \frac{1}{2E_\alpha(\mathbf{x})} H(\mathbf{x}) \equiv \frac{1}{2} (1_2 + \mathbf{b}_\alpha(\mathbf{x}) \cdot \boldsymbol{\sigma}), \quad (5)$$

where 1_2 is the 2×2 identity matrix and the *Bloch vector* $\mathbf{b}_\alpha(\mathbf{x})$ is given by

$$\mathbf{b}_\alpha(\mathbf{x}) = \frac{\mathbf{h}(\mathbf{x})}{E_\alpha(\mathbf{x})} = \alpha \mathbf{u}_h(\mathbf{x}). \quad (6)$$

It is immediately obvious that the definition of P_α (and \mathbf{b}_α) is completely unambiguous and unproblematic except at degeneracy points, *i.e.* when $E_+(\mathbf{x}_0) = E_-(\mathbf{x}_0) = 0$ for some $\mathbf{x} = \mathbf{x}_0$; this emphasizes the usefulness of the projectors.

Of course, the Bloch vector also defines a map $\mathbf{b}_\alpha(\mathbf{x})$ to a space that may be called the *eigenprojector's Bloch sphere* $\mathcal{B}_{P_\alpha}^{(2)}$; among the three kinds of Bloch spheres we are dealing with, it is perhaps the one most frequently referred to as a *Bloch sphere* in the literature. Importantly, the peculiarity and simplicity of two-band systems, as compared to the more general N -band case, consists in the fact that the eigenprojector's Bloch sphere is extremely simple, namely a unit two-sphere: $\mathcal{B}_{P_\alpha}^{(2)} = \mathcal{S}^2$, see Fig. 1(c). It is important to keep in mind, however, that the Hamiltonian's, the eigenstate's and the eigenprojector's Bloch spheres are *a priori distinct spaces*, even though they all happen to correspond to the unit two-sphere \mathcal{S}^2 in the $SU(2)$ case. This distinction is necessary to avoid considerable confusion in the $SU(N)$ generalization, as anticipated by Fig. 1(d)–(f).

A last important property of the eigenprojector P_α is that it is in some sense a more fundamental object than the eigenstate, namely it permits to construct the eigenstate $|\psi_\alpha\rangle$ from an arbitrary gauge freedom state $|\psi_g\rangle$. More concretely, a state equivalent to Eq. (4) is easily constructed as

$$|\psi_+\rangle = \frac{1}{\sqrt{\langle\psi_g|P_+|\psi_g\rangle}}P_+|\psi_g\rangle, \text{ with } |\psi_g\rangle = \begin{pmatrix} \cos\theta_g \\ \sin\theta_g e^{-i\phi_g} \end{pmatrix}, \quad (7)$$

where the gauge freedom angles (θ_g, ϕ_g) can be chosen at will at any point in parameter space \mathbf{x} , and independently for $\alpha = \pm$. For example, if $\cos\theta_g = 1$ and $\sin\theta_g = 0$, one exactly recovers the last expression in Eq. (4). Two important remarks are in order about the eigenstate obtained from Eq. (7). First, although this is not immediately obvious, the eigenstate's angles (θ_+, ϕ_+) stay unchanged upon varying (θ_g, ϕ_g) for fixed \mathbf{x} . In contrast, the global phase Γ_+ is changing, implying $\Gamma_+ \equiv \Gamma_+(\mathbf{x}, \theta_g, \phi_g)$. As a consequence, the possible singular behaviors of the wavefunction in parameter space are gauge-dependent. Second, the state $|\psi_g\rangle$ must not be orthogonal to the projector $P_\alpha(\mathbf{x})$, *i.e.* one requires $P_\alpha(\mathbf{x})|\psi_g\rangle \neq 0$. This constraint implies that it might be necessary to change the state $|\psi_g\rangle$ when the parameter \mathbf{x} is varying because it is never guaranteed that a single $|\psi_g\rangle$ (meaning a fixed gauge) is sufficient to describe a given eigenstate $|\psi_\alpha\rangle$ over the entire parameter space \mathbf{x} .

Quantum geometry

Having pointed out sufficient justification for abandoning energy eigenstates in favor of eigenprojectors, this idea may now be applied to quantum geometry. In other words, this section serves to explain how the *quantum geometric tensor (QGT)*, historically first introduced in terms of energy eigenstates, can be rewritten in terms of eigenprojectors and Bloch vectors, as is frequently done in the treatment of two-band systems. A similar procedure will then be developed for the $N > 2$ case in Sections 3 & 4.

The QGT originates from a Taylor expansion of the overlap $\langle\psi_\alpha(\mathbf{x})|\psi_\alpha(\mathbf{x} + d\mathbf{x})\rangle$ of states infinitesimally close in parameter space. Leaving the detailed derivation to Section 4.1, the QGT $T_{\alpha,ij}(\mathbf{x})$ associated to an eigenstate $|\psi_\alpha(\mathbf{x})\rangle$ may be written as:

$$\begin{aligned} T_{\alpha,ij}(\mathbf{x}) &= \langle\partial_i\psi_\alpha|\partial_j\psi_\alpha\rangle - \langle\partial_i\psi_\alpha|\psi_\alpha\rangle\langle\psi_\alpha|\partial_j\psi_\alpha\rangle, \\ g_{\alpha,ij}(\mathbf{x}) &= \text{Re } T_{\alpha,ij} = \text{Re } \langle\partial_i\psi_\alpha|\partial_j\psi_\alpha\rangle - \langle\partial_i\psi_\alpha|\psi_\alpha\rangle\langle\psi_\alpha|\partial_j\psi_\alpha\rangle, \\ \Omega_{\alpha,ij}(\mathbf{x}) &= -2\text{Im } T_{\alpha,ij} = -2\text{Im } \langle\partial_i\psi_\alpha|\partial_j\psi_\alpha\rangle, \end{aligned} \quad (8)$$

where $\partial_i \equiv \partial/\partial x_i$. The real part $g_{\alpha,ij}(\mathbf{x})$ of the QGT is the quantum metric tensor and is symmetric under the exchange of indices i, j . The imaginary part $\Omega_{\alpha,ij}(\mathbf{x})$ is the Berry curvature tensor and is antisymmetric in the indices i, j . This definition makes it clear that the explicit dimension and form of the matrix elements $g_{\alpha,ij}$ and $\Omega_{\alpha,ij}$ depend on the chosen set of parameters \mathbf{x} .

As an illustration, taking $\mathbf{x} = (\theta_h, \phi_h)$ ($\dim(\mathbf{x}) = 2$) and differentiating the state $|\psi_+\rangle$ [see Eq. (4)] as prescribed by Eq. (8), the associated quantum metric and Berry curvature tensors are 2×2 matrices that write as

$$g_{+,ij}(\theta_h, \phi_h) = \frac{1}{4} \begin{pmatrix} 1 & 0 \\ 0 & \sin^2\theta_h \end{pmatrix}, \quad \Omega_{+,ij}(\theta_h, \phi_h) = -\frac{1}{2} \begin{pmatrix} 0 & \sin\theta_h \\ -\sin\theta_h & 0 \end{pmatrix}, \quad (9)$$

which is a well-known result [16]. Taking instead $\mathbf{x} = (h_x, h_y, h_z)$ ($\dim(\mathbf{x}) = 3$), the quantum metric and Berry curvature tensors are now 3×3 matrices with matrix elements

$$g_{+,ij}(\mathbf{h}) = \frac{1}{4|\mathbf{h}|^2} \left(\delta_{ij} - \frac{h_i h_j}{|\mathbf{h}|^2} \right), \quad \Omega_{+,ij}(\mathbf{h}) = -\frac{1}{2|\mathbf{h}|^3} \epsilon_{ijk} h_k, \quad (10)$$

with ϵ_{ijk} the Levi-Civita antisymmetric tensor. Note that, in both of these cases, one easily finds $g_{-,ij} = g_{+,ij}$ and $\Omega_{-,ij} = -\Omega_{+,ij}$.

More generally, the quantum geometric tensor of interest is often related to the explicit dependency of the Hamiltonian vector $\mathbf{h}(\mathbf{x})$ on some vector of external parameters \mathbf{x} , with $\dim(\mathbf{x}) \geq 2$. For example, in condensed matter physics, one will often have $\mathbf{x} = \mathbf{k}$, where \mathbf{k} represents crystal momentum. In that situation, the corresponding QGT $T_{\alpha,ij}(\mathbf{x})$ may easily be obtained from either $T_{\alpha,kl}(\mathbf{h})$ or $T_{\alpha,kl}(\theta_h, \phi_h)$ by a simple composition rule as

$$T_{\alpha,ij}(\mathbf{x}) = \sum_{k,l} (\partial_i y_k)(\partial_j y_l) T_{\alpha,kl}(\mathbf{y}), \quad (11)$$

with $\mathbf{y} = \mathbf{h}$ or $\mathbf{y} = (\theta_h, \phi_h)$.

Within the eigenstate approach to the QGT [cf. Eq. (8) and point of view (i) of the Introduction], the derivation of the tensors $T_{+,ij}(\mathbf{h})$ or $T_{+,ij}(\theta_h, \phi_h)$ given by Eqs. (9) & (10) makes explicit use of the specific gauge choice that corresponds to the form of $|\psi_+\rangle$ given by Eq. (4). It is not immediately evident that these expressions of the quantum geometric tensors are gauge-invariant. There is, however, an obviously gauge-invariant formula that contains the same information as Eq. (8), but encodes it in terms of derivatives of the eigenprojector P_α [cf. point of view (ii) expressed in the Introduction]. This formula reads (see Section 4.1 for details)

$$T_{\alpha,ij}(\mathbf{x}) = \text{Tr} [(\partial_i P_\alpha) (1 - P_\alpha) (\partial_j P_\alpha)]. \quad (12)$$

For illustration, it is expedient to consider the specific example $\mathbf{x} = \mathbf{h}$, insert the expression $P_\alpha(\mathbf{h})$ as given by Eqs. (5) & (6) into Eq. (12), and to recover the QGT of Eq. (10).

The above formula (12) is extremely useful: in combination with Eq. (5), it can immediately be used for computing the QGT without eigenstates, assuming the matrix H and its eigenvalues are known. While this is sufficient for computational purposes, it is more instructive and convenient to resort to the vectorial language: equation (5) allows to first obtain a Bloch vector-based formula for the QGT, and using further Eq. (6) one gets the corresponding expression in terms of only the Hamiltonian vector and the energy eigenvalues $E_\alpha = \alpha|\mathbf{h}|$ [cf. point of view (iii) of the Introduction]. Both forms of writing for the quantum metric and Berry curvature tensors, and with a generic vector parameter \mathbf{x} [in the sense of either of Eqs. (9–11)], are summarized in the following expressions:

$$\begin{aligned} g_{\alpha,ij}(\mathbf{x}) &= \frac{1}{4} \mathbf{b}_\alpha^i \cdot \mathbf{b}_\alpha^j = \frac{1}{4|\mathbf{h}|^2} \left[\mathbf{h}^i \cdot \mathbf{h}^j - \frac{(\mathbf{h} \cdot \mathbf{h}^i)(\mathbf{h} \cdot \mathbf{h}^j)}{|\mathbf{h}|^2} \right], \\ \Omega_{\alpha,ij}(\mathbf{x}) &= -\frac{1}{2} \mathbf{b}_\alpha \cdot (\mathbf{b}_\alpha^i \times \mathbf{b}_\alpha^j) = -\frac{\alpha}{2|\mathbf{h}|^3} \mathbf{h} \cdot (\mathbf{h}^i \times \mathbf{h}^j), \end{aligned} \quad (13)$$

with the shorthand notation $\mathbf{m}^i \equiv \partial_i \mathbf{m} \equiv \partial \mathbf{m} / \partial x_i$ for the partial derivative of a vector \mathbf{m} . We will see that the strategy employed to obtain Eq. (13) applies in a completely analogous way to $SU(N > 2)$ systems. It will also become clear that, while the expressions of the quantum metric and Berry curvature tensors in terms of $\mathbf{h}(\mathbf{x})$ and its parametric derivatives are widely known, the reformulation directly in terms of Bloch vectors \mathbf{b}_α is actually the one that naturally pertains to the $SU(N)$ generalization of Eq. (13).

3 Eigenprojectors and Bloch vectors for N -band systems

Computing and understanding the quantum geometric properties of N -band systems – *i.e.* more specifically $N \times N$ Hermitian matrices $H(\mathbf{x})$ – is of interest for a wide variety of physical systems, not necessarily restricted to the quantum realm. The issues of eigenstates pointed out in the previous section of course generalize to the case $N > 2$ (and get harder to control). Now, one might tackle this problem by obtaining the eigenfunctions $|\psi_\alpha(\mathbf{x})\rangle$ numerically, and performing direct numerical computation of the geometric tensors. However, this strategy involves a necessarily discrete mesh in parameter space and possible difficulties related to spurious gauge dependencies and singularities. One never knows which effective *gauge* is chosen by the computer; moreover this effective gauge might be different at each point in parameter space and for each eigenstate.

In order to avoid such a complete numerical approach, the main goal here is to develop some analytical understanding of the eigenprojectors and geometric tensors, and to provide generalizations of Eqs. (5), (6) & (13) to $N > 2$. The strategy to do this is as follows. In a first step, each eigenprojector P_α is written as a polynomial of order $N - 1$ in the Hamiltonian matrix H , where each monomial coefficient is an explicit function of the associated energy eigenvalue E_α . The second step consists in expanding the Hamiltonian and the eigenprojectors in the basis of Gell-Mann matrices, such that they are described by an $SU(N)$ Hamiltonian vector \mathbf{h} and Bloch vectors \mathbf{b}_α , respectively. The Bloch vector \mathbf{b}_α is found to be a polynomial in \mathbf{h} , with monomial coefficients that are functions of E_α . The last step consists in computing the corresponding quantum geometric tensors, as is done in Section 4.

3.1 Eigenprojectors as polynomials in the Hamiltonian: $P_\alpha(H, E_\alpha)$

Our starting point is the following textbook formula for the eigenprojector P_α as a function of the $N \times N$ matrix H and the set $\{E_\beta, \beta = 1, \dots, N\}$ of all energy eigenvalues [46]:

$$P_\alpha = \prod_{\beta \neq \alpha} \frac{H - E_\beta \mathbf{1}_N}{E_\alpha - E_\beta}, \quad (14)$$

where $\mathbf{1}_N$ is the $N \times N$ identity matrix. Note that in the language of matrix theory, P_α is known as the *Frobenius covariant* of H . The goal is now to eliminate all $E_{\beta \neq \alpha}$ from this formula, such that P_α becomes a proper polynomial in H with coefficients that depend only on the single eigenvalue E_α . Notice that the denominator corresponds to the derivative of the Hamiltonian's characteristic polynomial: $p'_N(E_\alpha) = \prod_{\beta \neq \alpha} (E_\alpha - E_\beta)$. For more details on the characteristic polynomial $p_N(z)$, see Appendix A.

The products in the numerator and denominator of Eq. (14) can be rewritten as described in Appendix B. The result is

$$P_\alpha = \frac{\sum_{n=0}^{N-1} q_{N-1-n}(E_\alpha) H^n}{\sum_{n=0}^{N-1} q_{N-1-n}(E_\alpha) E_\alpha^n} = \frac{\sum_{n=0}^{N-1} q_{N-1-n}(E_\alpha) H^n}{\sum_{n=0}^{N-1} q_{N-1-n}(E_\alpha) C_n}, \quad (15)$$

where the C_n are (classical) *Casimir invariants* [47], which are defined as

$$C_n \equiv \text{Tr}(H^n) = \sum_{\alpha=1}^N E_\alpha^n. \quad (16)$$

Obviously, one has $C_0 = N$. Since one can always assume $\text{Tr } H = 0$ without loss of generality, see also Eq. (22) below, we will have $C_1 = 0$ throughout. Notice that from the second equality in Eq. (14), it is immediately clear that $\text{Tr } P_\alpha = 1$, as required.

| n | 1 | 2 | 3 | 4 | 5 | 6 |
|-------|---|------------------|------------------|-----------------------------------|-------------------------------------|--|
| c_n | 0 | $-\frac{C_2}{2}$ | $-\frac{C_3}{3}$ | $\frac{C_2^2}{8} - \frac{C_4}{4}$ | $\frac{C_2 C_3}{6} - \frac{C_5}{5}$ | $-\frac{C_2^3}{48} + \frac{C_3^2}{18} + \frac{C_2 C_4}{8} - \frac{C_6}{6}$ |

Table 1: Coefficients c_n determining the polynomial (17).

The polynomials $q_n(z)$ appearing in Eq. (14) are closely related to the Hamiltonian's characteristic polynomial and can be formally written as

$$q_n(z) \equiv \sum_{k=0}^n c_k z^{n-k}, \quad (17)$$

with $q_N(z) = p_N(z)$. Alternatively, one may construct them by starting from $q_0(z) = 1$ and using the simple recurrence relation

$$q_n(z) = z q_{n-1}(z) + c_n. \quad (18)$$

The c_n are derived in Appendix A and listed in Table 1 for $n \leq 6$.

As a concrete illustration of Eq. (15), we can immediately write down the eigenprojectors $P_\alpha(E_\alpha, H)$, as done here for the cases $N = 2$ to $N = 5$:

$$\begin{aligned} P_\alpha &= \frac{1}{2E_\alpha} (E_\alpha 1_2 + H), \\ P_\alpha &= \frac{1}{3E_\alpha^2 - \frac{C_2}{2}} \left[\left(E_\alpha^2 - \frac{C_2}{2} \right) 1_3 + E_\alpha H + H^2 \right], \\ P_\alpha &= \frac{1}{4E_\alpha^3 - C_2 E_\alpha - \frac{C_3}{3}} \left[\left(E_\alpha^3 - \frac{C_2}{2} E_\alpha - \frac{C_3}{3} \right) 1_4 + \left(E_\alpha^2 - \frac{C_2}{2} \right) H + E_\alpha H^2 + H^3 \right], \quad (19) \\ P_\alpha &= \frac{1}{5E_\alpha^4 - \frac{3C_2}{2} E_\alpha^2 - \frac{2C_3}{3} E_\alpha + \frac{C_2^2 - 2C_4}{8}} \left[\left(E_\alpha^4 - \frac{C_2}{2} E_\alpha^2 - \frac{C_3}{3} E_\alpha + \frac{C_2^2 - 2C_4}{8} \right) 1_5 \right. \\ &\quad \left. + \left(E_\alpha^3 - \frac{C_2}{2} E_\alpha - \frac{C_3}{3} \right) H + \left(E_\alpha^2 - \frac{C_2}{2} \right) H^2 + E_\alpha H^3 + H^4 \right]. \end{aligned}$$

Note that the $N = 2$ projector in the first line is the same as Eq. (5) discussed above. For given N , each eigenprojector is a polynomial of degree $N - 1$ in the Hamiltonian, in agreement with the Cayley-Hamilton theorem [48, 49]. Explicit formulas of this kind can be readily found for any higher N desired.

The eigenprojectors can be computed immediately for an arbitrary given Hamiltonian, provided the energy eigenvalues are known. In this context, one needs to distinguish the cases $N < 5$ and $N \geq 5$. In the former case, it is often simple to find the analytical form of $E_\alpha(\mathbf{x})$, and in principle it is always possible by using the analytical closed-form expressions for the eigenenergies given in Appendix C. In the latter case ($N \geq 5$), there are no closed-form solutions to the characteristic polynomial of a completely general H , but Eq. (15) can always be computed explicitly if the eigenvalues E_α (or approximate values thereof) are accessible by some means. This applies, for example, to the case of particle-hole symmetric energy spectra, discussed in Sections 5 & 6, where closed-form solutions for the eigenvalues exist for $N > 4$.

Beyond the simple computation of eigenprojectors, Eq. (15) has two important applications. First, it can be used to rewrite any function $f(H)$ as a polynomial of order $N - 1$ in

the Hamiltonian, which corresponds to an alternative version of *Sylvester's formula*:

$$f(H) = \sum_{\alpha=1}^N f(E_\alpha) \frac{\sum_{n=0}^{N-1} q_{N-1-n}(E_\alpha) H^n}{\sum_{n=0}^{N-1} q_{N-1-n}(E_\alpha) E_\alpha^n}. \quad (20)$$

Second, Eq. (15) may be employed for constructing energy eigenstates $|\psi_\alpha\rangle$ that can be used further to compute matrix elements of observables, or the Berry connection and other quantities of interest. More concretely, similarly to the case $N = 2$ discussed in Eq. (7), the N -band eigenstate $|\psi_\alpha\rangle$ in an arbitrary gauge may be obtained as

$$|\psi_\alpha\rangle = \frac{1}{\sqrt{\langle\psi_g| P_\alpha(H, E_\alpha) |\psi_g\rangle}} P_\alpha(H, E_\alpha) |\psi_g\rangle, \quad (21)$$

where the gauge freedom state $|\psi_g\rangle$ can be chosen arbitrarily². The resulting eigenstate $|\psi_\alpha\rangle$ has now N components that can be minimally encoded by a global phase Γ_α and $N - 1$ pairs of *eigenstate's angles* $(\theta_\alpha^i(\mathbf{x}), \phi_\alpha^i(\mathbf{x}))$ ($i = 1, \dots, N - 1$). These angles define a map from the parameter space to a $2(N - 1)$ -dimensional *eigenstate's Bloch sphere* $\mathcal{B}_\alpha^{(N)}$, which is depicted, for comparison with the $N = 2$ case, in Fig. 1(e).

3.2 Generalized Bloch vectors: $\mathbf{b}_\alpha(\mathbf{h}, E_\alpha)$

The above results on the eigenprojectors can now be translated into a vectorial language; this proves just as useful as in the $N = 2$ case.

Generalized Bloch vectors and generalized Bloch sphere

Similarly to the $N = 2$ case, one may define a Hamiltonian's vector \mathbf{h} and a (*generalized*) *Bloch vector* \mathbf{b}_α by expanding the (traceless) Hamiltonian H and the eigenprojector P_α as

$$H(\mathbf{x}) = \mathbf{h}(\mathbf{x}) \cdot \boldsymbol{\lambda}, \quad (22)$$

as well as [50]

$$P_\alpha(\mathbf{x}) = \frac{1}{N} \mathbf{1}_N + \frac{1}{2} \mathbf{b}_\alpha(\mathbf{x}) \cdot \boldsymbol{\lambda}. \quad (23)$$

Here, $\mathbf{h} \equiv \text{Tr}\{H\boldsymbol{\lambda}\}/2$ and $\mathbf{b}_\alpha \equiv \text{Tr}\{P_\alpha\boldsymbol{\lambda}\}$, where $\boldsymbol{\lambda} = (\lambda_1, \dots, \lambda_{N^2-1})$ is the vector composed of the $N^2 - 1$ *generalized Gell-Mann* (traceless Hermitian) matrices that are the elementary generators of the $SU(N)$ Lie group. Together with the identity matrix $\mathbf{1}_N$ they constitute a basis for the Lie algebra $\mathfrak{su}(N)$ [51]. For the reader's convenience, the Gell-Mann matrices for $N = 3$ and $N = 4$ are listed in Appendix D. Note that the vector \mathbf{b}_α is also called *coherence vector*, and that we choose the prefactor $\frac{1}{2}$ in front of \mathbf{b}_α , although various choices of this factor exist in the literature [52–54].

In the above, the vectors \mathbf{h} and \mathbf{b}_α have $N^2 - 1$ real-valued components, such that the unit vector $\mathbf{u}_h \equiv \mathbf{h}/|\mathbf{h}|$ can be parametrized by $N^2 - 2$ *Hamiltonian's angles*. In other words, $\mathbf{u}_h(\mathbf{x})$ defines a map from the parameter space to a *Hamiltonian's Bloch sphere* $\mathcal{B}_h^{(N)} = \mathcal{S}^{N^2-2}$, where \mathcal{S}^{N^2-2} is the unit $(N^2 - 2)$ -sphere, as depicted in Fig. 1(d). Naively, the map $\mathbf{b}_\alpha(\mathbf{x})$ (for given α) would similarly seem to define an $(N^2 - 2)$ -sphere, but there are actually constraints on

²The state $|\psi_g\rangle$ has now N components that are encoded by $N - 1$ pairs of gauge freedom angles (θ_g^i, ϕ_g^i) ($i = 1, \dots, N - 1$) that may be chosen independently for each eigenstate $|\psi_\alpha\rangle$ and at each point in parameter space \mathbf{x} . Even though it is far from obvious, it is expected that solely the global phase depends *both* on the gauge choice and on the parameters \mathbf{x} – that is, $\Gamma_\alpha \equiv \Gamma_\alpha(\mathbf{x}, \theta_g^i, \phi_g^i)$. In contrast, the angles $(\theta_\alpha^i, \phi_\alpha^i)$ should solely depend on \mathbf{x} .

the eigenprojectors which translate into constraints on the Bloch vectors [see the discussion in the context of Eq. (37) below]. Consequently, in contrast to the $N = 2$ case, \mathbf{h} and \mathbf{b}_α are no longer parallel for $N > 2$, such that $\mathbf{u}_h(\mathbf{x})$ and $\mathbf{b}_\alpha(\mathbf{x})$ are distinct maps.

Indeed, the vector $\mathbf{b}_\alpha(\mathbf{x})$ defines a map from parameter space not to an $(N^2 - 2)$ -sphere but to a $2(N - 1)$ -dimensional subset thereof, which may be called the *eigenprojector's Bloch sphere* $\mathcal{B}_{P_\alpha}^{(N)}$, or simply the *generalized Bloch sphere*. For comparing to the $N = 2$ case, $\mathcal{B}_{P_\alpha}^{(N)}$ is depicted schematically in Fig. 1(f). An understanding of the true geometrical structure of this Bloch sphere is not at all easy to acquire. Many efforts have been undertaken to figure out its properties for $N > 2$, which is a surprisingly nontrivial issue, see Refs. [52, 53, 55–60] and references therein. For the interested reader, we outline the main results about the generalized Bloch sphere in Appendix E. In summary, the eigenstate's Bloch sphere, the Hamiltonian's Bloch sphere, and the eigenprojector's Bloch sphere are all isomorphic spaces for $N = 2$, but all different spaces for $N > 2$.

Bloch vectors as a function of the Hamiltonian vector

We now detail the different steps that allow to find the concrete expression $\mathbf{b}_\alpha(\mathbf{h}, E_\alpha)$ from the eigenprojector formula $P_\alpha(H, E_\alpha)$ given by Eq. (15). The only missing ingredient is the explicit expansion of $H^n = (\mathbf{h} \cdot \boldsymbol{\lambda})^n$ in terms of generalized Gell-Mann matrices. Using the previous definition $C_n = \text{Tr}(H^n)$ and defining vectors $\boldsymbol{\eta}_n \equiv \text{Tr}(H^n \boldsymbol{\lambda})/2$, we can write:

$$H^n = (\mathbf{h} \cdot \boldsymbol{\lambda})^n = \frac{C_n}{N} \mathbf{1}_N + \boldsymbol{\eta}_n \cdot \boldsymbol{\lambda}, \quad (24)$$

where obviously $C_0 = N$, $C_1 = 0$, $\boldsymbol{\eta}_0 = 0$ and $\boldsymbol{\eta}_1 = \mathbf{h}$. Inserting into Eq. (15) and using Eq. (23), we obtain the intermediate result:

$$\mathbf{b}_\alpha = 2 \frac{\sum_{n=0}^{N-1} q_{N-1-n}(E_\alpha) \boldsymbol{\eta}_n}{\sum_{n=0}^{N-1} q_{N-1-n}(E_\alpha) E_\alpha^n}. \quad (25)$$

At this point it remains the task to find the explicit form of the vectors $\boldsymbol{\eta}_n(\mathbf{h})$ for $n > 1$.

To accomplish this task, one may first observe from Eq. (24) that both C_n and $\boldsymbol{\eta}_n$ can be written uniquely in terms of \mathbf{h} , have dimensions [energy] n , and therefore necessarily arise from products involving the vector \mathbf{h} . We therefore require a product identity generalizing the familiar SU(2) identity $(\mathbf{m} \cdot \boldsymbol{\sigma})(\mathbf{n} \cdot \boldsymbol{\sigma}) = \mathbf{m} \cdot \mathbf{n} \mathbf{1}_2 + i(\mathbf{m} \times \mathbf{n}) \cdot \boldsymbol{\sigma}$ to arbitrary N . This can be readily achieved by focusing on some properties of the Lie algebra $\mathfrak{su}(N)$, which are defined by the (anti)commutation relations of Gell-Mann matrices [61]:

$$\begin{aligned} [\lambda_a, \lambda_b] &= 2i f_{abc} \lambda_c, & f_{abc} &\equiv -\frac{i}{4} \text{Tr}([\lambda_a, \lambda_b] \lambda_c), \\ \{\lambda_a, \lambda_b\} &= \frac{4}{N} \delta_{ab} \mathbf{1}_N + 2d_{abc} \lambda_c, & d_{abc} &\equiv \frac{1}{4} \text{Tr}(\{\lambda_a, \lambda_b\} \lambda_c), \end{aligned} \quad (26)$$

where repeated lower indices imply summation (Einstein convention). Here, d_{abc} (f_{abc}) are the totally symmetric (antisymmetric) structure constants of $\mathfrak{su}(N)$, which are a known set of real numbers; for their explicit values in the $N = 3$ case, see for example Ref. [60]. Note also that for $N = 2$, where $\boldsymbol{\lambda} = \boldsymbol{\sigma}$, the d_{abc} vanish identically and $f_{abc} = \epsilon_{abc}$, where ϵ_{abc} is the Levi-Civita symbol. From Eq. (26) one easily obtains the product identity

$$\lambda_a \lambda_b = \frac{2}{N} \delta_{ab} \mathbf{1}_N + (d_{abc} + i f_{abc}) \lambda_c. \quad (27)$$

Since all generators are traceless, $\text{Tr } \lambda_c = 0$, the convenient trace orthogonality $\text{Tr}(\lambda_a \lambda_b) = 2\delta_{ab}$ holds. In order to translate Eq. (27) to its vectorial form, one may use the structure constants (26) to define dot, star and cross products of vectors:

$$\begin{aligned} \mathbf{m} \cdot \mathbf{n} &\equiv m_c n_c, \\ (\mathbf{m} \star \mathbf{n})_a &\equiv d_{abc} m_b n_c, \\ (\mathbf{m} \times \mathbf{n})_a &\equiv f_{abc} m_b n_c, \end{aligned} \tag{28}$$

where \mathbf{m} and \mathbf{n} are $(N^2 - 1)$ -dimensional. The star product does not play any role in $N = 2$ situations (where $d_{abc} = 0$) but is crucial for $N > 2$. Note that a different convention is sometimes used for defining the star product, which introduces N -dependent prefactors and is particularly popular in the treatment of qutrits [53, 60]. From Eqs. (27) & (28), one directly obtains the desired product identity in vector form:

$$(\mathbf{m} \cdot \boldsymbol{\lambda})(\mathbf{n} \cdot \boldsymbol{\lambda}) = \frac{2}{N} \mathbf{m} \cdot \mathbf{n} \mathbf{1}_N + (\mathbf{m} \star \mathbf{n} + i \mathbf{m} \times \mathbf{n}) \cdot \boldsymbol{\lambda}. \tag{29}$$

When computing $H^n = (\mathbf{h} \cdot \boldsymbol{\lambda})^n$ by applying Eq. (29) repeatedly, it is clear that star products of the kind $\mathbf{h} \star \mathbf{h}$ will appear. We may thus introduce the notation for repeated star products of a vector with itself:

$$\begin{aligned} \mathbf{m}_\star^{(0)} &= \mathbf{m}, \\ \mathbf{m}_\star^{(1)} &= \mathbf{m}_\star \equiv \mathbf{m} \star \mathbf{m}, \\ \mathbf{m}_\star^{(2)} &= \mathbf{m}_{\star\star} \equiv \mathbf{m} \star (\mathbf{m} \star \mathbf{m}), \\ \mathbf{m}_\star^{(k+1)} &= \mathbf{m}_{\star\star\dots} \equiv \mathbf{m} \star \mathbf{m}_\star^{(k)}. \end{aligned} \tag{30}$$

The resulting vectors have the following properties (with $n_1, n_2 \in \mathbb{N}_0$):

$$\begin{aligned} \mathbf{m}_\star^{(n_1)} \cdot \mathbf{m}_\star^{(n_2)} &= \left| \mathbf{m}_\star^{\left(\frac{n_1+n_2}{2}\right)} \right|^2 \quad \text{if } n_1 + n_2 \text{ even,} \\ \mathbf{m}_\star^{(n_1)} \times \mathbf{m}_\star^{(n_2)} &= 0. \end{aligned} \tag{31}$$

The former identity follows directly from the total symmetry of the structure constants (26), and the latter is a consequence of the second Jacobi identity, see Appendix F. More generally, from the generic properties of the algebra considered above, it is possible to establish useful generalized *vector* and *scalar* Jacobi identities, listed in Appendix G.

With all these prerequisites we may now calculate $(\mathbf{h} \cdot \boldsymbol{\lambda})^n$ *i.e.* determine $C_n(\mathbf{h})$ and $\boldsymbol{\eta}(\mathbf{h})$. In particular, we obtain the following simple recursion relations:

$$C_{n+1} = 2 \mathbf{h} \cdot \boldsymbol{\eta}_n, \quad \boldsymbol{\eta}_{n+1} = \mathbf{h} \star \boldsymbol{\eta}_n + \frac{C_n}{N} \mathbf{h}, \tag{32}$$

with initial conditions $C_0 = N$ and $\boldsymbol{\eta}_0 = 0$. (A more general but equivalent version of this recursion relation is established in Appendix H.) Applying this recursion, for a traceless Hamiltonian matrix, we obtain successively up to $n = 4$ the important identities

$$\begin{aligned} C_1 &= 0, & \boldsymbol{\eta}_1 &= \mathbf{h}, \\ C_2 &= 2|\mathbf{h}|^2, & \boldsymbol{\eta}_2 &= \mathbf{h}_\star, \\ C_3 &= 2 \mathbf{h} \cdot \mathbf{h}_\star, & \boldsymbol{\eta}_3 &= \frac{C_2}{N} \mathbf{h} + \mathbf{h}_{\star\star}, \\ C_4 &= \frac{4|\mathbf{h}|^4}{N} + 2|\mathbf{h}_\star|^2, & \boldsymbol{\eta}_4 &= \frac{C_3}{N} \mathbf{h} + \frac{C_2}{N} \mathbf{h}_\star + \mathbf{h}_{\star\star\star}. \end{aligned} \tag{33}$$

More generally, for a generic $N > 1$, the form of the vector $\boldsymbol{\eta}_n(\mathbf{h})$ is compactly written as:

$$\boldsymbol{\eta}_n = \frac{1}{N} \sum_{p=0}^{n-1} C_p \mathbf{h}_\star^{(n-1-p)}. \quad (34)$$

The final step required for completing our task of finding the explicit expressions of the Bloch vector $\mathbf{b}_\alpha(\mathbf{h}, E_\alpha)$ consists in substituting Eqs. (33) & (34) into Eq. (25). The Bloch vectors for $N = 2$ to $N = 5$ are then found to be

$$\begin{aligned} \mathbf{b}_\alpha &= \frac{2}{2E_\alpha} \mathbf{h}, \\ \mathbf{b}_\alpha &= \frac{2}{3E_\alpha^2 - \frac{C_2}{2}} (E_\alpha \mathbf{h} + \mathbf{h}_\star), \\ \mathbf{b}_\alpha &= \frac{2}{4E_\alpha^3 - C_2 E_\alpha - \frac{C_3}{3}} \left[\left(E_\alpha^2 - \frac{C_2}{4} \right) \mathbf{h} + E_\alpha \mathbf{h}_\star + \mathbf{h}_{\star\star} \right], \\ \mathbf{b}_\alpha &= \frac{2}{5E_\alpha^4 - \frac{3C_2}{2} E_\alpha^2 - \frac{2C_3}{3} E_\alpha + \frac{C_2^2 - 2C_4}{8}} \left[\left(E_\alpha^3 - \frac{3C_2}{10} E_\alpha - \frac{2C_3}{15} \right) \mathbf{h} \right. \\ &\quad \left. + \left(E_\alpha^2 - \frac{3C_2}{10} \right) \mathbf{h}_\star + E_\alpha \mathbf{h}_{\star\star} + \mathbf{h}_{\star\star\star} \right], \end{aligned} \quad (35)$$

respectively. In the first line, Eq. (6) is recovered. Equation (35) contains the same information as Eq. (19), and clearly illustrates that the Bloch vector is no longer parallel to the Hamiltonian vector \mathbf{h} for $N > 2$. Indeed, for given N , each Bloch vector is a kind of "vector polynomial" of degree $N - 1$ in "star product powers" of \mathbf{h} , which can be viewed as a consequence of the Cayley-Hamilton theorem [48, 49]. Writing down analogous formulas for the $N \geq 6$ Bloch vectors is straightforward using Eq. (25) and Eqs. (32)–(34). Note also that for explicitly calculating the Bloch vectors, one needs to know the energy eigenvalues; concerning this point, the same discussion as conducted below Eq. (19) applies.

It is important to be aware that, for given N , only $C_{n \leq N}$ and $\boldsymbol{\eta}_{n < N}$ are relevant, and there are only $N - 1$ independent vectors $\mathbf{h}_\star^{(k)}$, $k = 0, \dots, N - 2$. For example, for $N = 3$, all information we need is encoded in C_2 , C_3 , \mathbf{h} and \mathbf{h}_\star . This again follows from the Cayley-Hamilton theorem, which states that $q_{n=N}(H) = p_N(H) = 0$. From this property it is easy to establish the following useful identities:

$$\begin{aligned} N = 3 : \quad &\mathbf{h}_{\star\star} = \frac{C_2}{6} \mathbf{h}, \quad \mathbf{h}_\star \star \mathbf{h}_\star = \frac{C_3}{3} \mathbf{h} - \frac{C_2}{6} \mathbf{h}_\star, \\ N = 4 : \quad &\mathbf{h}_{\star\star\star} = \frac{C_3}{12} \mathbf{h} + \frac{C_2}{4} \mathbf{h}_\star, \quad \mathbf{h}_\star \star \mathbf{h}_\star = \frac{C_3}{3} \mathbf{h}, \quad \mathbf{h}_\star \star \mathbf{h}_{\star\star} = \frac{|\mathbf{h}_\star|^2}{2} \mathbf{h} + \frac{C_3}{12} \mathbf{h}_\star. \end{aligned} \quad (36)$$

In closing this section, some further general remarks on the Bloch vectors are in order. The usual orthogonality relation $P_\alpha P_\beta = \delta_{\alpha\beta} P_\alpha$ and completeness relation $\sum_\alpha P_\alpha = 1_N$ of eigen-projectors translate to the Bloch vector picture as:

$$\begin{aligned} \mathbf{b}_\alpha \cdot \mathbf{b}_\beta &= 2 \left(\delta_{\alpha\beta} - \frac{1}{N} \right), \\ \mathbf{b}_\alpha \star \mathbf{b}_\beta &= \left(\delta_{\alpha\beta} - \frac{2}{N} \right) (\mathbf{b}_\alpha + \mathbf{b}_\beta), \\ \mathbf{b}_\alpha \times \mathbf{b}_\beta &= 0, \\ \sum_\alpha \mathbf{b}_\alpha &= 0. \end{aligned} \quad (37)$$

The star product constraint can be viewed as being responsible for the complicated shape of the generalized Bloch sphere described in Appendix E.

4 Quantum geometric tensor without eigenstates

The results of the preceding section can now be used for the discussion of quantum geometry. We first recall the derivation of the quantum geometric tensor (QGT) based on the expansion of the overlap of neighboring eigenstates in parameter space. Second, it is reformulated in terms of eigenprojectors and then in terms of generalized Bloch vectors. Finally, it is considered in detail how to write the QGT in terms of only the Hamiltonian vector \mathbf{h} and the eigenenergy E_α . Along this path, we will encounter many expressions for Berry curvature and quantum metric that are extremely useful for practical computations.

4.1 From eigenstate to projector picture

The QGT is a tensor quantifying the overlap of two states that are "infinitesimally close" in parameter space [13]: $\langle \psi_\alpha(\mathbf{x}) | \psi_\alpha(\mathbf{x} + d\mathbf{x}) \rangle = \mathcal{F}_\alpha(\mathbf{x}) e^{i\phi_\alpha(\mathbf{x})}$, where the modulus $\mathcal{F}_\alpha(\mathbf{x})$ has come to be known as *fidelity* [62]. For a given eigenstate $|\psi_\alpha\rangle$, the form of the QGT depends on the choice of parameter space, *i.e.* on the meaning of the vector \mathbf{x} (cf. the discussion in Section 2). The fidelity is related to the quantum metric, while the phase $\phi_\alpha(\mathbf{x})$ gives rise to the Berry curvature. This can be seen by expanding

$$\begin{aligned} \langle \psi_\alpha(\mathbf{x}) | \psi_\alpha(\mathbf{x} + d\mathbf{x}) \rangle &= 1 + \sum_i \langle \psi_\alpha(\mathbf{x}) | \partial_i \psi_\alpha(\mathbf{x}) \rangle dx_i \\ &\quad + \frac{1}{2} \sum_{ij} \langle \psi_\alpha(\mathbf{x}) | \partial_{ij} \psi_\alpha(\mathbf{x}) \rangle dx_i dx_j + \mathcal{O}(|d\mathbf{x}|^3), \end{aligned} \quad (38)$$

where $\partial_i \equiv \partial/\partial x_i$ as before. Noting that $\text{Re} \langle \psi_\alpha(\mathbf{x}) | \partial_{ij} \psi_\alpha(\mathbf{x}) \rangle = -\text{Re} \langle \partial_i \psi_\alpha(\mathbf{x}) | \partial_j \psi_\alpha(\mathbf{x}) \rangle$ and introducing the Berry connection $\mathcal{A}_{\alpha,i}(\mathbf{x}) \equiv i \langle \psi_\alpha(\mathbf{x}) | \partial_i \psi_\alpha(\mathbf{x}) \rangle = -\text{Im} \langle \psi_\alpha(\mathbf{x}) | \partial_i \psi_\alpha(\mathbf{x}) \rangle$, one immediately finds

$$\begin{aligned} \mathcal{F}_\alpha^2(\mathbf{x}) &= [\text{Re} \langle \psi_\alpha(\mathbf{x}) | \psi_\alpha(\mathbf{x} + d\mathbf{x}) \rangle]^2 + [\text{Im} \langle \psi_\alpha(\mathbf{x}) | \psi_\alpha(\mathbf{x} + d\mathbf{x}) \rangle]^2 \\ &= 1 - \sum_{ij} [\text{Re} \langle \partial_i \psi_\alpha(\mathbf{x}) | \partial_j \psi_\alpha(\mathbf{x}) \rangle - \mathcal{A}_{\alpha,i}(\mathbf{x}) \mathcal{A}_{\alpha,j}(\mathbf{x})] dx_i dx_j + \mathcal{O}(|d\mathbf{x}|^3). \end{aligned} \quad (39)$$

Now, the quantum metric tensor $g_{\alpha,ij}(\mathbf{x})$ is defined [13, 33] by $\sum_{ij} g_{\alpha,ij} dx_i dx_j \equiv 1 - \mathcal{F}_\alpha^2$, such that

$$g_{\alpha,ij}(\mathbf{x}) = \text{Re} \langle \partial_i \psi_\alpha | \partial_j \psi_\alpha \rangle + \langle \psi_\alpha | \partial_i \psi_\alpha \rangle \langle \psi_\alpha | \partial_j \psi_\alpha \rangle. \quad (40)$$

Upon calculating the Berry curvature $\Omega_{\alpha,ij}(\mathbf{x}) \equiv \partial_i \mathcal{A}_{\alpha,j} - \partial_j \mathcal{A}_{\alpha,i}$, one can observe that $g_{\alpha,ij}$ and $\Omega_{\alpha,ij}$ are parts of a single complex tensor, the *quantum geometric tensor (QGT)*, first introduced by Berry in Ref. [14]:

$$\begin{aligned} T_{\alpha,ij}(\mathbf{x}) &= \langle \partial_i \psi_\alpha | \partial_j \psi_\alpha \rangle - \langle \partial_i \psi_\alpha | \psi_\alpha \rangle \langle \psi_\alpha | \partial_j \psi_\alpha \rangle, \\ g_{\alpha,ij}(\mathbf{x}) &= \text{Re} T_{\alpha,ij} = \text{Re} \langle \partial_i \psi_\alpha | \partial_j \psi_\alpha \rangle - \langle \partial_i \psi_\alpha | \psi_\alpha \rangle \langle \psi_\alpha | \partial_j \psi_\alpha \rangle, \\ \Omega_{\alpha,ij}(\mathbf{x}) &= -2 \text{Im} T_{\alpha,ij} = -2 \text{Im} \langle \partial_i \psi_\alpha | \partial_j \psi_\alpha \rangle. \end{aligned} \quad (41)$$

From a practical point of view, the derivatives acting on energy eigenstates that appear in Eq. (41) are not very convenient; in particular, recalling Eq. (21), they might introduce spurious effects due to the global phase difference $\Gamma_\alpha(\mathbf{x} + d\mathbf{x}) - \Gamma_\alpha(\mathbf{x})$ – the latter might not

be perturbative in $d\mathbf{x}$ if the states $|\psi_\alpha\rangle$ at \mathbf{x} and $\mathbf{x} + d\mathbf{x}$ are not calculated in the same gauge, *i.e.* from the same $|\psi\rangle$.

To circumvent this problem, there is an alternative expression of Eq. (41) in terms of matrix elements of the parametric velocity operators $\partial_i H$, which reads as

$$T_{\alpha,ij} = \sum_{\beta \neq \alpha} \frac{\langle \psi_\alpha | \partial_i H | \psi_\beta \rangle \langle \psi_\beta | \partial_j H | \psi_\alpha \rangle}{(E_\alpha - E_\beta)^2}. \quad (42)$$

Using the formal identity $\langle \psi_\alpha | \partial_i H | \psi_\beta \rangle = \langle \partial_i \psi_\alpha | \psi_\beta \rangle (E_\alpha - E_\beta)$, valid for $\alpha \neq \beta$, the energies in the denominator can be eliminated to recover Eq. (41). Equation (42) may further be written in an explicitly gauge-invariant form:

$$T_{\alpha,ij} = \sum_{\beta \neq \alpha} \frac{\text{Tr} \{ P_\alpha (\partial_i H) P_\beta (\partial_j H) \}}{(E_\alpha - E_\beta)^2}, \quad (43)$$

where we used the identity $\langle \psi_\alpha | O | \psi_\alpha \rangle = \text{Tr} \{ P_\alpha O P_\alpha \} = \text{Tr} \{ P_\alpha O \}$. From there, by inserting $H = \sum_\gamma E_\gamma P_\gamma$, it is straightforward to show that Eq. (43) is equivalent to

$$T_{\alpha,ij} = \text{Tr} \{ (\partial_i P_\alpha) (1 - P_\alpha) (\partial_j P_\alpha) \}. \quad (44)$$

This equation for the eigenprojectors is very useful. For purely computational purposes, it is already sufficient to compute the QGT for an $N > 2$ system: for a given H whose eigenvalues are known, Eq. (19) can be immediately combined with Eq. (44). However, similarly to the $N = 2$ case, it turns out to be much more instructive and convenient to transfer Eq. (44) to the vectorial language.

4.2 Two alternative Bloch vector pictures

In order to obtain a Bloch vector picture of the geometric tensors, one can simply substitute Eq. (23) for the projector P_α in terms of the Bloch vector \mathbf{b}_α into Eq. (43) or Eq. (44).

The most compact expression is obtained in the latter case, using the identities (29) & (37) that imply $\mathbf{b}_\alpha \star \mathbf{b}_\alpha^i = (1 - 2/N)\mathbf{b}_\alpha^i$. The QGT can then be expressed through Bloch vectors as

$$\begin{aligned} g_{\alpha,ij} &= \frac{1}{4} \mathbf{b}_\alpha^i \cdot \mathbf{b}_\alpha^j, \\ \Omega_{\alpha,ij} &= -\frac{1}{2} \mathbf{b}_\alpha \cdot (\mathbf{b}_\alpha^i \times \mathbf{b}_\alpha^j), \end{aligned} \quad (45)$$

for *arbitrary* values of N (again with the shorthand notation $\mathbf{m}^i \equiv \partial_i \mathbf{m}$). For $N = 2$, Eq. (13) is recovered. For higher N , the only difference is the meaning of the dot and vector products, which have to be interpreted using the structure constants of Eq. (28). For the SU(3) case, an equivalent way of writing Berry curvature and quantum metric was already encountered in Refs. [40, 41] and [42], respectively; for the SU(N) case, Pozo and de Juan very recently found an equivalent formula in terms of what they call *1-generators* [43]. While conceptually important, Eq. (45) is not necessarily in the most practical form for concrete calculations of the QGT, as it involves explicit parametric derivatives of the Bloch vector; this is potentially complicated, as cumbersome expressions follow from applying the product rule to Eq. (35). (As we will see below, such complications can be eliminated for the Berry curvature due to orthogonality relations, but not for the quantum metric.)

An alternative form of writing the QGT that does not involve such explicit derivatives of the Bloch vectors can be obtained by instead inserting Eq. (23) into Eq. (43) and exploiting

the identity (115):

$$g_{\alpha,ij} = \sum_{\beta \neq \alpha} \frac{S_{\alpha\beta}^{ij}}{(E_\alpha - E_\beta)^2}, \quad \Omega_{\alpha,ij} = - \sum_{\beta \neq \alpha} \frac{A_{\alpha\beta}^{ij}}{(E_\alpha - E_\beta)^2}, \quad (46)$$

with

$$\begin{aligned} S_{\alpha\beta}^{ij} &= \frac{4}{N^2} \mathbf{h}^i \cdot \mathbf{h}^j + \frac{1}{N} [(\mathbf{b}_\alpha \cdot \mathbf{h}^i)(\mathbf{b}_\beta \cdot \mathbf{h}^j) + (\mathbf{b}_\alpha \cdot \mathbf{h}^j)(\mathbf{b}_\beta \cdot \mathbf{h}^i)] \\ &\quad + \frac{2}{N} (\mathbf{b}_\alpha + \mathbf{b}_\beta) \cdot (\mathbf{h}^i \star \mathbf{h}^j) + \frac{1}{2} [(\mathbf{b}_\alpha \star \mathbf{h}^i) \cdot (\mathbf{b}_\beta \star \mathbf{h}^j) + (\mathbf{b}_\alpha \star \mathbf{h}^j) \cdot (\mathbf{b}_\beta \star \mathbf{h}^i)], \quad (47) \\ A_{\alpha\beta}^{ij} &= \frac{2}{N} (\mathbf{b}_\alpha - \mathbf{b}_\beta) \cdot (\mathbf{h}^i \times \mathbf{h}^j) + (\mathbf{b}_\alpha \star \mathbf{h}^i) \cdot (\mathbf{b}_\beta \times \mathbf{h}^j) + (\mathbf{b}_\alpha \times \mathbf{h}^i) \cdot (\mathbf{b}_\beta \star \mathbf{h}^j). \end{aligned}$$

It is straightforward to check that $S_{\alpha\beta}^{ij}$ is symmetric under the exchange of indices i, j (or of α, β), whereas $A_{\alpha\beta}^{ij}$ is antisymmetric under such exchange, and as a consequence $\sum_\alpha \Omega_{\alpha,ij} = 0$. While apparently much less compact than Eq. (45), the expressions above appear more convenient to numerically calculate the QGT. Conceptually, they mainly distinguish themselves from Eq. (45) in that, on the one hand, they involve solely the parametric derivatives of the Hamiltonian vector, while on the other hand they also illustrate the interband nature of the two geometric tensors, and lastly they also show explicitly the importance of the *star product* for both the N -band quantum metric and Berry curvature.

4.3 N -band Berry curvature from the Hamiltonian vector

Having established the general expressions (45)–(47) for *arbitrary* values of N , the final step towards obtaining a closed-form formula for the QGT in terms of the Hamiltonian vector \mathbf{h} and the eigenenergy E_α consists in inserting the explicit formula for $\mathbf{b}_\alpha(\mathbf{h}, E_\alpha)$. In practice, for $N > 2$, writing down such an explicit analytical formula proves too cumbersome for the quantum metric, but can be achieved using Eq. (45) for the Berry curvature (for details, see Appendix I). This is illustrated here for $N = 3$ and $N = 4$, for comparison with the simple $N = 2$ expression (13); the $N = 5$ formula as well as the discussion for arbitrary N is given in Appendix I.

In the $N = 3$ case, the Berry curvature tensor is found to be given by

$$\Omega_{\alpha,ij} = - \frac{4(E_\alpha \mathbf{h} + \mathbf{h}_\star)}{(3E_\alpha^2 - |\mathbf{h}|^2)^3} \cdot [(E_\alpha \mathbf{h}^i + \mathbf{h}_\star^i) \times (E_\alpha \mathbf{h}^j + \mathbf{h}_\star^j)], \quad (48)$$

with $\mathbf{h}_\star^i \equiv \partial_i \mathbf{h}_\star = 2 \mathbf{h} \star \mathbf{h}^i$. This expression recovers the result from Barnett *et al.* [40] if one inserts the closed-form energy parametrization (102). Interestingly, Eq. (48) can be simplified to the following more compact form (cf. Appendix I):

$$\begin{aligned} \Omega_{\alpha,ij} &= \frac{-4}{(3E_\alpha^2 - |\mathbf{h}|^2)^3} \{ E_\alpha [|\mathbf{h}|^2 \mathbf{h} \cdot (\mathbf{h}^i \times \mathbf{h}^j) + 3 \mathbf{h} \cdot (\mathbf{h}_\star^i \times \mathbf{h}_\star^j)] \\ &\quad + (3E_\alpha^2 + |\mathbf{h}|^2) \mathbf{h}_\star \cdot (\mathbf{h}^i \times \mathbf{h}^j) \}. \end{aligned} \quad (49)$$

It may be verified that $\sum_\alpha E_\alpha (3E_\alpha^2 - |\mathbf{h}|^2)^{-3} = 0$ and $\sum_\alpha (3E_\alpha^2 + |\mathbf{h}|^2) (3E_\alpha^2 - |\mathbf{h}|^2)^{-3} = 0$ such that the Berry curvature sum rule $\sum_\alpha \Omega_{\alpha,ij} = 0$ holds.

Analogously, for arbitrary $N = 4$ systems, we have

$$\Omega_{\alpha,ij} = - \frac{4(Q_\alpha \mathbf{h} + E_\alpha \mathbf{h}_\star + \mathbf{h}_{\star\star})}{(4E_\alpha Q_\alpha - \frac{2}{3} \mathbf{h} \cdot \mathbf{h}_\star)^3} \cdot [(Q_\alpha \mathbf{h}^i + E_\alpha \mathbf{h}_\star^i + \mathbf{h}_{\star\star}^i) \times (Q_\alpha \mathbf{h}^j + E_\alpha \mathbf{h}_\star^j + \mathbf{h}_{\star\star}^j)], \quad (50)$$

with $Q_\alpha \equiv E_\alpha^2 - |\mathbf{h}|^2/2$. One could proceed to develop further this expression using $SU(4)$ Jacobi identities, to derive the $SU(4)$ analog of Eq. (49). This is outlined in Appendix I, but it leads to a rather lengthy expression that we will not write explicitly. For practical implementation, Eq. (50) is already in a convenient form.

The procedure for $N > 4$ is described in Appendix I.

5 N -band systems with particle-hole symmetric energy spectrum

It is worthwhile to consider the above generic results in more detail for special cases of practical interest. In the present section, we will therefore restrict to the special class of $N \times N$ Hamiltonians with a particle-hole symmetric (PHS) energy spectrum. This is of interest for many physical applications and corresponds to Hamiltonians characterized by an effective chiral and/or charge conjugation symmetry. In the case of a PHS spectrum, the Hamiltonian's characteristic polynomial is drastically simplified. Consequently, the eigenenergies entering into the projector and Bloch vector expansions (19) & (35) are of quite simple form, allowing us to proceed yet a bit further in the analytical treatment than is possible in the case of fully generic E_α . In particular, the Berry curvature formulas of Section 4.3 simplify considerably, and it becomes possible to write down tractable closed-form expressions for the quantum metric.

5.1 Definition of a particle-hole symmetric spectrum

We define a *particle-hole symmetric (PHS)* energy spectrum (or band structure) as a (in general \mathbf{x} -dependent) set of energy eigenvalues

$$\begin{aligned} \{E_\alpha\} &= \{\pm\epsilon_1, \dots, \pm\epsilon_k, \dots, \pm\epsilon_{\frac{N}{2}}\}, & \text{if } N \text{ even,} \\ \{E_\alpha\} &= \{0, \pm\epsilon_1, \dots, \pm\epsilon_k, \dots, \pm\epsilon_{\frac{N-1}{2}}\}, & \text{if } N \text{ odd,} \end{aligned} \quad (51)$$

of the Hamiltonian (22), where $\epsilon_k < \epsilon_{k+1}$. According to the *tenfold way* symmetry classification [63], such a PHS spectrum can be caused by a chiral symmetry and/or charge conjugation symmetry. (Note that some authors use the term "particle-hole symmetry" instead of "charge conjugation symmetry". We will employ the latter term throughout to avoid confusion; importantly, there can be a PHS spectrum (51) in the absence of charge conjugation symmetry.)

If the spectrum is PHS, the Casimir invariants (16) take a particularly simple form:

$$\begin{aligned} C_{2n} &= 2 \sum_{k=1}^{\lfloor N/2 \rfloor} \epsilon_k^{2n}, \\ C_{2n+1} &= 0, \end{aligned} \quad (52)$$

where $n \in \mathbb{N}_0$. Conversely, one can use the Casimir invariants to check whether the spectrum of a given $SU(N)$ Hamiltonian H is PHS. For N even (odd), all odd (even) powers in the characteristic polynomial (92) vanish if $C_{2n+1} = \text{Tr}(H^{2n+1}) = 0, \forall 2n+1 \leq N$, in which case all solutions of the characteristic equation occur in pairs of opposite sign. In other words, if one computes the Casimir invariants C_{2n+1} , $2n+1 \leq N$, and if they all vanish, then the spectrum of H is PHS.

Let us restrict to $N < 6$ for simplicity. For $N = 3, 4$ it is obvious that (since we have $C_1 = \text{Tr } H = 0$ by construction) the condition for a PHS spectrum is simply $C_3 = 0$, *i.e.* $\mathbf{h} \cdot \mathbf{h}_* = 0$

according to Eq. (33). For $N = 5$, one needs $C_5 = 0$ additionally, which further requires $\mathbf{h} \cdot \mathbf{h}_{\star\star} = 0$. From Eq. (52) one then immediately obtains

$$\begin{aligned} N = 2 \text{ and } N = 3 : \quad \epsilon_1 &= \sqrt{\frac{C_2}{2}}, \\ N = 4 \text{ and } N = 5 : \quad \epsilon_{1,2} &= \sqrt{\frac{C_2}{4} \mp \frac{1}{2} \sqrt{C_4 - \frac{C_2^2}{4}}}, \end{aligned} \quad (53)$$

where $C_2 = 2|\mathbf{h}|^2$ and $C_4 = 4|\mathbf{h}|^4/N + 2|\mathbf{h}_\star|^2$, cf. Eq. (33). Any PHS energy spectrum can thus always be written in the form

$$\begin{aligned} N = 2 : \quad E_\alpha &= \alpha|\mathbf{h}|, & \alpha &= \{\pm 1\}, \\ N = 3 : \quad E_\alpha &= \alpha|\mathbf{h}|, & \alpha &= \{0, \pm 1\}, \\ N = 4 : \quad E_{\alpha_1\alpha_2} &= \alpha_1 \sqrt{\frac{|\mathbf{h}|^2}{2} + \alpha_2 \frac{|\mathbf{h}_\star|}{\sqrt{2}}}, & \alpha_1 &= \{\pm 1\}, \alpha_2 = \{\pm 1\}, \\ N = 5 : \quad E_{\alpha_1\alpha_2} &= \alpha_1 \sqrt{\frac{|\mathbf{h}|^2}{2} + \alpha_2 \sqrt{\frac{|\mathbf{h}_\star|^2}{2} - \frac{|\mathbf{h}|^4}{20}}}, & \alpha_1 &= \{0, \pm 1\}, \alpha_2 = \{\pm 1\}. \end{aligned} \quad (54)$$

Note finally that from Eq. (33), the orthogonality relation

$$\mathbf{h}_\star^{(2n)} \cdot \mathbf{h}_\star^{(2m+1)} = 0 \quad (55)$$

is implied by the vanishing of odd invariants C_{2n+1} .

5.2 Eigenprojectors, Bloch vectors and quantum geometric tensor

The above properties of PHS spectra can now be used to obtain the eigenprojectors, Bloch vectors and quantum geometry for this particular class of Hamiltonians. Here, the cases $N = 3$ and $N = 4$ are exposed in detail and, for completeness, the $N = 5$ case is discussed in Appendix J.

Three-band systems

Under the constraint of a particle hole-symmetric spectrum, the eigenprojectors and Bloch vectors take a particularly simple form:

$$\begin{aligned} P_\alpha &= \frac{1}{3\alpha^2 - 1} \left[(\alpha^2 - 1)1_3 + \alpha \sqrt{\frac{2}{C_2}} H + \frac{2}{C_2} H^2 \right], \\ \mathbf{b}_\alpha &= \frac{2}{3\alpha^2 - 1} \left(\alpha \mathbf{u}_0 + \frac{1}{\sqrt{3}} \mathbf{u}_1 \right), \end{aligned} \quad (56)$$

with $\alpha = 0, \pm$, as well as $C_2 = \sqrt{2C_4} = 2|\mathbf{h}|^2$, $|\mathbf{h}_\star| = |\mathbf{h}|^2/\sqrt{3}$, $\mathbf{u}_0 \equiv \mathbf{h}/|\mathbf{h}|$ and $\mathbf{u}_1 \equiv \mathbf{h}_\star/|\mathbf{h}_\star|$, such that $\{\mathbf{u}_0, \mathbf{u}_1\}$ form an orthonormal set. It is easily checked that $\text{Tr } P_\alpha = 1$ and $|\mathbf{b}_\alpha|^2 = 4/3$ independently of α , as required by Eq. (37).

The Berry curvature is immediately obtained from Eq. (49) as:

$$\Omega_{\alpha,ij} = \frac{-4}{(3\alpha^2 - 1)^3 |\mathbf{h}|^3} \left[\alpha \mathbf{h} \cdot (\mathbf{h}^i \times \mathbf{h}^j) + \frac{3\alpha}{|\mathbf{h}|^2} \mathbf{h} \cdot (\mathbf{h}_\star^i \times \mathbf{h}_\star^j) + \frac{3\alpha^2 + 1}{|\mathbf{h}|} \mathbf{h}_\star \cdot (\mathbf{h}^i \times \mathbf{h}^j) \right]. \quad (57)$$

It is easily checked that the sum over α of each contribution vanishes. The quantum metric is most compactly expressed as a function of \mathbf{u}_0 and \mathbf{u}_1 , by inserting Eq. (56) into Eq. (45):

$$g_{\alpha,ij} = \frac{1}{(3\alpha^2 - 1)^2} \left(\alpha \mathbf{u}_0^i + \frac{1}{\sqrt{3}} \mathbf{u}_1^i \right) \cdot \left(\alpha \mathbf{u}_0^j + \frac{1}{\sqrt{3}} \mathbf{u}_1^j \right). \quad (58)$$

Carrying out the derivatives on \mathbf{u}_0 and \mathbf{u}_1 , one may express this more explicitly as

$$\begin{aligned} g_{\alpha,ij} = \frac{1}{(3\alpha^2 - 1)^2} & \left\{ \frac{\alpha^2}{|\mathbf{h}|^2} \left[\mathbf{h}^i \cdot \mathbf{h}^j - \frac{(\mathbf{h} \cdot \mathbf{h}^i)(\mathbf{h} \cdot \mathbf{h}^j)}{|\mathbf{h}|^2} \right] + \frac{\alpha}{|\mathbf{h}|^3} [\mathbf{h}^i \cdot \mathbf{h}_\star^j + \mathbf{h}_\star^i \cdot \mathbf{h}^j] \right. \\ & \left. + \frac{1}{|\mathbf{h}|^4} \left[\mathbf{h}_\star^i \cdot \mathbf{h}_\star^j - \frac{4}{3} (\mathbf{h} \cdot \mathbf{h}^i)(\mathbf{h} \cdot \mathbf{h}^j) \right] \right\}, \end{aligned} \quad (59)$$

where it was used that $\mathbf{h}_\star \cdot \mathbf{h}^i = -\mathbf{h}_\star^i \cdot \mathbf{h} = -2(\mathbf{h}^i \star \mathbf{h}) \cdot \mathbf{h} = 0$ due to PHS. This result may be compared with Eq. (13). Evidently, the quantum metric is a rather complicated object, even under the constraint of a PHS spectrum.

Four-band systems

In this case it proves convenient to rewrite the eigenenergies as $E_{\alpha_1\alpha_2} = \alpha_1 \mathcal{E}_{\alpha_2}$ with $\mathcal{E}_{\alpha_2} = (|\mathbf{h}|^2/2 + \alpha_2 |\mathbf{h}_\star|/\sqrt{2})^{1/2}$ according to Eq. (54). For the projector and the Bloch vector one then obtains

$$\begin{aligned} P_{\alpha_1\alpha_2} &= \frac{1}{4\mathcal{E}_{\alpha_2}^2 - C_2} \left[\left(\mathcal{E}_{\alpha_2}^2 - \frac{C_2}{2} \right) \mathbf{1}_4 + \alpha_1 \left(\mathcal{E}_{\alpha_2} - \frac{C_2}{2\mathcal{E}_{\alpha_2}} \right) \mathbf{H} + \mathbf{H}^2 + \frac{\alpha_1}{\mathcal{E}_{\alpha_2}} \mathbf{H}^3 \right], \\ \mathbf{b}_{\alpha_1\alpha_2} &= \alpha_1 \mathbf{u}_{\alpha_2} + \frac{\alpha_2}{\sqrt{2}} \mathbf{u}_1 \equiv \alpha_1 \frac{\mathbf{u}_0 + \alpha_2 \mathbf{u}_2}{|\mathbf{u}_0 + \alpha_2 \mathbf{u}_2|} + \frac{\alpha_2}{\sqrt{2}} \mathbf{u}_1, \end{aligned} \quad (60)$$

where $\mathbf{u}_0 \equiv \mathbf{h}/|\mathbf{h}|$, $\mathbf{u}_1 \equiv \mathbf{h}_\star/|\mathbf{h}_\star|$, $\mathbf{u}_2 \equiv \mathbf{h}_{\star\star}/|\mathbf{h}_{\star\star}|$ and with $|\mathbf{h}_{\star\star}| = |\mathbf{h}||\mathbf{h}_\star|/\sqrt{2}$. The vectors $\{\mathbf{u}_+, \mathbf{u}_-, \mathbf{u}_1\}$ form an orthonormal set, however $\mathbf{u}_0 \cdot \mathbf{u}_2 = |\mathbf{h}_\star|/(\sqrt{2}|\mathbf{h}|)$. It is straightforward to check that $\text{Tr } P_{\alpha_1\alpha_2} = 1$ and $|\mathbf{b}_{\alpha_1\alpha_2}|^2 = 3/2$, independently of α_1, α_2 .

Using Eq. (50), the Berry curvature in terms of \mathbf{h} reads:

$$\begin{aligned} \Omega_{\alpha_1\alpha_2,ij} = -\frac{\alpha_1\alpha_2}{4\sqrt{2}|\mathbf{h}_\star|^3\mathcal{E}_{\alpha_2}^3} & \left(\frac{\alpha_2}{\sqrt{2}} |\mathbf{h}_\star| \mathbf{h} + \alpha_1 \mathcal{E}_{\alpha_2} \mathbf{h}_\star + \mathbf{h}_{\star\star} \right) \\ & \cdot \left[\left(\frac{\alpha_2}{\sqrt{2}} |\mathbf{h}_\star| \mathbf{h}^i + \alpha_1 \mathcal{E}_{\alpha_2} \mathbf{h}_\star^i + \mathbf{h}_{\star\star}^i \right) \times \left(\frac{\alpha_2}{\sqrt{2}} |\mathbf{h}_\star| \mathbf{h}^j + \alpha_1 \mathcal{E}_{\alpha_2} \mathbf{h}_\star^j + \mathbf{h}_{\star\star}^j \right) \right]. \end{aligned} \quad (61)$$

For the quantum metric it is again simple to write it in terms of the unit vectors:

$$g_{\alpha_1\alpha_2,ij} = \frac{1}{4} \left[\alpha_1 \mathbf{u}_{\alpha_2}^i + \frac{\alpha_2}{\sqrt{2}} \mathbf{u}_1^i \right] \cdot \left[\alpha_1 \mathbf{u}_{\alpha_2}^j + \frac{\alpha_2}{\sqrt{2}} \mathbf{u}_1^j \right], \quad (62)$$

however the corresponding expression in terms of \mathbf{h} becomes too lengthy to be provided explicitly.

For completeness, the five-band case is discussed in Appendix J.

6 Application to multifold linear band crossings with distinct topology

Let us now illustrate the formalism developed above by applying it to concrete $N = 3$ and $N = 4$ systems with interesting quantum geometric properties. The vector of parameters \mathbf{x}

is crucial for the form of the quantum geometric tensor (QGT) and can take a large variety of different meanings depending on the physical system considered. In solid-state physics, where it is common to work in the Fourier space of the real-space periodic lattice, it is known since Zak's seminal paper [64] at the latest that taking $\mathbf{x} = \mathbf{k}$ to be the crystal momentum is a natural choice for the analysis of Berry phases and related geometrical and topological properties of solids. More generally, in modern condensed matter physics, taking $\mathbf{x} = \mathbf{q}$ to be a quasi-momentum of some kind is the starting point for the analysis of many different kinds of geometrical and topological effects, with various physical meanings attached to \mathbf{q} [20, 65–69]. It is in this general sense, not restricted to purely crystalline systems, that \mathbf{q} should be understood here.

While the formalism developed in this paper applies just as well to Hamiltonians set up on a lattice (typically some tight-binding model), the models that are considered in the following will, for concreteness, all belong to the class of *multifold (Dirac) fermions* (or *multifold linear band crossings*), terms that we will use as referring to a Hamiltonian of the form

$$\begin{aligned} H(\mathbf{q}) &= \sum_i q_i \mathbf{v}_i \cdot \boldsymbol{\lambda}, \\ \mathbf{h}(\mathbf{q}) &= \sum_i q_i \mathbf{v}_i, \end{aligned} \tag{63}$$

where the number of terms in the sum represents the dimension of the quasi-momentum \mathbf{q} -space; for example $\mathbf{q} = (q_x, q_y, q_z)$ for a three-dimensional model. The matrices $\{\lambda_j\}$ are the generalized Gell-Mann metrices introduced in the context of Eq. (22). The vectors \mathbf{v}_i , which contain all relevant information about the model, should be understood as \mathbf{q} -independent parametric velocities, $\mathbf{v}_i = \frac{1}{2} \text{Tr}\{(\partial_{q_i} H)\boldsymbol{\lambda}\}$.

For generic velocity vectors \mathbf{v}_i the energy spectrum of the Hamiltonian (63) is composed of N bands that exhibit a linear band crossing with an N -fold degeneracy at $\mathbf{q} = 0$. Importantly, the existence of such a degenerate point implies a strong coupling between the bands, which should be reflected in the quantum geometric properties (Berry curvature and quantum metric). In particular, in the familiar case of a three-dimensional (3D) quasi-momentum space, depending on the effective symmetries (charge conjugation, time-reversal and/or chirality) that are implicitly encoded in the velocity vectors \mathbf{v}_i , the Berry curvature may take the form of an effective topological monopole that gives rise to an integer quantized Berry flux (measured by the first Chern number) through a surface enclosing the degeneracy point. In the more exotic case of a four-dimensional (4D) quasi-momentum space, it was recently shown that the degeneracy point may act as a tensor monopole, in which case the quantum metric appears as the key ingredient for characterizing another kind of integer topological number, called Dixmier-Douady invariant [70–72]. More generally, the peculiar quantum geometric properties of linear Dirac Hamiltonians of the form (63) are known to play a key role in many physical phenomena, as is evident already from the simplest example of a two-fold degeneracy in graphene and Weyl semimetals. The more complicated case involving multiply degenerate points ($N > 2$) is currently intensely investigated in many different experimental contexts [73–91].

Hereafter, for concreteness, we restrict to a certain class of multifold fermions and discuss the cases $N = 3$ and $N = 4$ in detail. Since we wish to focus on instructive models with a simple band structure, we may impose certain constraints on the Hamiltonian, which can be formulated in terms of the \mathbf{v}_i as discussed in Section 6.1. Section 6.2 will serve to present explicit examples for Hamiltonians subject to those constraints; in particular, we will compare the quantum geometry and topology of pseudospin- S fermions to multifold fermions beyond spin- S .

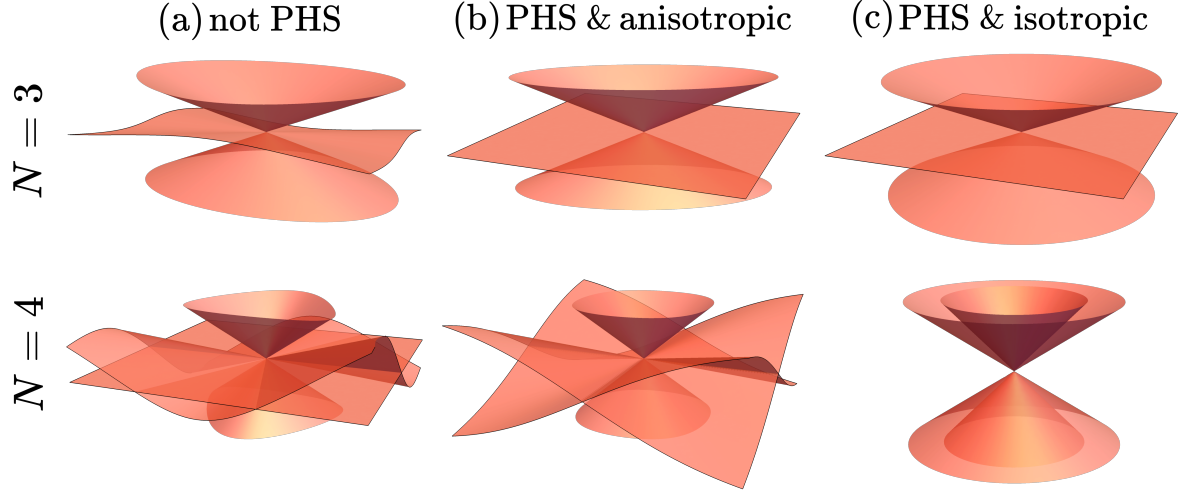


Figure 2: Schematic illustration of possible energy band structures (in \mathbf{q} -space) in the vicinity of the N -fold degeneracy at $\mathbf{q} = 0$, using the examples $N = 3$ and $N = 4$. Different band structures can be grouped into (a) not PHS, (b) PHS but anisotropic, (c) PHS and isotropic.

6.1 Particle-hole symmetric isotropic multifold fermions in 3D

All multifold fermion models (63) that we will consider are constrained as explained in the following. First, we take the quasi-momentum space to be 3D, *i.e.* $\mathbf{q} = (q_x, q_y, q_z)$. Second, we will only consider mutually orthogonal velocity vectors with

$$\mathbf{v}_i \cdot \mathbf{v}_j = c_0 \delta_{ij}, \quad (64)$$

where c_0 is a positive real constant. In the case $N = 2$ the energy spectrum is automatically particle-hole symmetric (PHS) due to the traceless character of H . For $N = 3$ and $N = 4$, the band structure is not automatically PHS. Instead, different kinds of band structures are possible, as illustrated schematically in Fig. 2.

As a third constraint, we are thus interested in $N = 3$ and $N = 4$ models that exhibit an energy band structure with the two main properties illustrated in Fig. 2(c), namely it should be PHS and isotropic in quasi-momentum space. For $N = 2$, the orthogonality condition (64) is sufficient to ensure an isotropic spectrum (in \mathbf{q} -space), *i.e.* $E_{\pm} = \pm\sqrt{c_0}|\mathbf{q}|$. Notice however that, for $N > 2$, Eqs. (63) & (64) alone are not sufficient for rendering the band structure PHS and/or isotropic; instead, additional constraints on the \mathbf{v}_i are necessary. As a last constraint, the energy bands should be non-degenerate for $\mathbf{q} \neq 0$ and *not explicitly dependent* on the three velocity vectors $\mathbf{v}_{x,y,z}$.

The point we wish to make is that, despite these rather restrictive constraints, it is possible to find several classes of models that exhibit distinct quantum geometry (sometimes *explicitly dependent* on \mathbf{v}_i), as well as distinct topological properties as reflected by the first Chern number.

To see how the above constraints on the energy spectrum can be imposed quantitatively, let us first observe that, for $N = 3$ and $N = 4$, the identity

$$(\mathbf{v}_i \star \mathbf{v}_j) \cdot \mathbf{v}_k = 0, \quad \text{for any triple } (i, j, k), \quad (65)$$

is necessary and sufficient to satisfy the constraint of a PHS spectrum – this simply represents the identity $C_3 = \text{Tr}(H^3) = 0$ in vector form, cf. Eq. (33).

For $N = 3$, once Eq. (65) is verified, the orthogonality (64) automatically imposes the desired additional constraint of an isotropic energy spectrum

$$E_\alpha(\mathbf{q}) = \alpha\sqrt{c_0}|\mathbf{q}|, \quad \text{where } \alpha = 0, \pm 1, \quad (66)$$

implying a Dirac cone along with a zero-energy flat band. For $N = 4$, however, in addition to the two constraints (64) & (65) on the \mathbf{v}_i , one further requires the condition that $|\mathbf{h}_s|$ be proportional to $|\mathbf{h}|^2$, *i.e.* $\sqrt{2}|\sum_{i,j} q_i q_j (\mathbf{v}_i \star \mathbf{v}_j)| = d_0|\mathbf{q}|^2$, for obtaining an isotropic spectrum

$$E_{\alpha_1\alpha_2}(\mathbf{q}) = \frac{\alpha_1}{\sqrt{2}}\sqrt{c_0 + \alpha_2 d_0}|\mathbf{q}|, \quad \text{where } \alpha_1 = \pm 1, \alpha_2 = \pm 1, \quad (67)$$

as can be verified from Eq. (54). Here, $d_0 \leq c_0$ is a non-negative real constant; in the limiting case $d_0 = 0$ ($d_0 = c_0$), the double-cone structure implied by Eq. (67) reduces to two degenerate Dirac cones (a Dirac cone and two degenerate flat bands).

6.2 Pseudospin- S multifold fermions and beyond

We can now distinguish several classes of multifold fermions featuring a band structure of the type just described. Models belonging to different classes have distinct geometrical and topological properties. The standard way of demonstrating that the topological properties of any two models are distinct consists in showing that they have different effective symmetries that place them in different topological classes according to the tenfold way classification [63]. In short, whenever a multifold fermion model exhibits a PHS spectrum, it is due to the presence of one or both of the following effective symmetries: (a) A *chiral symmetry* $\mathcal{S}^\dagger H(\mathbf{q})\mathcal{S} = -H(\mathbf{q})$ of the first-quantized Hamiltonian matrix, represented by a unitary matrix \mathcal{S} . (b) A *charge conjugation symmetry* $\mathcal{C}^\dagger H^*(\mathbf{q})\mathcal{C} = -H(\mathbf{q})$, represented by a unitary matrix \mathcal{C} . Since all of our models are PHS, their topological properties can be distinguished according to whether only one or both of the matrices \mathcal{S} and \mathcal{C} can be found, and further according to the sign of the product $\mathcal{C}\mathcal{C}^* = \pm 1_N$.

One obvious class consists of simple pseudospin- S fermions [where $S = (N - 1)/2$] and is considered in Section 6.2.1. This provides both a consistency check for our formalism and a pedagogical example for how the Hamiltonian vectors, Bloch vectors, Berry curvature formulas *et cetera*, introduced throughout this paper, can be used in practice. In the language of the \mathbf{v}_i , we will see that the class of pseudospin- S fermions encompasses all models for which the three orthogonal velocity vectors verify the identity

$$\mathbf{v}_i \times \mathbf{v}_j = \frac{1}{2}\epsilon_{ijk}\mathbf{v}_k, \quad \text{for any triple } (i, j, k). \quad (68)$$

All such models possess a global charge conjugation symmetry with $\mathcal{C}\mathcal{C}^* = (-1)^{2S}1_{2S+1}$ and the quantum geometry is fully *independent* of the \mathbf{v}_i ; the Berry curvature takes the form of a topological monopole that gives rise to an integer quantized Berry flux (first Chern number).

Two other classes of multifold fermions, going beyond pseudospin- S but exhibiting the same type of band structure, are considered in Section 6.2.2. The first class, for which we present both $N = 3$ and $N = 4$ examples, corresponds to models that have a global chiral symmetry, in which case the velocity vectors verify the identity

$$(\mathbf{v}_i \times \mathbf{v}_j) \cdot \mathbf{v}_k = 0, \quad \text{for any triple } (i, j, k). \quad (69)$$

Importantly, in that situation the quantum geometry is in general *anisotropic* and *tunable* by the velocity vectors, despite the band structure being isotropic and fixed. Correspondingly,

there is no finite Berry flux associated to the Berry curvature. For $N = 4$, there is a second class that corresponds to models such that

$$(\mathbf{v}_i \times \mathbf{v}_j) \cdot \mathbf{v}_k = f_0 \epsilon_{ijk}, \quad \text{for any triple } (i, j, k), \quad (70)$$

with $\mathbf{v}_i \times \mathbf{v}_j \neq \frac{1}{2} \epsilon_{ijk} \mathbf{v}_k$ for at least one triple (i, j, k) and where f_0 is a non-zero positive constant (it is a function of c_0 and d_0). In this case, there is again a global charge conjugation symmetry, but now $\mathcal{CC}^* = 1_N$ in contrast to a pseudospin-3/2. The quantum geometry again appears to be independent of the velocity vectors, and the point $\mathbf{q} = 0$ again corresponds to a topological monopole; its quantized charge, however, is in general different from the one of a pseudospin-3/2.

6.2.1 Pseudospin- S multifold fermions

The simplest setup for a (pseudo)spin- S multifold fermion involves three spin matrices $S_{x,y,z}$ that satisfy a spin algebra

$$[S_i, S_j] = i \epsilon_{ijk} S_k, \quad \text{for any triple } (i, j, k). \quad (71)$$

as well as $\mathbf{S}^2 = S(S+1)1_N$ with $N = 2S+1$, and in terms of which the Hamiltonian can be written as

$$H(\mathbf{q}) = q_x S_x + q_y S_y + q_z S_z. \quad (72)$$

It may be checked that the matrix $\mathcal{C} = e^{i\pi S_y}$ plays the role of an effective charge-conjugation symmetry. As a consequence, the band spectrum of $H(\mathbf{q})$ is particle-hole symmetric. It is given by $E_m(\mathbf{q}) = m|\mathbf{q}|$, with $m = -S, \dots, +S$.

Eigenstate approach

In the conventional eigenstate picture, one may construct the \mathbf{q} -dependent spin eigenstates $|S, m, \mathbf{q}\rangle$ as rotated eigenstates of the form $|S, m, \mathbf{q}\rangle = e^{i\theta_{\mathbf{q}}(\sin \varphi_{\mathbf{q}} S_x - \cos \varphi_{\mathbf{q}} S_y)} |S, m\rangle$, where $S_z |S, m\rangle = m |S, m\rangle$ and $\cos \theta_{\mathbf{q}} = q_z / |\mathbf{q}|$, $\tan \varphi_{\mathbf{q}} = q_y / q_x$. One may then use Eq. (42) and the spin eigenstates $|S, m, \mathbf{q}\rangle$ to obtain the Berry curvature tensor $\Omega_{m,ij}(\mathbf{q})$ in the 3D parameter space $\mathbf{q} = (q_x, q_y, q_z)$. Defining the three-component Berry curvature pseudo-vector $\Omega_m \equiv (\Omega_{m,yz}, \Omega_{m,zx}, \Omega_{m,xy})$, it takes the form of a topological monopole [5]:

$$\Omega_m(\mathbf{q}) = -m \frac{\mathbf{q}}{|\mathbf{q}|^3}. \quad (73)$$

The flux of this monopole through any surface enclosing $\mathbf{q} = 0$ results in a topological charge measured by the first Chern number $\mathcal{C}_m = -2m$. As is well known, \mathcal{C}_m is odd for half-integer spin because $\mathcal{CC}^* = -1$, whereas \mathcal{C}_m is even for integer spin because $\mathcal{CC}^* = 1$.

Eigenprojector (Bloch vector) approach

As a first simple check, it is now shown for the spin-1 and spin-3/2 cases (corresponding to three-band and four-band Hamiltonians, respectively) that the result (73) for the Berry curvature can also be obtained without constructing spin eigenstates when our general method is used. For completing the full QGT we will also compute the quantum metric. Of course, in the present case of a simple spin- S , using the eigenprojector formalism is not at all necessary to find the QGT, but the spin Hamiltonian provides a suitable opportunity to get familiar with the general procedure that can be carried out for an *arbitrary* Hamiltonian. Indeed,

in more complicated situations (see for example Section 6.2.2), the formalism proves very advantageous, avoiding any considerations involving eigenstates.

To start with, we rewrite the Hamiltonian (72) in the multifold fermions form of Eq. (63) by defining velocity vectors as $\mathbf{v}_i = \frac{1}{2} \text{Tr}(S_i \boldsymbol{\lambda})$, or equivalently $S_i = \mathbf{v}_i \cdot \boldsymbol{\lambda}$. Each vector \mathbf{v}_i has $N^2 - 1 = 4S(S+1)$ components, but it appears that only $2S$ components are non-zero (using the conventional matrix representation for spin matrices in Appendix D). It is clear that the velocity vectors \mathbf{v}_i are orthogonal, however their norm depends on S as³

$$|\mathbf{v}_i|^2 = \frac{S(S+1)(2S+1)}{6}. \quad (74)$$

Likewise, note that the spin matrix commutation relations (71) translate immediately into the vector identity (68). Recall further that the Hamiltonian vector \mathbf{h} and the star products constructed from it are key ingredients for the eigenprojector (Bloch vector) formalism. In the present case, the Hamiltonian vector is given by Eq. (63) and leads to $\mathbf{h}_\star = \sum_{i,j} q_i q_j (\mathbf{v}_i \star \mathbf{v}_j)$, $\mathbf{h}_{\star\star} = \sum_{i,j,k} q_i q_j q_k (\mathbf{v}_i \star \mathbf{v}_j) \star \mathbf{v}_k$, *et cetera*. Be finally reminded that the star and vector product operations that we use here very frequently are determined by the character of the associated $\mathfrak{su}(N)$ algebra, cf. Section 3.2, and thus depend on the spin size S .

At this point we separate the analysis for the spin-1 and spin-3/2 cases. Consider first the spin-1 case ($N = 3$ bands), where each vector \mathbf{v}_i has $N^2 - 1 = 8$ components. Introducing Cartesian basis vectors \mathbf{e}_j in this 8D space, *i.e.* writing $\mathbf{v}_i = \sum_j v_i^j \mathbf{e}_j$, one gets from the relation (104) between spin-1 matrices and SU(3) Gell-Mann matrices: $\mathbf{v}_x = \frac{1}{\sqrt{2}}(\mathbf{e}_1 + \mathbf{e}_6)$, $\mathbf{v}_y = \frac{1}{\sqrt{2}}(\mathbf{e}_2 + \mathbf{e}_7)$ and $\mathbf{v}_z = \frac{1}{2}(\mathbf{e}_3 + \sqrt{3}\mathbf{e}_8)$. The vectors \mathbf{h} and \mathbf{h}_\star follow as

$$\begin{aligned} \mathbf{h}(\mathbf{q}) &= \frac{1}{2}(\sqrt{2}q_x, \sqrt{2}q_y, q_z, 0, 0, \sqrt{2}q_x, \sqrt{2}q_y, \sqrt{3}q_z), \\ \mathbf{h}_\star(\mathbf{q}) &= \left(\frac{q_x q_z}{\sqrt{2}}, \frac{q_y q_z}{\sqrt{2}}, \frac{3q_z^2 - |\mathbf{q}|^2}{4}, \frac{q_x^2 - q_y^2}{2}, q_x q_y, -\frac{q_x q_z}{\sqrt{2}}, -\frac{q_y q_z}{\sqrt{2}}, \frac{|\mathbf{q}|^2 - 3q_z^2}{4\sqrt{3}} \right). \end{aligned} \quad (75)$$

The spectrum $E_m = m|\mathbf{q}|$, where $m = 0, \pm 1$, is of the form (66) with a normalization factor $c_0 = 1$, in agreement with Eq. (74). Upon evaluating $C_2 = \sum_m E_m^2 = 2|\mathbf{q}|^2$, the Bloch vectors for a pseudospin-1 fermion are readily obtained from Eq. (35):

$$\mathbf{b}_m(\mathbf{q}) = \frac{2}{3m^2 - 1} \left(m \frac{\mathbf{h}}{|\mathbf{q}|} + \frac{\mathbf{h}_\star}{|\mathbf{q}|^2} \right). \quad (76)$$

Equivalently, the eigenprojectors follow immediately from Eq. (19) or simply by inserting the Bloch vector (76) into Eq. (23):

$$\begin{aligned} P_m(\mathbf{q}) &= \frac{1}{3m^2 - 1} \left[(m^2 - 1) \mathbf{1}_3 + \frac{m}{|\mathbf{q}|} \mathbf{H} + \frac{1}{|\mathbf{q}|^2} \mathbf{H}^2 \right] \\ &= \frac{1}{3} \mathbf{1}_3 + \frac{1}{3m^2 - 1} \left(m \frac{\mathbf{h}}{|\mathbf{q}|} + \frac{\mathbf{h}_\star}{|\mathbf{q}|^2} \right) \cdot \boldsymbol{\lambda}. \end{aligned} \quad (77)$$

We are now ready to compute the Berry curvature from either of the formulas (45), (49) or (57) – the last one is the most convenient here. Inserting the vectors \mathbf{h} and \mathbf{h}_\star , one recovers Eq. (73) as expected. Note that in obtaining this result, the last term of Eq. (57) vanishes,

³This can be obtained by calculating on the one hand $\mathbf{S}^2 = \sum_i (\mathbf{v}_i \cdot \boldsymbol{\lambda})^2$ from Eq. (29), and using on the other hand $\mathbf{S}^2 = S(S+1)\mathbf{1}_{2S+1}$; we also find the velocity vector identities $\mathbf{v}_z \star \mathbf{v}_z = 0$ and $\mathbf{v}_x \star \mathbf{v}_x = -\mathbf{v}_y \star \mathbf{v}_y$.

$\mathbf{h}_\star \cdot (\mathbf{h}^i \times \mathbf{h}^j) = 0$, while $\mathbf{h} \cdot (\mathbf{h}_\star^i \times \mathbf{h}_\star^j)/|\mathbf{h}|^2 = \mathbf{h} \cdot (\mathbf{h}^i \times \mathbf{h}^j)$. We can also quickly compute the quantum metric tensor for each band, from either of Eqs. (45), (58) or (59):

$$g_{m,ij}(\mathbf{q}) = \frac{2-m^2}{2|\mathbf{q}|^2} \left(\delta_{ij} - \frac{q_i q_j}{|\mathbf{q}|^2} \right), \quad (78)$$

Drawing on Ref. [92], we can indeed see that this is the spin-1 special case of the quantum metric formula

$$g_{m,ij}(\mathbf{q}) = \frac{S(S+1)-m^2}{2|\mathbf{q}|^2} \left(\delta_{ij} - \frac{q_i q_j}{|\mathbf{q}|^2} \right) \quad (79)$$

for a generic spin- S fermion.

Similarly, considering now the spin-3/2 case ($N = 4$ bands), each vector \mathbf{v}_i has $N^2-1 = 15$ components, and introducing Cartesian basis vectors \mathbf{e}_j in this 15-dimensional space one has $\mathbf{v}_x = \frac{1}{2}(\sqrt{3}\mathbf{e}_1 + 2\mathbf{e}_6 + \sqrt{3}\mathbf{e}_{13})$, $\mathbf{v}_y = \frac{1}{2}(\sqrt{3}\mathbf{e}_2 + 2\mathbf{e}_7 + \sqrt{3}\mathbf{e}_{14})$, $\mathbf{v}_z = \frac{1}{2}(\mathbf{e}_3 + \sqrt{3}\mathbf{e}_8 + \sqrt{6}\mathbf{e}_{15})$ from the relation (105) between spin-3/2 matrices and SU(4) Gell-Mann matrices. The vector \mathbf{h} then follows as

$$\mathbf{h}(\mathbf{q}) = \frac{1}{2}(\sqrt{3}q_x, \sqrt{3}q_y, q_z, 0, 0, 2q_x, 2q_y, \sqrt{3}q_z, 0, 0, 0, 0, \sqrt{3}q_x, \sqrt{3}q_y, \sqrt{6}q_z), \quad (80)$$

from which one can now obtain \mathbf{h}_\star and $\mathbf{h}_{\star\star}$. The spectrum $E_m = m|\mathbf{q}|$, where now $m = \pm\frac{3}{2}, \pm\frac{1}{2}$, is of the form (67) with $c_0 = 5/2$ and $d_0 = 2$. Upon evaluating $C_2 = \sum_m E_m^2 = 5|\mathbf{q}|^2$ and using $C_3 = 0$ we obtain the corresponding Bloch vectors from Eq. (35) as

$$\mathbf{b}_m(\mathbf{q}) = \frac{1}{2m(m^2 - \frac{5}{4})} \left[\left(m^2 - \frac{5}{4} \right) \frac{\mathbf{h}}{|\mathbf{q}|} + m \frac{\mathbf{h}_\star}{|\mathbf{q}|^2} + \frac{\mathbf{h}_{\star\star}}{|\mathbf{q}|^3} \right]. \quad (81)$$

Using this expression and either of the formulas provided in Sections 4 & 5, we find that the Berry curvature again takes the expected form (73), and the quantum metric is given by Eq. (79) with $S(S+1) = 15/4$.

6.2.2 Beyond spin- S multifold fermions

As announced earlier, the purpose of this last section is to show, using examples with $N = 3$ and $N = 4$ bands, that there are many possibilities to design Hamiltonians that drastically *differ* from a simple pseudospin on the level of the eigenprojectors, geometry and topology, even if the band structure is indistinguishable, *i.e.* of the form (66) & (67). Conveniently, no information about eigenstates whatsoever will be required for this discussion.

Three-band models

In the $N = 3$ case, we find that a 3D multifold fermion Hamiltonian (63) with a spectrum of the form (66) can only be of two kinds: either it is non-spin-like, which is the case if it exhibits a global chiral symmetry, represented by a matrix \mathcal{S} . Or it is spin-like, in which case it exhibits a global charge conjugation symmetry with $\mathcal{CC}^* = 1_3$.

Chiral models: Two examples for this class are given by the family of Hamiltonians $H_A^{(\theta)}$, determined by $\mathbf{v}_x = \mathbf{e}_1$, $\mathbf{v}_y = \mathbf{e}_6$, $\mathbf{v}_z = c_\theta \mathbf{e}_2 + s_\theta \mathbf{e}_7$, and the family $H_B^{(\theta)}$, determined by $\mathbf{v}_x = c_\theta \mathbf{e}_1 + s_\theta \mathbf{e}_6$, $\mathbf{v}_y = c_\theta \mathbf{e}_2 - s_\theta \mathbf{e}_7$, $\mathbf{v}_z = \mathbf{e}_5$. Here, θ is a free parameter, abbreviations $s_\theta \equiv \sin \theta$ and $c_\theta \equiv \cos \theta$ are used and we again employ Cartesian basis vectors \mathbf{e}_j in 8D space.

In matrix form, these models simply read

$$H_A^{(\theta)} = \begin{pmatrix} 0 & q_x - ic_\theta q_z & 0 \\ \dots & 0 & q_y - is_\theta q_z \\ \dots & \dots & 0 \end{pmatrix}, \quad H_B^{(\theta)} = \begin{pmatrix} 0 & c_\theta(q_x - iq_y) & -iq_z \\ \dots & 0 & s_\theta(q_x + iq_y) \\ \dots & \dots & 0 \end{pmatrix}, \quad (82)$$

where the lower left matrix elements are obtained by complex conjugating the upper right ones. For $H_A^{(\theta)}$, the presence of a chiral symmetry is immediately obvious, with $\mathcal{S} = \text{diag}(-1, 1, -1) = -\frac{1}{3}\mathbf{1}_3 - \lambda_3 + \frac{1}{\sqrt{3}}\lambda_8$. For $H_B^{(\theta)}$, this is less evident, but it is possible to construct a symmetry operator $\mathcal{S} = -\frac{1}{3}\mathbf{1}_3 + c_\theta^2\lambda_3 + 2s_\theta c_\theta \lambda_4 + \frac{1}{\sqrt{3}}(c_\theta^2 - 2s_\theta^2)\lambda_8$. Note that this symmetry is truly global in the sense that it is \mathbf{q} -independent.

For the models $H_A^{(\theta)}$ and $H_B^{(\theta)}$ we have $c_0 = 1$, *i.e.* their spectrum is θ -independent and exactly the same as for the spin-1 fermion discussed in Section 6.2.1. However, both models are far from being a spin-1, since instead of verifying Eq. (68) they share the property (69). Indeed, the same is true for any other chiral model that we can find – assuming each such model to have a spectrum (66). Interestingly, the vector identity (69) appears to provide a quick and direct way to check for a chiral symmetry that is much simpler than the explicit construction of a matrix \mathcal{S} .

Moreover, for any of our chiral models the QGT for all bands $\alpha = 0, \pm 1$ [obtained either from Eq. (45) with the Bloch vector (56), or more directly from Eqs. (57) & (58)] can be summarized in compact form as

$$\begin{aligned} \boldsymbol{\Omega}_\alpha(\mathbf{q}) &= (2 - 3\alpha^2)(\mathbf{q} \cdot \boldsymbol{\mu}) \frac{\mathbf{q}}{|\mathbf{q}|^4}, \\ g_{\alpha,ij}(\mathbf{q}) &= \frac{2 - \alpha^2}{2|\mathbf{q}|^2} \left[\delta_{ij} - \frac{q_i q_j}{|\mathbf{q}|^2} - \frac{2 - \alpha^2}{2|\mathbf{q}|^2} (\mathbf{q} \times \boldsymbol{\mu})_i (\mathbf{q} \times \boldsymbol{\mu})_j \right], \end{aligned} \quad (83)$$

where we again introduced a Berry curvature pseudovector $\boldsymbol{\Omega}_\alpha$ and where $\boldsymbol{\mu}$ is a function of the velocity vectors \mathbf{v}_i . For the particular example H_A , we have $\boldsymbol{\mu} = (s_\theta, c_\theta, 0)$, while $\boldsymbol{\mu} = (0, 0, 1)$ for the model H_B .

There are several notable features of Eq. (83). First, the Berry curvature is completely different from its spin-1 analog (73) and yields zero upon integration over a closed surface around the degeneracy, *i.e.* all Chern numbers \mathcal{C}_α vanish. Second, the quantum metric contains a part that is exactly like for a spin-1 [cf. Eq. (78)], plus an additional term. Third and importantly, both Berry curvature and quantum metric are *anisotropic* for any choice of $\boldsymbol{\mu}$ and *tunable* by the velocity vectors; in particular, the QGT is a function of θ for the Hamiltonian $H_A^{(\theta)}$.

Spin-like models: Two simple examples for this class are the Hamiltonian H_C , determined by $\mathbf{v}_x = \mathbf{e}_2$, $\mathbf{v}_y = \mathbf{e}_5$, $\mathbf{v}_z = \mathbf{e}_7$, and the family $H_D^{(\theta)}$, determined by $\mathbf{v}_x = c_\theta \mathbf{e}_1 + s_\theta \mathbf{e}_2$, $\mathbf{v}_y = c_\theta \mathbf{e}_6 - s_\theta \mathbf{e}_7$, $\mathbf{v}_z = \mathbf{e}_5$, or in matrix form

$$H_C = \begin{pmatrix} 0 & -iq_x & -iq_y \\ \dots & 0 & -iq_z \\ \dots & \dots & 0 \end{pmatrix}, \quad H_D^{(\theta)} = \begin{pmatrix} 0 & e^{-i\theta} q_x & -iq_z \\ \dots & 0 & e^{i\theta} q_y \\ \dots & \dots & 0 \end{pmatrix}. \quad (84)$$

These models have a global charge conjugation symmetry represented by matrices $\mathcal{C} = \mathbf{1}_3$ and $\mathcal{C} = \text{diag}(1, -e^{-2i\theta}, 1)$, respectively, with $\mathcal{C}\mathcal{C}^* = 1$.

For H_C and $H_D^{(\theta)}$ we also have a θ -independent spectrum with $c_0 = 1$, but in contrast to the chiral models above the present models are indeed pseudospin-1 fermions. We may see this by checking that they verify Eq. (68), which means that they can be written in the form of Eq. (72), with some spin matrices that are in general different from the standard spin-1 representation (104). Moreover, the Berry curvature vector $\Omega_\alpha(\mathbf{q})$ and quantum metric $g_{\alpha,ij}(\mathbf{q})$ of these models (calculated from the same Eqs. as used above) are indeed given by Eqs. (73) and (78), respectively (with $m \rightarrow \alpha$), further corroborating their spin-1 nature.

Four-band models

In the $N = 4$ case, we find that a 3D multifold fermion with a spectrum of the form (67) can be of three types. First, it may be of type spin-3/2, in which case it has all the properties discussed in Section 6.2.1. Here we focus on the two possible types of non-spin-like fermions: either the model exhibits a global chiral symmetry, or it exhibits a global charge conjugation symmetry with $\mathcal{CC}^* = 1_N$. Examples for both classes are provided below. Be aware that constructing models that have a PHS and isotropic band structure is now much harder to construct than for the $N = 3$ case. In particular, it is very difficult to verify the isotropy condition stated just before Eq. (67).

Chiral models: The Hamiltonian that we will consider as a representative example for the chiral class is inspired by the 4D topological semimetal model of Ref. [71] and is given by $\mathbf{v}_x = a(\mathbf{e}_1 - \mathbf{e}_{13}) + b(\mathbf{e}_4 - \mathbf{e}_{11})$, $\mathbf{v}_y = a(\mathbf{e}_2 - \mathbf{e}_{14}) + b(\mathbf{e}_5 - \mathbf{e}_{12})$, $\mathbf{v}_z = a[c_\theta(\mathbf{e}_4 + \mathbf{e}_{11}) + s_\theta(\mathbf{e}_5 + \mathbf{e}_{12})] + b[c_\theta(\mathbf{e}_1 + \mathbf{e}_{13}) + s_\theta(\mathbf{e}_2 + \mathbf{e}_{14})]$, where a, b are non-negative real parameters, or in matrix form

$$H_E^{(\theta)} = \begin{pmatrix} 0 & aq_- + be^{-i\theta}q_z & bq_- + ae^{-i\theta}q_z & 0 \\ \dots & 0 & 0 & -bq_- + ae^{-i\theta}q_z \\ \dots & \dots & 0 & -aq_- + be^{-i\theta}q_z \\ \dots & \dots & \dots & 0 \end{pmatrix}, \quad (85)$$

where $q_- \equiv q_x - iq_y$. This model exhibits a global chiral symmetry $\mathcal{S} = \text{diag}(1, -1, -, 1, 1)$, and a band structure of the form (67) with $c_0 = 2(a^2 + b^2)$ and $d_0 = 4ab$, i.e. $E_{\alpha_1\alpha_2} = \alpha_1(a + \alpha_2 b)|\mathbf{q}|$; notice that this is again θ -independent. Fermions with a spectrum of this kind, with two different effective Dirac velocities, have been dubbed *birefringent fermions* in the 2D case [93]. Two flat bands along with a Dirac cone (two degenerate Dirac cones) appear for $a = b$ ($a = 0$ or $b = 0$), and the band structure of a pseudospin-3/2 fermion is recovered in the special case $a = 2b = 1$.

However, for *any* possible values of a and b , including the case $a = 2b$ where the spectrum is the same as for a pseudospin-3/2, the model $H_E^{(\theta)}$ is not at all a pseudospin-3/2; just like the chiral models that we considered in the $N = 3$ case, the velocity vectors have the property (69) instead of verifying Eq. (68). Thus, identity (69) indeed appears to be a generic feature of chiral Hamiltonians with a PHS and isotropic band structure.

The QGT for the Hamiltonian $H_E^{(\theta)}$ [obtained either from Eq. (45) with the Bloch vector (60), or more directly from Eqs. (61) & (62)] can be written in compact form as

$$\begin{aligned} \Omega_{\alpha_1\alpha_2}(\mathbf{q}) &= -\alpha_2(\mathbf{q} \cdot \boldsymbol{\mu}) \frac{\mathbf{q}}{|\mathbf{q}|^4}, \\ g_{\alpha_1\alpha_2,ij}(\mathbf{q}) &= \frac{1}{2|\mathbf{q}|^2} \left[\delta_{ij} - \frac{q_i q_j}{|\mathbf{q}|^2} - \frac{1}{2|\mathbf{q}|^2} (\mathbf{q} \times \boldsymbol{\mu})_i (\mathbf{q} \times \boldsymbol{\mu})_j \right], \end{aligned} \quad (86)$$

where $\mu = (c_\theta, s_\theta, 0)$. Though the coefficients are slightly different (in particular the quantum metric is the same for all bands), this is exactly of the same form as the result (83) for the $N = 3$ chiral models, and the same interesting features are present. Moreover, note the fundamentally different role of the parameters: a and b affect the spectrum but not the quantum geometry, while the role of θ is the very opposite. The model $H_E^{(\theta)}$ thus allows to tune band structure and quantum geometry completely independently.

Charge conjugation models: For this class, two examples are given by

$$H_F = \begin{pmatrix} 0 & -i(aq_x + bq_z) & -i(bq_x + aq_y) & i(bq_y - aq_z) \\ \dots & 0 & -i(bq_y + aq_z) & -i(bq_x - aq_y) \\ \dots & \dots & 0 & -i(aq_x - bq_z) \\ \dots & \dots & \dots & 0 \end{pmatrix},$$

$$H_G = \begin{pmatrix} 0 & aq_y + bq_z & -i(aq_x + bq_y) & bq_x - aq_z \\ \dots & 0 & bq_x + aq_z & i(aq_x - bq_y) \\ \dots & \dots & 0 & aq_y - bq_z \\ \dots & \dots & \dots & 0 \end{pmatrix},$$
(87)

where the Hamiltonian H_F is determined by $\mathbf{v}_x = a(\mathbf{e}_2 + \mathbf{e}_{14}) + b(\mathbf{e}_5 + \mathbf{e}_{12})$, $\mathbf{v}_y = a(\mathbf{e}_5 - \mathbf{e}_{12}) + b(\mathbf{e}_7 - \mathbf{e}_{10})$, $\mathbf{v}_z = a(\mathbf{e}_7 + \mathbf{e}_{10}) + b(\mathbf{e}_2 - \mathbf{e}_{14})$ in vector language, and H_G by $\mathbf{v}_x = a(\mathbf{e}_5 - \mathbf{e}_{12}) + b(\mathbf{e}_6 + \mathbf{e}_9)$, $\mathbf{v}_y = a(\mathbf{e}_1 + \mathbf{e}_{13}) + b(\mathbf{e}_5 + \mathbf{e}_{12})$, $\mathbf{v}_z = a(\mathbf{e}_6 - \mathbf{e}_9) + b(\mathbf{e}_1 - \mathbf{e}_{13})$. These models have a global charge conjugation symmetry represented by matrices $\mathcal{C} = 1_4$ and $\mathcal{C} = \text{diag}(1, -1, 1, -1)$, respectively. Moreover, they both have a spectrum $E_{\alpha_1 \alpha_2} = \alpha_1(a + \alpha_2 b)|\mathbf{q}|$ that is exactly the same as the spectrum of $H_E^{(\theta)}$, but H_F and H_G are in fact neither chiral nor spin-like. We may see this by checking that they violate Eqs. (68) & (69) but satisfy Eq. (70) with $f_0 = 2(a^3 + b^3)$.

The Berry curvature and quantum metric of these models (calculated in the same way as for the chiral case above) are given by

$$\Omega_{\alpha_1 \alpha_2}(\mathbf{q}) = -\alpha_1(1 + \alpha_2) \frac{\mathbf{q}}{2|\mathbf{q}|^3},$$

$$g_{\alpha_1 \alpha_2, ij}(\mathbf{q}) = \frac{1}{2|\mathbf{q}|^2} \left(\delta_{ij} - \frac{q_i q_j}{|\mathbf{q}|^2} \right),$$
(88)

which is again completely independent of a and b . Though this result is reminiscent of a spin-like fermion, the models are in fact not of spin-like type; indeed, according to the Chern numbers obtained from Eq. (88), and also according to the quantum metric, the models differ from any spin- S fermion.

Summary of multifold fermion models

For any N , the simplest class of linear band crossings that are PHS and isotropic consists of pseudospin- S fermions, where $S = (N - 1)/2$. Such models are characterized by a global charge conjugation symmetry $\mathcal{CC}^* = (-1)^{N-1} 1_N$, the velocity vectors verify Eq. (68), and the QGT is of the well-known form (73) & (79), as visualized in Fig. 3.

For $N = 3$ and $N = 4$, we focused on classes that are not of this spin-like type but exhibit exactly the same spectrum, of the form (66) and (67), respectively. The results are visualized in Fig. 3 and can be stated as follows:

(a) Charge conjugation class: This class exists for $N = 4$ but not for $N = 3$. The Hamiltonian H has a global charge conjugation symmetry with $\mathcal{CC}^* = 1_N$, the velocity vectors verify Eq. (70), and the QGT is of the form (88).

(b) Chiral class: This class exists for both $N = 3$ and $N = 4$. The Hamiltonian H has a global chiral symmetry, the velocity vectors verify Eq. (69), and the QGT is given by Eqs. (83) and (86), respectively. Importantly, the QGT is anisotropic and tunable by a vector μ that does not affect the spectrum.

Note the important role of the word "global". A system with a global chiral symmetry may exhibit a local (*i.e.* \mathbf{q} -dependent) charge conjugation symmetry, as is the case for the model $H_B^{(\theta)}$. Likewise, there can be a local chiral symmetry in the presence of a global charge conjugation symmetry, as for model $H_D^{(\theta)}$. The global symmetries appear to be decisive for the resulting type of monopole (*i.e.* for the form of the QGT).

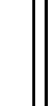
| 3D multifold fermions | (a) Charge conjugation symmetry | | (b) Chiral symmetry | |
|---|---|--|---|---|
| | $\Omega_\alpha(\mathbf{q}) = \mathcal{C}_\alpha \frac{\mathbf{q}}{2 \mathbf{q} ^3}$ | $g_{\alpha,ij}(\mathbf{q}) = \frac{\nu_\alpha}{ \mathbf{q} ^2} \left(\delta_{ij} - \frac{q_i q_j}{ \mathbf{q} ^2} \right)$ | $\Omega_\alpha(\mathbf{q}, \mu) = \kappa_\alpha (\mathbf{q} \cdot \mu) \frac{\mathbf{q}}{ \mathbf{q} ^4}$ | $g_{\alpha,ij}(\mathbf{q}, \mu) = \frac{\tilde{\nu}_\alpha}{ \mathbf{q} ^2} \left(\delta_{ij} - \frac{q_i q_j}{ \mathbf{q} ^2} \right) - \left(\frac{\tilde{\nu}_\alpha}{ \mathbf{q} ^2} \right)^2 (\mathbf{q} \times \mu)_i (\mathbf{q} \times \mu)_j$ |
| Geometry & topology \rightarrow varying Band structure fixed: PHS & isotropic \downarrow | $\mathcal{CC}^* = -1_N$ | $\mathcal{CC}^* = 1_N$ | $\mathcal{S}^2 = 1_N$ | |
| Band index α | \mathcal{C}_α ν_α | $-2 \ 1/2$  $0 \ 1$ $2 \ 1/2$ | κ_α $\tilde{\nu}_\alpha$ | $-1 \ 1/2$ $2 \ 1$ $-1 \ 1/2$ |
| $N = 3$ | 1 0 -1 | not possible | | |
| $N = 4$ | Band index $\alpha = (\alpha_1, \alpha_2)$ 1 1 1 -1 -1 -1 -1 1 | \mathcal{C}_α ν_α  $-3 \ 3/4$ $-1 \ 7/4$ $1 \ 7/4$ $3 \ 3/4$ | \mathcal{C}_α ν_α $-2 \ 1/2$ $0 \ 1/2$ $0 \ 1/2$ $2 \ 1/2$ | κ_α $\tilde{\nu}_\alpha$ $-1 \ 1/2$ $1 \ 1/2$ $1 \ 1/2$ $-1 \ 1/2$ |

Figure 3: Quantum geometry for 3D multifold fermions with a spectrum (66) or (67). In case (a) the Chern number C_α is odd for $\mathcal{CC}^* = -1_N$, even for $\mathcal{CC}^* = 1_N$, and flips sign within each particle-hole conjugate band pair. The quantum metric is determined by $\nu_\alpha = \frac{1}{2} \text{Tr } g_\alpha(\mathbf{q}) |\mathbf{q}|^2$. In case (b) one has $C_\alpha = 0$ for all bands; the Berry curvature is determined by a number κ_α that is identical within each particle-hole conjugate band pair. The QGT is *anisotropic and tunable* by a vector μ that is a function of the velocity vectors \mathbf{v}_i .

7 Summary and conclusions

For a physical system described by a Hermitian $N \times N$ Hamiltonian matrix $H = H(\mathbf{x})$, where the vector \mathbf{x} represents some parameters, there are situations in which it is useful to recall that any eigenstate $|\psi_\alpha(\mathbf{x})\rangle$ ($\alpha = 1, \dots, N$) of H is more fundamentally encoded in the *eigenprojector matrix* $P_\alpha(\mathbf{x}) = |\psi_\alpha(\mathbf{x})\rangle \langle \psi_\alpha(\mathbf{x})|$. We here use the term "more fundamental" in the sense that, while $|\psi_\alpha\rangle$ and P_α can always be constructed from one another, P_α does not suffer from gauge arbitrariness and uncontrollable singularities. The inconvenience of these latter features of eigenstates is apparent already in the simple $N = 2$ case, as reviewed in Section 2.

Consequently, for a given quantity of interest whose standard expression is known in terms of eigenstates, it can prove rewarding to aim for a reformulation in terms of eigenprojectors, which will entirely eliminate the necessity for computing $|\psi_\alpha\rangle$ explicitly. Such a reformulation can be done for *any physical quantity* in principle. The present work demonstrates this by selecting as a prominent example the special case where the quantities of interest are the quantum metric and Berry curvature tensors (forming together what is known as the quantum geometric tensor, QGT). Selecting the QGT is natural for two reasons. First, it is relatively simple (compared to more involved quantities like the orbital magnetic susceptibility), and therefore serves well for illustrating the main features of the eigenprojector approach, which are preserved in the treatment of more complicated observables. Second, the inconvenient features of eigenstates become particularly problematic when one is interested in geometrical quantities; therefore, the QGT is one of the observables for which the projector formalism is the most powerful and beneficial.

The most striking qualitative conclusion that can be drawn from the eigenprojector approach is that any quantity of interest can be computed *from the knowledge of H and its eigenvalues E_α alone*, in agreement with recent results of Pozo and de Juan [43] (who used a somewhat different mathematical framework). At the origin of this conclusion is the fact that the eigenprojector is a *matrix polynomial* of degree $N - 1$ in H , according to the Cayley-Hamilton theorem. This result, though implicitly known for a long time in the form of Eq. (14), is perhaps most useful to physicists when reformulated as an explicit function $P_\alpha(E_\alpha, H)$ of a single eigenvalue, as we have done in Section 3.1, see in particular Eqs. (15) & (19). These expressions for $P_\alpha(E_\alpha, H)$ represent our first intermediate result.

The realization that the knowledge of H as well as its eigenenergies *immediately yields* the eigenprojectors implies that any physical quantity of interest can be computed without eigenstates in the following way:

- (1) Express the quantity in terms of eigenprojectors.
- (2) Explicitly insert the function $P_\alpha(E_\alpha, H)$.

In the course of carrying out this procedure, it proves extremely enlightening to switch between two "languages" where appropriate. The first language simply employs the relevant matrices (H , P_α , etc.), while the second one expands those matrices in the (generalized) Gell-Mann matrices. As explained in Section 3.2, in this second (vectorial) language the Hamiltonian H is given by a real vector \mathbf{h} , and its powers are given by *star products* of \mathbf{h} , which are totally symmetric vector products defined through the underlying Lie algebra. Similarly, the eigenprojector P_α is given by a real (*generalized*) *Bloch vector* \mathbf{b}_α . In the vector language, the analog of the matrix function $P_\alpha(E_\alpha, H)$ is the vector function $\mathbf{b}_\alpha(E_\alpha, \mathbf{h})$, see in particular the important result (35). Both languages contain exactly the same information, such that the above protocol can be equivalently formulated as:

- (1) Express the quantity in terms of Bloch vectors.
- (2) Explicitly insert the function $\mathbf{b}_\alpha(E_\alpha, \mathbf{h})$.

In the present paper, starting in Section 4, the above protocol was carried out for the QGT, and the systematic application to other, more complicated observables will be published elsewhere [44]. The known formula (44) for the QGT in terms of eigenprojectors can be written in the vectorial language as described in Section 4.2 [cf. in particular Eq. (45)], which proves quite handy for practical computations and completes step (1). Step (2) was carried out in Section 4.3, where we obtained the Berry curvature tensor $\Omega_{\alpha,ij}$ in terms of the vector \mathbf{h} and the relevant energy eigenvalue E_α only. This generalizes the well-known Berry curvature expression (13) to arbitrary N , although it gets rather cumbersome for $N \gtrsim 5$.

Equipped with these general results, it proved instructive to consider some simplified cases. For example, many physical systems exhibit an (effective) chiral or charge conjugation symmetry in the sense of the tenfold way classification [63]. In the presence of such symmetries, the eigenvalues occur in pairs of opposite sign, *i.e.* the energy spectrum is *particle-hole symmetric (PHS)*. In Section 5, it was discussed how the eigenprojectors, Bloch vectors as well as the QGT simplify in the PHS case. This discussion of PHS spectra can again easily be extended to more complicated physical observables.

As a concrete illustration of all of the above, and especially of the results obtained for the QGT, Section 6 served to present models belonging to the class of *multifold Dirac fermions*, characterized by an N -fold degenerate nodal point accompanied by a linear band crossing. The discussion of pseudospin- S fermions, conducted in Section 6.2.1, provided us with interesting Bloch vector expressions for spin-1 and spin-3/2 fermions that yield a QGT consistent with the literature. The multifold Dirac fermion models of Section 6.2.2 emphasize that different Hamiltonians can exhibit completely distinct geometrical and topological properties despite being indistinguishable according to their band structure, as summarized in Fig. 3; especially the chiral models with their tunable band geometry may serve as interesting platforms for studying effects such as orbital magnetism or Friedel oscillations, similar to the $\alpha - T_3$ model [45].

To close this paper, we mention a few immediate perspectives of our work. First, as already mentioned, it is worthwhile to apply the eigenprojector approach to observables that are not purely of geometric origin. In particular, this will help to unveil and distinguish purely spectral and geometrical contributions to such observables, similar in spirit to what has been done for the orbital magnetic susceptibility of two-band models in Ref. [24], superconducting stiffness or non-linear responses and more generalized thermodynamic stiffnesses.

Second, it would be interesting to establish a better understanding of the geometry and topology of multifold fermion models with linear but also quadratic band crossings. More concretely, how to systematically design models that share a PHS and/or isotropic spectrum but belong to different topological classes according to the tenfold way classification? How exactly do the quantum geometric properties and their associated topological characterization depend on the number N of bands and on the dimensionality of quasi-momentum parameter space?

Finally, note that the validity of the formalism developed in this paper goes beyond the case of Hermitian Hamiltonian matrices. In particular, the key expressions Eq. (19) for the eigenprojector $P_\alpha(E_\alpha, H)$ and Eq. (35) for the Bloch vector $\mathbf{b}_\alpha(E_\alpha, \mathbf{h})$ stay valid for systems where the Hermiticity condition is relaxed [94, 95]. These expressions explicitly encode the fact that the eigenprojectors retain all the properties (Hermiticity/non-Hermiticity) and symmetries of the Hamiltonian. Importantly, for non-Hermitian systems the eigenprojectors naturally rewrite as $P_\alpha(E_\alpha, H) = |\psi_\alpha^R\rangle\langle\psi_\alpha^L|$ in terms of the corresponding left and right

eigenstates. When necessary, the left/right eigenstates could be recovered by applying the eigenprojector to some left/right gauge freedom states under an appropriate adaptation of Eq. (21).

Acknowledgements

We thank Mark-Oliver Goerbig and Andrej Mesaros for fruitful discussions.

A Characteristic polynomial

The *characteristic polynomial* of an $N \times N$ matrix A is given by [96]

$$\tilde{p}_N(z) = \det(z1_N - A) = \sum_{k=0}^N \tilde{c}_k z^{N-k} = \prod_{\alpha=1}^N (z - a_\alpha), \quad (89)$$

where a_α denotes an eigenvalue of A and $\tilde{c}_0 = 1$. According to the Faddeev-Le Verrier algorithm [96], the coefficients \tilde{c}_k may be computed from the traces $s_k \equiv \text{Tr } A^k$ of powers of A as

$$\begin{aligned} \tilde{c}_k &= -\frac{1}{k}(s_k + \tilde{c}_1 s_{k-1} + \dots + \tilde{c}_{k-1} s_1) \\ &= \frac{(-1)^k}{k!} Y_k(s_1, \dots, (-1)^{k-1}(k-1)!s_k). \end{aligned} \quad (90)$$

The second equality involves (*exponential*) *complete Bell polynomials* $Y_k(z_1, \dots, z_k)$ [97, 98], the first few of which read explicitly

$$\begin{aligned} Y_0 &= 1, \\ Y_1(z_1) &= z_1, \\ Y_2(z_1, z_2) &= z_1^2 + z_2, \\ Y_3(z_1, z_2, z_3) &= z_1^3 + 3z_1 z_2 + z_3, \\ Y_4(z_1, z_2, z_3, z_4) &= z_1^4 + 6z_1^2 z_2 + 4z_1 z_3 + 3z_2^2 + z_4. \end{aligned} \quad (91)$$

Focusing now on the case where $A = H$ represents an $N \times N$ Hamiltonian matrix, we have the Hamiltonian's characteristic polynomial

$$p_N(z) = \det(z1_N - H) = \sum_{k=0}^N c_k z^{N-k} = \prod_{\alpha=1}^N (z - E_\alpha). \quad (92)$$

Using the traceless character of the Hamiltonian, cf. Eq. (22), and the Casimir invariants defined in Eq. (16), the coefficients are given by

$$c_k = \frac{(-1)^k}{k!} Y_k(0, -C_2, \dots, (-1)^{k-1}(k-1)!C_k), \quad (93)$$

and the first few of them read explicitly

$$\begin{aligned} c_0 &= 1, & c_1 &= 0, \\ c_2 &= -\frac{C_2}{2}, & c_3 &= -\frac{C_3}{3}, \\ c_4 &= \frac{C_2^2}{8} - \frac{C_4}{4}, & c_5 &= \frac{C_2 C_3}{6} - \frac{C_5}{5}, \\ c_6 &= -\frac{C_2^3}{48} + \frac{C_3^2}{18} + \frac{C_2 C_4}{8} - \frac{C_6}{6}. \end{aligned} \quad (94)$$

B Derivation of Eq. (15)

Consider first the numerator of Eq. (14) and note that by explicit multiplication one may write

$$\prod_{\beta \neq \alpha} (H - E_\beta 1_N) = \sum_{n=0}^{N-1} (-1)^n e_n(E_1, \dots, E_{\alpha-1}, E_{\alpha+1}, \dots, E_N) H^{N-1-n}, \quad (95)$$

where $e_n = e_n(E_1, \dots, E_{\alpha-1}, E_{\alpha+1}, \dots, E_N)$ are known as *elementary symmetric polynomials* [99]. One has $e_0 = 1$ and all higher e_n are determined recursively by Newton's identities:

$$e_n = \frac{1}{n} \sum_{k=1}^n (-1)^{k-1} (C_k - E_\alpha^k) e_{n-k}, \quad (96)$$

where the C_k are the Casimir invariants of Eq. (16) and it was exploited that $\sum_{\beta \neq \alpha} E_\beta^k = C_k - E_\alpha^k$. This may further be rewritten as

$$e_n = (-1)^n \sum_{k=0}^n c_k E_\alpha^{n-k}, \quad (97)$$

where c_k are the coefficients (93) of the characteristic polynomial. If we now define polynomials

$$q_n(z) \equiv \sum_{k=0}^n c_k z^{n-k}, \quad (98)$$

it is clear that $q_N(z) = p_N(z)$ is the characteristic polynomial (92), and $q_n(E_\alpha) = (-1)^n e_n$. Moreover, inserting into Eq. (95), we have

$$\prod_{\beta \neq \alpha} (H - E_\beta 1_N) = \sum_{n=0}^{N-1} q_{N-1-n}(E_\alpha) H^n. \quad (99)$$

Similarly, for the numerator of Eq. (14), exactly the same procedure as above (where H gets replaced by E_α) leads to

$$\prod_{\beta \neq \alpha} (E_\alpha - E_\beta) = \sum_{n=0}^{N-1} q_{N-1-n}(E_\alpha) E_\alpha^n. \quad (100)$$

As mentioned in the main text, $\prod_{\beta \neq \alpha} (E_\alpha - E_\beta)$ is equal to the derivative $p'_N(E_\alpha)$ of the characteristic polynomial. From this one may also show that $\prod_{\beta \neq \alpha} (E_\alpha - E_\beta) = \sum_{n=0}^{N-1} q_{N-1-n}(E_\alpha) C_n$. Combining all of these results, one arrives at Eq. (15).

C Closed-form solutions for energy eigenvalues

The solutions of the characteristic equation $p_N(z) = 0$, with $p_N(z)$ given by Eq. (92), are the eigenvalues of H . For $N = 2$, the solution of $p_2(E_\alpha) = E_\alpha^2 - C_2/2 = 0$ is simple, cf. Eq. (3). For $N > 2$, the complexity of the function $E_\alpha(\{C_n\})$ grows very quickly. For $N = 3$, the solutions of $p_3(E_\alpha) = E_\alpha^3 - (C_2/2)E_\alpha - C_3/3 = 0$ can be parametrized as [100, 101]

$$\begin{aligned} E_\alpha &= \frac{(-1)^\alpha}{1 + |\alpha|} (S_+ + S_-) + \alpha \frac{i\sqrt{3}}{2} (S_+ - S_-), \quad \alpha = 0, \pm 1, \\ S_\pm &\equiv \frac{1}{6^{\frac{1}{3}}} \left(C_3 \pm i\sqrt{\frac{C_2^3}{6} - C_3^2} \right)^{\frac{1}{3}}. \end{aligned} \quad (101)$$

Note that since $C_2^3 \geq 6C_3^2$, all E_α are of course real [100, 102]. This allows to interpret the eigenvalues as lying on a circle, *i.e.* one may parametrize the solutions using trigonometric functions, see for example Ref. [102]:

$$\begin{aligned} E_\alpha &= \sqrt{\frac{2C_2}{3}} \cos \left[\frac{1}{3} \arccos \left(\frac{\sqrt{6}C_3}{C_2^{\frac{3}{2}}} \right) + \frac{2(\alpha+2)\pi}{3} \right], \quad \alpha = 0, \pm 1, \\ &= \frac{2|\mathbf{h}|}{\sqrt{3}} \cos \phi_\alpha, \\ \phi_\alpha &\equiv \frac{1}{3} \left[\arccos \left(\sqrt{3}\mathbf{h} \cdot \mathbf{h}_\star / |\mathbf{h}|^3 \right) + 2(\alpha+2)\pi \right]. \end{aligned} \quad (102)$$

In either of Eqs. (101) & (102) the Casimir invariants can easily be expressed as a function of \mathbf{h} using Eq. (33).

For $N = 4$, there are again several ways to parametrize the solutions of $p_4(E_\alpha) = E_\alpha^4 - (C_2/2)E_\alpha^2 - (C_3/3)E_\alpha + C_2^2/8 - C_4/4 = 0$, for example [100, 103]

$$\begin{aligned} E_\alpha &= \frac{\text{sgn}(\alpha)}{2\sqrt{3}} \left[R + (-1)^\alpha \sqrt{2C_2 - D + \text{sgn}(\alpha) \frac{2\sqrt{3}C_3}{R}} \right], \quad \alpha = \pm 1, \pm 2, \\ R &\equiv \sqrt{D + C_2}, \\ D &\equiv B \left(\frac{2}{A + \sqrt{A^2 - 4B^3}} \right)^{1/3} + \left(\frac{A + \sqrt{A^2 - 4B^3}}{2} \right)^{1/3}, \\ A &\equiv 3C_3^2 + C_2 \left(\frac{17}{4}C_2^2 - 9C_4 \right), \\ B &\equiv \frac{7}{4}C_2^2 - 3C_4. \end{aligned} \quad (103)$$

Again, the transition to the function $E_\alpha(\mathbf{h})$ is done by inserting Eq. (33) for the Casimir invariants.

For $N \geq 5$, closed-form solutions $E_\alpha(\{C_n\})$ of the characteristic equation are unknown [104].

D Gell-Mann and spin matrices

Here we list the $N = 3$ ($N = 4$) Gell-Mann matrices and relate them to spin-1 (spin-3/2) matrices. Note that the generalization to $N \geq 5$ Gell-Mann matrices (not listed here explicitly) is straightforward, see for example Refs. [51, 54]: There are $N(N-1)/2$ symmetric matrices (purely real), $N(N-1)/2$ antisymmetric matrices (purely imaginary), and $N-1$ diagonal matrices.

The $N = 3$ Gell-Mann matrices [105] are given by

$$\lambda_1 = \begin{pmatrix} 0 & 1 & 0 \\ 1 & 0 & 0 \\ 0 & 0 & 0 \end{pmatrix}, \quad \lambda_2 = \begin{pmatrix} 0 & -i & 0 \\ i & 0 & 0 \\ 0 & 0 & 0 \end{pmatrix}, \quad \lambda_3 = \begin{pmatrix} 1 & 0 & 0 \\ 0 & -1 & 0 \\ 0 & 0 & 0 \end{pmatrix}, \quad \lambda_4 = \begin{pmatrix} 0 & 0 & 1 \\ 0 & 0 & 0 \\ 1 & 0 & 0 \end{pmatrix},$$

$$\lambda_5 = \begin{pmatrix} 0 & 0 & -i \\ 0 & 0 & 0 \\ i & 0 & 0 \end{pmatrix}, \quad \lambda_6 = \begin{pmatrix} 0 & 0 & 0 \\ 0 & 0 & 1 \\ 0 & 1 & 0 \end{pmatrix}, \quad \lambda_7 = \begin{pmatrix} 0 & 0 & 0 \\ 0 & 0 & -i \\ 0 & i & 0 \end{pmatrix}, \quad \lambda_8 = \frac{1}{\sqrt{3}} \begin{pmatrix} 1 & 0 & 0 \\ 0 & 1 & 0 \\ 0 & 0 & -2 \end{pmatrix}.$$

They can easily be related to spin-1 operators, which fulfill the algebra $[S_i, S_j] = i\epsilon_{ijk}S_k$. In the most commonly employed representation of spin-1 operators, we have

$$\begin{aligned} S_x &= \frac{1}{\sqrt{2}}(\lambda_1 + \lambda_6), \\ S_y &= \frac{1}{\sqrt{2}}(\lambda_2 + \lambda_7), \\ S_z &= \frac{1}{2}(\lambda_3 + \sqrt{3}\lambda_8). \end{aligned} \tag{104}$$

The $N = 4$ Gell-Mann matrices in the defining representation [51, 54] are given by the extended SU(3) Gell-Mann matrices,

$$\lambda_1 = \begin{pmatrix} 0 & 1 & 0 & 0 \\ 1 & 0 & 0 & 0 \\ 0 & 0 & 0 & 0 \\ 0 & 0 & 0 & 0 \end{pmatrix}, \quad \lambda_2 = \begin{pmatrix} 0 & -i & 0 & 0 \\ i & 0 & 0 & 0 \\ 0 & 0 & 0 & 0 \\ 0 & 0 & 0 & 0 \end{pmatrix}, \quad \lambda_3 = \begin{pmatrix} 1 & 0 & 0 & 0 \\ 0 & -1 & 0 & 0 \\ 0 & 0 & 0 & 0 \\ 0 & 0 & 0 & 0 \end{pmatrix},$$

$$\lambda_4 = \begin{pmatrix} 0 & 0 & 1 & 0 \\ 0 & 0 & 0 & 0 \\ 1 & 0 & 0 & 0 \\ 0 & 0 & 0 & 0 \end{pmatrix}, \quad \lambda_5 = \begin{pmatrix} 0 & 0 & -i & 0 \\ 0 & 0 & 0 & 0 \\ i & 0 & 0 & 0 \\ 0 & 0 & 0 & 0 \end{pmatrix}, \quad \lambda_6 = \begin{pmatrix} 0 & 0 & 0 & 0 \\ 0 & 0 & 1 & 0 \\ 0 & 1 & 0 & 0 \\ 0 & 0 & 0 & 0 \end{pmatrix},$$

$$\lambda_7 = \begin{pmatrix} 0 & 0 & 0 & 0 \\ 0 & 0 & -i & 0 \\ 0 & i & 0 & 0 \\ 0 & 0 & 0 & 0 \end{pmatrix}, \quad \lambda_8 = \frac{1}{\sqrt{3}} \begin{pmatrix} 1 & 0 & 0 & 0 \\ 0 & 1 & 0 & 0 \\ 0 & 0 & -2 & 0 \\ 0 & 0 & 0 & 0 \end{pmatrix},$$

plus an additional seven matrices

$$\begin{aligned}
\lambda_9 &= \begin{pmatrix} 0 & 0 & 0 & 1 \\ 0 & 0 & 0 & 0 \\ 0 & 0 & 0 & 0 \\ 1 & 0 & 0 & 0 \end{pmatrix}, & \lambda_{10} &= \begin{pmatrix} 0 & 0 & 0 & -i \\ 0 & 0 & 0 & 0 \\ 0 & 0 & 0 & 0 \\ i & 0 & 0 & 0 \end{pmatrix}, & \lambda_{11} &= \begin{pmatrix} 0 & 0 & 0 & 0 \\ 0 & 0 & 0 & 1 \\ 0 & 0 & 0 & 0 \\ 0 & 1 & 0 & 0 \end{pmatrix}, \\
\lambda_{12} &= \begin{pmatrix} 0 & 0 & 0 & 0 \\ 0 & 0 & 0 & -i \\ 0 & 0 & 0 & 0 \\ 0 & i & 0 & 0 \end{pmatrix}, & \lambda_{13} &= \begin{pmatrix} 0 & 0 & 0 & 0 \\ 0 & 0 & 0 & 0 \\ 0 & 0 & 0 & 1 \\ 0 & 0 & 1 & 0 \end{pmatrix}, & \lambda_{14} &= \begin{pmatrix} 0 & 0 & 0 & 0 \\ 0 & 0 & 0 & 0 \\ 0 & 0 & 0 & -i \\ 0 & 0 & i & 0 \end{pmatrix}, \\
\lambda_{15} &= \frac{1}{\sqrt{6}} \begin{pmatrix} 1 & 0 & 0 & 0 \\ 0 & 1 & 0 & 0 \\ 0 & 0 & 1 & 0 \\ 0 & 0 & 0 & -3 \end{pmatrix}.
\end{aligned}$$

This can easily be used to represent the common definition of spin-3/2 operators:

$$\begin{aligned}
S_x &= \frac{1}{2}(\sqrt{3}\lambda_1 + 2\lambda_6 + \sqrt{3}\lambda_{13}), \\
S_y &= \frac{1}{2}(\sqrt{3}\lambda_2 + 2\lambda_7 + \sqrt{3}\lambda_{14}), \\
S_z &= \frac{1}{2}(\lambda_3 + \sqrt{3}\lambda_8 + \sqrt{6}\lambda_{15}).
\end{aligned} \tag{105}$$

E The generalized Bloch sphere

We give here a short summary of the concept of a *generalized Bloch sphere* [*i.e.* the $SU(N)$ eigenprojector's Bloch sphere $\mathcal{B}_{P_\alpha}^{(N)}$ introduced in Section 3.2], drawing largely on Refs. [52, 53, 55–60].

For an N -dimensional Hilbert space, the three defining properties of a (mixed state) density matrix ρ_α representing an N -component (mixed) quantum state $|\psi_\alpha\rangle$, where $\alpha = 1, \dots, N$, are hermiticity $\rho_\alpha^\dagger = \rho_\alpha$, probability conservation $\text{Tr } \rho_\alpha = 1$ and positive semidefiniteness, $\rho_\alpha \geq 0$. Pure states have, in addition, $\rho_\alpha^2 = \rho_\alpha$, in which case $\rho_\alpha = P_\alpha$ is an eigenprojector. An expansion in the basis of generalized Gell-Mann matrices analogous to Eq. (23) can be made for a general (mixed state) density matrix:

$$\rho_\alpha = \frac{1}{N} \mathbf{1}_N + \frac{1}{2} \mathbf{b}_\alpha \cdot \boldsymbol{\lambda}, \tag{106}$$

where now $|\mathbf{b}_\alpha|$ can take various values depending on the pureness of the state. In the pure state case, we have $|\mathbf{b}_\alpha| = \sqrt{2(N-1)/N}$, in agreement with Eq. (37). Considering the vector space \mathbb{R}^{N^2-1} , and denoting the (N^2-1) -dimensional subspace accessible to the (mixed state) Bloch vector \mathbf{b}_α as $\Sigma_{\rho_\alpha}^{(N)}$, one needs to distinguish between two kinds of boundaries, namely

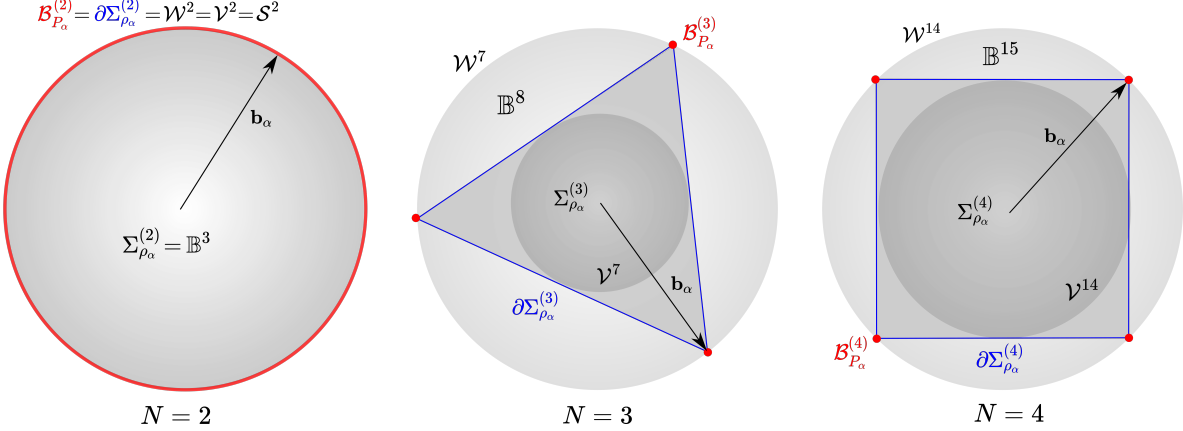


Figure 4: Schematic illustration of the generalized Bloch sphere and other relevant sets, for $N = 2, 3, 4$. The large $(N^2 - 2)$ -sphere \mathcal{W}^{N^2-2} , of radius $\sqrt{2(N-1)/N}$, corresponds to the highest permissible length of a Bloch vector. In its interior, the Ball \mathbb{B}^{N^2-1} , there is the space $\Sigma_{\rho_\alpha}^{(N)}$ accessible to a mixed state of type (106), with topological boundary $\partial\Sigma_{\rho_\alpha}^{(N)}$, and in the interior of $\Sigma_{\rho_\alpha}^{(N)}$ there is the small $(N^2 - 2)$ -sphere \mathcal{V}^{N^2-2} , of radius $\sqrt{2/[N(N-1)]}$. The extremal boundary $\mathcal{B}_{P_\alpha}^{(N)}$ of $\Sigma_{\rho_\alpha}^{(N)}$, which is the intersection of $\Sigma_{\rho_\alpha}^{(N)}$ with the large sphere, is the generalized (eigenprojector's) Bloch sphere that interests us in the discussion of Section 3.2. For the familiar $N = 2$ case, these complications are hidden, since all of the relevant sets coincide.

its $(N^2 - 2)$ -dimensional *topological boundary* $\partial\Sigma_{\rho_\alpha}^{(N)}$ and its *extremal boundary* $\mathcal{B}_{P_\alpha}^{(N)}$. The latter is of dimension $2(N - 1)$, and it comprises the vectors of maximal $|\mathbf{b}_\alpha|$, *i.e.* it is the space of pure state Bloch vectors, or in other words the *generalized Bloch sphere*, sketched in Fig. 4. The dimensionality of $\mathcal{B}_{P_\alpha}^{(N)}$ is in agreement with the fact that one needs $2(N - 1)$ angles to parametrize a given pure state, see the discussion below Eq. (21).

Another set of immediate interest in this discussion is the sphere

$$\mathcal{W}^{N^2-2} \equiv \left\{ \mathbf{r} \in \mathbb{R}^{N^2-1} \mid |\mathbf{r}| = \sqrt{\frac{2(N-1)}{N}} \right\} \quad (107)$$

that contains all pure state Bloch vectors; in other words, it is the surface of the ball \mathbb{B}^{N^2-1} , the smallest ball that contains $\Sigma_{\rho_\alpha}^{(N)}$. For $N = 2$, one trivially has $\partial\Sigma_{\rho_\alpha}^{(2)} = \mathcal{B}_{P_\alpha}^{(2)} = \mathcal{W}^2$ (and $\mathcal{W}^2 = \mathcal{S}^2$, with the unit two-sphere \mathcal{S}^2), as illustrated in Fig. 4; but for higher N the three spaces are different. One has $\mathcal{B}_{P_\alpha}^{(N)} \subset \partial\Sigma_{\rho_\alpha}^{(N)}$ and $\mathcal{B}_{P_\alpha}^{(N)} \subset \mathcal{W}^{N^2-2}$, *i.e.* the generalized Bloch sphere is a proper subset of (i) the boundary of the space of mixed states and (ii) the sphere \mathcal{W}^{N^2-2} ; in fact, it is their intersection: $\partial\Sigma_{\rho_\alpha}^{(N)} \cap \mathcal{W}^{N^2-2} = \mathcal{B}_{P_\alpha}^{(N)}$. In other words, if \mathbf{b}_α corresponds to a pure state, it lies on \mathcal{W}^{N^2-2} , but not necessarily the other way around, *i.e.* not all points on \mathcal{W}^{N^2-2} represent physically valid pure states.

Analogously, the interior of \mathcal{W}^{N^2-2} , *i.e.* the ball \mathbb{B}^{N^2-1} , is not composed of only physically valid mixed states. In fact, calculations [57] of the volume of $\Sigma_{\rho_\alpha}^{(N)}$ show that $\text{vol}(\Sigma_{\rho_\alpha}^{(3)})/\text{vol}(\mathbb{B}^8) \approx 0.26$ and $\text{vol}(\Sigma_{\rho_\alpha}^{(4)})/\text{vol}(\mathbb{B}^{15}) \approx 0.12$, meaning that most points in \mathbb{B}^{N^2-1} do actually not represent physically valid states as soon as $N > 2$.

At the origin of all of these complications is the constraint of positive definiteness, $\rho_\alpha \geq 0$: for $N = 1$, this condition is trivially fulfilled. For $N = 2$, it is equivalent to $\text{Tr}(\rho_\alpha^2) \leq 1$, so for a given density matrix there is *one additional constraint* as compared to $N = 1$. In the same

way, whenever N increases by one, one additional constraint involving traces $D_{\alpha,n} \equiv \text{Tr}(\rho_\alpha^n)$ needs to be fulfilled in order to have positive definiteness. For example, for $N = 3$, there are the three constraints [52] $D_{\alpha,1} = 1$, $D_{\alpha,2} \leq 1$, and $-2D_{\alpha,3} + 3D_{\alpha,2} \leq 1$, which can be translated to constraints on the Bloch vectors via Eq. (106). This restrict the elements of \mathbb{B}^8 that represent physically valid states. As a consequence, the relevant sets (including the generalized Bloch sphere) acquire a very nontrivial shape already for $N = 3$ [60]:

$$\begin{aligned}\mathcal{B}_{P_\alpha}^{(3)} &= \left\{ \mathbf{b}_\alpha \in \mathbb{R}^8 \mid |\mathbf{b}_\alpha|^2 = \frac{4}{3}, |\mathbf{b}_\alpha|^2 - \mathbf{b}_\alpha \cdot (\mathbf{b}_\alpha \star \mathbf{b}_\alpha) = \frac{4}{9} \right\}, \\ \partial\Sigma_{\rho_\alpha}^{(3)} &= \left\{ \mathbf{b}_\alpha \in \mathbb{R}^8 \mid |\mathbf{b}_\alpha|^2 \leq \frac{4}{3}, |\mathbf{b}_\alpha|^2 - \mathbf{b}_\alpha \cdot (\mathbf{b}_\alpha \star \mathbf{b}_\alpha) = \frac{4}{9} \right\}, \\ \Sigma_{\rho_\alpha}^{(3)} &= \left\{ \mathbf{b}_\alpha \in \mathbb{R}^8 \mid |\mathbf{b}_\alpha|^2 \leq \frac{4}{3}, |\mathbf{b}_\alpha|^2 - \mathbf{b}_\alpha \cdot (\mathbf{b}_\alpha \star \mathbf{b}_\alpha) \leq \frac{4}{9} \right\},\end{aligned}\quad (108)$$

where the star product is defined in Eq. (28), and the agreement of the first line with Eq. (37) is to be noted. Similarly, more complicated constraints can be obtained for higher N . For more details on this procedure, see Ref. [52].

Finally, note that there exists another sphere

$$\mathcal{V}^{N^2-2} \equiv \left\{ \mathbf{r} \in \mathbb{R}^{N^2-1} \mid |\mathbf{r}| = \sqrt{\frac{2}{N(N-1)}} \right\} \quad (109)$$

inscribed inside $\Sigma_{\rho_\alpha}^{(N)}$, *i.e.* $\partial\Sigma_{\rho_\alpha}^{(N)}$ lies between \mathcal{V}^{N^2-2} and \mathcal{W}^{N^2-2} .

The essence of all of these established facts is visualized schematically in Fig. 4. Note that the figure is only a rough sketch supposed to highlight the different sets involved. A visual insight into the true (very complicated) shape of those sets can be gained by considering two- or three-sections, see for instance Refs. [56, 58–60].

F Proof of orthogonality relation (31)

We first prove

$$\mathbf{h} \times \mathbf{h}_\star^{(n)} = 0, \quad \forall n \in \mathbb{N}_0, \quad (110)$$

by induction. The base case $\mathbf{h} \times \mathbf{h}_\star^{(0)} = \mathbf{h} \times \mathbf{h} = 0$ is obviously verified. We now assume $\mathbf{h} \times \mathbf{h}_\star^{(n)} = 0$ and show that it implies $\mathbf{h} \times \mathbf{h}_\star^{(n+1)} = 0$:

$$(\mathbf{h} \times \mathbf{h}_\star^{(n+1)})_l = f_{lkm} h_k (\mathbf{h}_\star^{(n+1)})_m = d_{ijm} f_{lkm} h_k h_i (\mathbf{h}_\star^{(n)})_j = 0. \quad (111)$$

This is easily verified from the second Jacobi identity (114). Equation (110) is thus proven and we use it to prove $\mathbf{h}_\star^{(n_1)} \times \mathbf{h}_\star^{(n_2)} = 0$ by induction in two variables. The base cases are $\mathbf{h}_\star^{(n_1)} \times \mathbf{h} = \mathbf{h} \times \mathbf{h}_\star^{(n_2)} = 0$. We now assume $\mathbf{h}_\star^{(n_1)} \times \mathbf{h}_\star^{(n_2)} = 0$ and show that it implies both $\mathbf{h}_\star^{(n_1)} \times \mathbf{h}_\star^{(n_2+1)} = 0$ and $\mathbf{h}_\star^{(n_1+1)} \times \mathbf{h}_\star^{(n_2)} = 0$:

$$\begin{aligned}(\mathbf{h}_\star^{(n_1)} \times \mathbf{h}_\star^{(n_2+1)})_l &= d_{ijm} f_{lkm} (\mathbf{h}_\star^{(n_1)})_k h_i (\mathbf{h}_\star^{(n_2)})_j = 0, \\ (\mathbf{h}_\star^{(n_1+1)} \times \mathbf{h}_\star^{(n_2)})_l &= d_{ijk} f_{lkm} h_i (\mathbf{h}_\star^{(n_1)})_j (\mathbf{h}_\star^{(n_2)})_m = 0.\end{aligned}\quad (112)$$

This concludes the proof.

G $SU(N)$ Jacobi identities

The *first Jacobi identity* [61, 106] can be written alternatively for the generator matrices, the antisymmetric structure constants and the $SU(N)$ vectors as

$$\begin{aligned} [[\lambda_i, \lambda_j], \lambda_k] + [[\lambda_j, \lambda_k], \lambda_i] + [[\lambda_k, \lambda_i], \lambda_j] &= 0, \\ f_{ijm}f_{klm} + f_{ikm}f_{ljm} + f_{ilm}f_{jkm} &= 0, \\ \mathbf{m} \times (\mathbf{n} \times \mathbf{o}) + \mathbf{n} \times (\mathbf{o} \times \mathbf{m}) + \mathbf{o} \times (\mathbf{m} \times \mathbf{n}) &= 0, \\ (\mathbf{m} \times \mathbf{n}) \cdot (\mathbf{o} \times \mathbf{p}) + (\mathbf{m} \times \mathbf{o}) \cdot (\mathbf{p} \times \mathbf{n}) + (\mathbf{m} \times \mathbf{p}) \cdot (\mathbf{n} \times \mathbf{o}) &= 0, \end{aligned} \quad (113)$$

where the third and fourth lines are obtained from the second line depending on whether or not one keeps a free index. Similarly, the *second Jacobi identity* is given by

$$\begin{aligned} [\{\lambda_i, \lambda_j\}, \lambda_k] + [\{\lambda_j, \lambda_k\}, \lambda_i] + [\{\lambda_k, \lambda_i\}, \lambda_j] &= 0, \\ f_{ijm}d_{klm} + f_{ikm}d_{ljm} + f_{ilm}d_{jkm} &= 0, \\ \mathbf{m} \times (\mathbf{n} \star \mathbf{o}) + \mathbf{n} \times (\mathbf{o} \star \mathbf{m}) + \mathbf{o} \times (\mathbf{m} \star \mathbf{n}) &= 0, \\ (\mathbf{m} \times \mathbf{n}) \cdot (\mathbf{o} \star \mathbf{p}) + (\mathbf{m} \times \mathbf{o}) \cdot (\mathbf{p} \star \mathbf{n}) + (\mathbf{m} \times \mathbf{p}) \cdot (\mathbf{n} \star \mathbf{o}) &= 0. \end{aligned} \quad (114)$$

Furthermore, there is the identity

$$\begin{aligned} [\lambda_i, [\lambda_j, \lambda_k]] &= \{\lambda_k, \{\lambda_i, \lambda_j\}\} - \{\lambda_j, \{\lambda_i, \lambda_k\}\}, \\ f_{ijm}f_{klm} &= \frac{2}{N}(\delta_{ik}\delta_{jl} - \delta_{il}\delta_{jk}) + d_{ikm}d_{jlm} - d_{ilm}d_{jkm}, \\ \mathbf{m} \times (\mathbf{n} \times \mathbf{o}) &= \frac{2}{N}[(\mathbf{m} \cdot \mathbf{o})\mathbf{n} - (\mathbf{m} \cdot \mathbf{n})\mathbf{o}] + (\mathbf{m} \star \mathbf{o}) \star \mathbf{n} - (\mathbf{m} \star \mathbf{n}) \star \mathbf{o}, \\ (\mathbf{m} \times \mathbf{n}) \cdot (\mathbf{o} \times \mathbf{p}) &= \frac{2}{N}[(\mathbf{m} \cdot \mathbf{o})(\mathbf{n} \cdot \mathbf{p}) - (\mathbf{m} \cdot \mathbf{p})(\mathbf{n} \cdot \mathbf{o})] \\ &\quad + (\mathbf{m} \star \mathbf{o}) \cdot (\mathbf{n} \star \mathbf{p}) - (\mathbf{m} \star \mathbf{p}) \cdot (\mathbf{n} \star \mathbf{o}). \end{aligned} \quad (115)$$

H Recursion relations for powers of H

Equation (24), together with the product prescription (29), leads to the recursion relations

$$\begin{aligned} C_n &= \frac{C_{n-q}C_q}{N} + 2\boldsymbol{\eta}_{n-q} \cdot \boldsymbol{\eta}_q, \\ \boldsymbol{\eta}_n &= \frac{1}{N}(C_{n-q}\boldsymbol{\eta}_q + C_q\boldsymbol{\eta}_{n-q}) + \boldsymbol{\eta}_{n-q} \star \boldsymbol{\eta}_q, \end{aligned} \quad (116)$$

which hold for $n \geq q \geq 0$. In obtaining the second line of Eq. (116), we made use of the fact that $\boldsymbol{\eta}_n$ and the structure constants f_{abc} are real by definition, establishing the identity

$$\boldsymbol{\eta}_{n_1} \times \boldsymbol{\eta}_{n_2} = 0, \quad \forall n_1, n_2 \in \mathbb{N}_0. \quad (117)$$

Note also that $\boldsymbol{\eta}_n$ can, according to the recursion (116), be expressed as Eq. (34) given in the main text. The orthogonality relation (117) then also agrees with Eq. (31).

I Berry curvature formula for N -band systems

The Berry curvature formula for arbitrary $SU(N)$ systems follows from combining Eqs. (25), (34) & (45), together with the total antisymmetry of the triple product $\mathbf{m} \cdot (\mathbf{n} \times \mathbf{o}) = f_{abc}n_a o_b m_c$

and the orthogonality relation (117) [or, similarly, the orthogonality relation (31)]. Consequently, for arbitrary N , the Berry curvature can be written as

$$\Omega_{\alpha,ij} = -\frac{2\mathbf{b}_\alpha}{[q'_N(E_\alpha)]^2} \cdot \left(\sum_{n,m=1}^{N-1} q_{N-1-n}(E_\alpha) q_{N-1-m}(E_\alpha) \boldsymbol{\tau}_n^{(i)} \times \boldsymbol{\tau}_m^{(j)} \right), \quad (118)$$

with vectors

$$\boldsymbol{\tau}_n^{(i)} \equiv \frac{1}{N} \sum_{p=0}^{n-1} C_p \partial_i \mathbf{h}_\star^{(n-1-p)}. \quad (119)$$

With the notation $\mathbf{m}^i \equiv \partial_i \mathbf{m}$, the first few $\boldsymbol{\tau}_n^{(i)}$ read

$$\boldsymbol{\tau}_1^{(i)} = \mathbf{h}^i, \quad \boldsymbol{\tau}_2^{(i)} = \mathbf{h}_\star^i, \quad \boldsymbol{\tau}_3^{(i)} = \frac{C_2}{N} \mathbf{h}^i + \mathbf{h}_{\star\star}^i. \quad (120)$$

From Eq. (118) and using the results for \mathbf{b}_α and $q_n(E_\alpha)$ from Section 3, the $N = 2$ formula (13) is immediately obtained.

For $N = 3$, analogously, we have

$$\Omega_{\alpha,ij} = -\frac{4(E_\alpha \mathbf{h} + \mathbf{h}_\star)}{(3E_\alpha^2 - \frac{C_2}{2})^3} \cdot [E_\alpha^2 \mathbf{h}^i \times \mathbf{h}^j + E_\alpha (\mathbf{h}^i \times \mathbf{h}_\star^j + \mathbf{h}_\star^i \times \mathbf{h}^j) + \mathbf{h}_\star^i \times \mathbf{h}_\star^j], \quad (121)$$

or equivalently Eq. (48) in the main text. Importantly, we find that this result can be considerably simplified, due to the following identities:

$$\begin{aligned} \mathbf{h} \cdot (\mathbf{h}^i \times \mathbf{h}_\star^j) &= \mathbf{h} \cdot (\mathbf{h}_\star^i \times \mathbf{h}^j) = \mathbf{h}_\star \cdot (\mathbf{h}^i \times \mathbf{h}^j), \\ \mathbf{h}_\star \cdot (\mathbf{h}^i \times \mathbf{h}_\star^j) &= \mathbf{h}_\star \cdot (\mathbf{h}_\star^i \times \mathbf{h}^j) = \mathbf{h} \cdot (\mathbf{h}_\star^i \times \mathbf{h}_\star^j), \\ \mathbf{h}_\star \cdot (\mathbf{h}_\star^i \times \mathbf{h}_\star^j) &= \left[-\frac{2}{3}(\mathbf{h} \cdot \mathbf{h}_\star) \mathbf{h} + |\mathbf{h}|^2 \mathbf{h}_\star \right] \cdot (\mathbf{h}^i \times \mathbf{h}^j). \end{aligned} \quad (122)$$

The first two lines are valid for general N and can be proved using the second Jacobi identity (114). The proof of the third line requires the Jacobi identity as well, but additionally the SU(3)-specific identities (36). Inserting all of these identities into Eq. (121), and exploiting the characteristic equation $E_\alpha^3 = \frac{C_2}{2} E_\alpha + \frac{C_3}{3}$, one obtains the generic SU(3) Berry curvature formula (49) provided in the main text.

Equivalently, the SU(4) Berry curvature is obtained as

$$\begin{aligned} \Omega_{\alpha,ij} &= -\frac{4[(E_\alpha^2 - \frac{C_2}{4}) \mathbf{h} + E_\alpha \mathbf{h}_\star + \mathbf{h}_{\star\star}]}{[4E_\alpha(E_\alpha^2 - \frac{C_2}{4}) - \frac{C_3}{3}]^3} \\ &\cdot \left[\left(E_\alpha^2 - \frac{C_2}{4} \right)^2 \mathbf{h}^i \times \mathbf{h}^j + E_\alpha \left(E_\alpha^2 - \frac{C_2}{4} \right) (\mathbf{h}^i \times \mathbf{h}_\star^j + \mathbf{h}_\star^i \times \mathbf{h}^j) + E_\alpha^2 \mathbf{h}_\star^i \times \mathbf{h}_\star^j \right. \\ &\quad \left. + \left(E_\alpha^2 - \frac{C_2}{4} \right) (\mathbf{h}^i \times \mathbf{h}_{\star\star}^j + \mathbf{h}_{\star\star}^i \times \mathbf{h}^j) + E_\alpha (\mathbf{h}_\star^i \times \mathbf{h}_{\star\star}^j + \mathbf{h}_{\star\star}^i \times \mathbf{h}_\star^j) + \mathbf{h}_{\star\star}^i \times \mathbf{h}_{\star\star}^j \right], \end{aligned} \quad (123)$$

which is equivalent to Eq. (50) in the main text. Again, we may exploit several vector identities to reduce the number of terms. The first two lines of Eq. (122) still hold, but the third one is changed [cf. Eq. (36)], and other identities are needed as well, which are again proved by the second Jacobi identity:

$$\begin{aligned} \mathbf{h}_\star \cdot (\mathbf{h}_\star^i \times \mathbf{h}_\star^j) &= -\frac{2}{3}(\mathbf{h} \cdot \mathbf{h}_\star) \mathbf{h} \cdot (\mathbf{h}^i \times \mathbf{h}^j) + \mathbf{h}_{\star\star} \cdot (\mathbf{h}_\star^i \times \mathbf{h}^j + \mathbf{h}^i \times \mathbf{h}_\star^j), \\ \mathbf{h} \cdot (\mathbf{h}^i \times \mathbf{h}_{\star\star}^j) &= \mathbf{h} \cdot (\mathbf{h}_{\star\star}^i \times \mathbf{h}^j) = \mathbf{h}_{\star\star} \cdot (\mathbf{h}^i \times \mathbf{h}^j), \\ \mathbf{h} \cdot (\mathbf{h}_\star^i \times \mathbf{h}_{\star\star}^j) &= \mathbf{h} \cdot (\mathbf{h}_{\star\star}^i \times \mathbf{h}_\star^j) = \frac{1}{2} \mathbf{h}_{\star\star} \cdot (\mathbf{h}_\star^i \times \mathbf{h}^j + \mathbf{h}^i \times \mathbf{h}_\star^j), \end{aligned} \quad (124)$$

et cetera. Putting all of this together, one may derive the SU(4) analog of Eq. (49), which will contain nine independent terms instead of the 27 terms in Eq. (50). However, this will give rise to quite lengthy coefficients, so we deem Eq. (50) to be in the simplest possible form for practical purposes.

Finally, for arbitrary SU(5) systems, the Berry curvature is given by

$$\Omega_{\alpha,ij} = -\frac{4(R_\alpha \mathbf{h} + \tilde{R}_\alpha \mathbf{h}_\star + E_\alpha \mathbf{h}_{\star\star} + \mathbf{h}_{\star\star\star})}{[q'_5(E_\alpha)]^3} \cdot \left[(R_\alpha \mathbf{h}^i + \tilde{R}_\alpha \mathbf{h}_\star^i + E_\alpha \mathbf{h}_{\star\star}^i + \mathbf{h}_{\star\star\star}^i) \times (R_\alpha \mathbf{h}^j + \tilde{R}_\alpha \mathbf{h}_\star^j + E_\alpha \mathbf{h}_{\star\star}^j + \mathbf{h}_{\star\star\star}^j) \right], \quad (125)$$

where $q'_5(E_\alpha) = 5E_\alpha R_\alpha + \frac{3}{10}|\mathbf{h}|^4 - \frac{1}{2}|\mathbf{h}_\star|^2$, with $R_\alpha \equiv E_\alpha \tilde{R}_\alpha - \frac{4}{15}\mathbf{h} \cdot \mathbf{h}_\star$ and $\tilde{R}_\alpha \equiv E_\alpha^2 - \frac{3}{5}|\mathbf{h}|^2$.

J Quantum geometry of five-band Hamiltonians with a PHS spectrum

In the PHS case (see Section 5), the SU(5) projectors read off Eqs. (19) & (54) are

$$\begin{aligned} P_{\alpha_1=0} &= 1_5 + \frac{2C_2}{C_4 - \frac{C_2^2}{2}} H^2 - \frac{4}{C_4 - \frac{C_2^2}{2}} H^4, \\ P_{\alpha_1 \neq 0, \alpha_2} &= \frac{1}{C_4 + C_2(\mathcal{E}_{\alpha_2}^2 - \frac{C_2}{2})} \left[\alpha_1 \mathcal{E}_{\alpha_2} \left(\mathcal{E}_{\alpha_2}^2 - \frac{C_2}{2} \right) H + \left(\mathcal{E}_{\alpha_2}^2 - \frac{C_2}{2} \right) H^2 \right. \\ &\quad \left. + \alpha_1 \mathcal{E}_{\alpha_2} H^3 + H^4 \right], \end{aligned} \quad (126)$$

where the energy was written as $E_{\alpha_1 \neq 0, \alpha_2} = \alpha_1 \mathcal{E}_{\alpha_2}$ with $\mathcal{E}_{\alpha_2} \equiv (C_2/4 + \frac{\alpha_2}{2}\sqrt{C_4 - C_2^2/4})^{1/2}$. It can be readily verified that these projectors fulfill the unit trace and completeness relations. In the Bloch vector picture, this translates to

$$\begin{aligned} \mathbf{b}_{\alpha_1=0} &= \frac{-\frac{3}{5}|\mathbf{h}|^2 \mathbf{h}_\star + \mathbf{h}_{\star\star\star}}{\frac{3}{20}|\mathbf{h}|^4 - \frac{1}{4}|\mathbf{h}_\star|^2}, \\ \mathbf{b}_{\alpha_1 \neq 0, \alpha_2} &= \frac{\alpha_1 \mathcal{E}_{\alpha_2} R_{\alpha_2} \mathbf{h} + R_{\alpha_2} \mathbf{h}_\star + \alpha_1 \mathcal{E}_{\alpha_2} \mathbf{h}_{\star\star} + \mathbf{h}_{\star\star\star}}{\frac{5}{2} \mathcal{E}_{\alpha_2}^2 R_{\alpha_2} + \frac{3}{20}|\mathbf{h}|^4 - \frac{1}{4}|\mathbf{h}_\star|^2}, \end{aligned} \quad (127)$$

where $R_{\alpha_2} \equiv \mathcal{E}_{\alpha_2}^2 - \frac{3}{5}|\mathbf{h}|^2$. We only write the Berry curvature explicitly, which is easily obtained from Eq. (125):

$$\begin{aligned} \Omega_{\alpha_1=0,ij} &= -\frac{1}{2} \frac{-\frac{3}{5}|\mathbf{h}|^2 \mathbf{h}_\star + \mathbf{h}_{\star\star\star}}{\left(\frac{3}{20}|\mathbf{h}|^4 - \frac{1}{4}|\mathbf{h}_\star|^2 \right)^3} \cdot \left[\left(-\frac{3}{5}|\mathbf{h}|^2 \mathbf{h}_\star^i + \mathbf{h}_{\star\star\star}^i \right) \times \left(-\frac{3}{5}|\mathbf{h}|^2 \mathbf{h}_\star^j + \mathbf{h}_{\star\star\star}^j \right) \right], \\ \Omega_{\alpha_1 \neq 0, \alpha_2, ij} &= -\frac{1}{2} \frac{\alpha_1 \mathcal{E}_{\alpha_2} R_{\alpha_2} \mathbf{h} + R_{\alpha_2} \mathbf{h}_\star + \alpha_1 \mathcal{E}_{\alpha_2} \mathbf{h}_{\star\star} + \mathbf{h}_{\star\star\star}}{\left(\frac{5}{2} \mathcal{E}_{\alpha_2}^2 R_{\alpha_2} + \frac{3}{20}|\mathbf{h}|^4 - \frac{1}{4}|\mathbf{h}_\star|^2 \right)^3} \\ &\quad \cdot \left[(\alpha_1 \mathcal{E}_{\alpha_2} R_{\alpha_2} \mathbf{h}^i + R_{\alpha_2} \mathbf{h}_\star^i + \alpha_1 \mathcal{E}_{\alpha_2} \mathbf{h}_{\star\star}^i + \mathbf{h}_{\star\star\star}^i) \right. \\ &\quad \left. \times (\alpha_1 \mathcal{E}_{\alpha_2} R_{\alpha_2} \mathbf{h}^j + R_{\alpha_2} \mathbf{h}_\star^j + \alpha_1 \mathcal{E}_{\alpha_2} \mathbf{h}_{\star\star}^j + \mathbf{h}_{\star\star\star}^j) \right]. \end{aligned} \quad (128)$$

The quantum metric can be obtained by combining Eqs. (45) & (127).

References

- [1] W Ehrenberg and R E Siday. “The Refractive Index in Electron Optics and the Principles of Dynamics”. In: *Proceedings of the Physical Society. Section B* 62.1 (1949), pp. 8–21. DOI: [10.1088/0370-1301/62/1/303](https://doi.org/10.1088/0370-1301/62/1/303).
- [2] Y. Aharonov and D. Bohm. “Significance of Electromagnetic Potentials in the Quantum Theory”. In: *Phys. Rev.* 115 (3 1959), pp. 485–491. DOI: [10.1103/PhysRev.115.485](https://doi.org/10.1103/PhysRev.115.485).
- [3] S. Pancharatnam. “Generalized theory of interference, and its applications”. In: *Proceedings of the Indian Academy of Sciences - Section A* 44.5 (Nov. 1956), pp. 247–262. ISSN: 0370-0089. DOI: [10.1007/BF03046050](https://doi.org/10.1007/BF03046050).
- [4] A. J. Stone and Hugh Christopher Longuet-Higgins. “Spin-orbit coupling and the intersection of potential energy surfaces in polyatomic molecules”. In: *Proceedings of the Royal Society of London. A. Mathematical and Physical Sciences* 351.1664 (Oct. 1976), pp. 141–150. DOI: [10.1098/rspa.1976.0134](https://doi.org/10.1098/rspa.1976.0134).
- [5] M. V. Berry. “Quantal Phase Factors Accompanying Adiabatic Changes”. In: *Proceedings of the Royal Society of London. Series A, Mathematical and Physical Sciences* 392.1802 (1984), pp. 45–57. ISSN: 00804630. DOI: [10.1098/rspa.1984.0023](https://doi.org/10.1098/rspa.1984.0023).
- [6] Barry Simon. “Holonomy, the Quantum Adiabatic Theorem, and Berry’s Phase”. In: *Phys. Rev. Lett.* 51 (24 1983), pp. 2167–2170. DOI: [10.1103/PhysRevLett.51.2167](https://doi.org/10.1103/PhysRevLett.51.2167).
- [7] Frank Wilczek and A. Zee. “Appearance of Gauge Structure in Simple Dynamical Systems”. In: *Phys. Rev. Lett.* 52 (24 1984), pp. 2111–2114. DOI: [10.1103/PhysRevLett.52.2111](https://doi.org/10.1103/PhysRevLett.52.2111).
- [8] M. V. Berry. “Classical adiabatic angles and quantal adiabatic phase”. In: *Journal of Physics A: Mathematical and General* 18.1 (Jan. 1985), pp. 15–27. ISSN: 1361-6447. DOI: [10.1088/0305-4470/18/1/012](https://doi.org/10.1088/0305-4470/18/1/012).
- [9] J H Hannay. “Angle variable holonomy in adiabatic excursion of an integrable Hamiltonian”. In: *Journal of Physics A: Mathematical and General* 18.2 (1985), pp. 221–230. DOI: [10.1088/0305-4470/18/2/011](https://doi.org/10.1088/0305-4470/18/2/011).
- [10] Y. Aharonov and J. Anandan. “Phase change during a cyclic quantum evolution”. In: *Phys. Rev. Lett.* 58 (16 1987), pp. 1593–1596. DOI: [10.1103/PhysRevLett.58.1593](https://doi.org/10.1103/PhysRevLett.58.1593).
- [11] Don N. Page. “Geometrical description of Berry’s phase”. In: *Phys. Rev. A* 36 (7 1987), pp. 3479–3481. DOI: [10.1103/PhysRevA.36.3479](https://doi.org/10.1103/PhysRevA.36.3479).
- [12] E. I. Blount. “Formalisms of Band Theory”. In: *Solid State Physics*. Ed. by Frederick Seitz and David Turnbull. Vol. 13. Academic Press, Jan. 1962, pp. 305–373. DOI: [10.1016/S0081-1947\(08\)60459-2](https://doi.org/10.1016/S0081-1947(08)60459-2).
- [13] J. P. Provost and G. Vallee. “Riemannian structure on manifolds of quantum states”. In: *Comm. Math. Phys.* 76.3 (1980), pp. 289–301. DOI: [10.1007/BF02193559](https://doi.org/10.1007/BF02193559).
- [14] M. V. Berry. “The Quantum Phase, Five Years After”. In: *Geometric Phases in Physics*. Ed. by F. Wilczek and A. Shapere. Advanced series in mathematical physics. World Scientific, 1989. ISBN: 9789971506216. DOI: [10.1142/9789812798381_0001](https://doi.org/10.1142/9789812798381_0001).
- [15] R. Resta. “The insulating state of matter: a geometrical theory”. In: *The European Physical Journal B* 79.2 (Jan. 2011), pp. 121–137. ISSN: 1434-6036. DOI: [10.1140/epjb/e2010-10874-4](https://doi.org/10.1140/epjb/e2010-10874-4).

[16] Michael Kolodrubetz et al. “Geometry and non-adiabatic response in quantum and classical systems”. In: *Physics Reports* 697 (2017). Geometry and non-adiabatic response in quantum and classical systems, pp. 1 –87. ISSN: 0370-1573. DOI: <https://doi.org/10.1016/j.physrep.2017.07.001>.

[17] D. J. Thouless et al. “Quantized Hall Conductance in a Two-Dimensional Periodic Potential”. In: *Phys. Rev. Lett.* 49 (6 1982), pp. 405–408. DOI: [10.1103/PhysRevLett.49.405](https://doi.org/10.1103/PhysRevLett.49.405).

[18] Naoto Nagaosa et al. “Anomalous Hall effect”. In: *Rev. Mod. Phys.* 82 (2 2010), pp. 1539–1592. DOI: [10.1103/RevModPhys.82.1539](https://doi.org/10.1103/RevModPhys.82.1539).

[19] Di Xiao, Ming-Che Chang, and Qian Niu. “Berry phase effects on electronic properties”. In: *Rev. Mod. Phys.* 82 (3 2010), pp. 1959–2007. DOI: [10.1103/RevModPhys.82.1959](https://doi.org/10.1103/RevModPhys.82.1959).

[20] Xiao-Liang Qi and Shou-Cheng Zhang. “Topological insulators and superconductors”. In: *Reviews of Modern Physics* 83.4 (2011), 1057–1110. ISSN: 1539-0756. DOI: [10.1103/revmodphys.83.1057](https://doi.org/10.1103/revmodphys.83.1057).

[21] Jairo Sinova et al. “Spin Hall effects”. In: *Rev. Mod. Phys.* 87 (4 2015), pp. 1213–1260. DOI: [10.1103/RevModPhys.87.1213](https://doi.org/10.1103/RevModPhys.87.1213).

[22] Paolo Zanardi, Paolo Giorda, and Marco Cozzini. “Information-Theoretic Differential Geometry of Quantum Phase Transitions”. In: *Phys. Rev. Lett.* 99 (10 2007), p. 100603. DOI: [10.1103/PhysRevLett.99.100603](https://doi.org/10.1103/PhysRevLett.99.100603).

[23] Ajit Srivastava and Atac Imamoglu. “Signatures of Bloch-Band Geometry on Excitons: Nonhydrogenic Spectra in Transition-Metal Dichalcogenides”. In: *Phys. Rev. Lett.* 115 (16 2015), p. 166802. DOI: [10.1103/PhysRevLett.115.166802](https://doi.org/10.1103/PhysRevLett.115.166802).

[24] Arnaud Raoux et al. “Orbital magnetism in coupled-bands models”. In: *Physical Review B* 91.8 (2015). ISSN: 1550-235X. DOI: [10.1103/physrevb.91.085120](https://doi.org/10.1103/physrevb.91.085120).

[25] Martin Claassen et al. “Position-Momentum Duality and Fractional Quantum Hall Effect in Chern Insulators”. In: *Phys. Rev. Lett.* 114 (23 2015), p. 236802. DOI: [10.1103/PhysRevLett.114.236802](https://doi.org/10.1103/PhysRevLett.114.236802).

[26] Yang Gao, Shengyuan A. Yang, and Qian Niu. “Geometrical effects in orbital magnetic susceptibility”. In: *Phys. Rev. B* 91 (21 2015), p. 214405. DOI: [10.1103/PhysRevB.91.214405](https://doi.org/10.1103/PhysRevB.91.214405).

[27] Frédéric Piéchon et al. “Geometric orbital susceptibility: Quantum metric without Berry curvature”. In: *Phys. Rev. B* 94 (13 2016), p. 134423. DOI: [10.1103/PhysRevB.94.134423](https://doi.org/10.1103/PhysRevB.94.134423).

[28] Aleksi Jalkku et al. “Geometric Origin of Superfluidity in the Lieb-Lattice Flat Band”. In: *Phys. Rev. Lett.* 117 (4 2016), p. 045303. DOI: [10.1103/PhysRevLett.117.045303](https://doi.org/10.1103/PhysRevLett.117.045303).

[29] Frank Freimuth, Stefan Blügel, and Yuriy Mokrousov. “Geometrical contributions to the exchange constants: Free electrons with spin-orbit interaction”. In: *Phys. Rev. B* 95 (18 2017), p. 184428. DOI: [10.1103/PhysRevB.95.184428](https://doi.org/10.1103/PhysRevB.95.184428).

[30] Matthew F. Lapa and Taylor L. Hughes. “Semiclassical wave packet dynamics in nonuniform electric fields”. In: *Phys. Rev. B* 99 (12 2019), p. 121111. DOI: [10.1103/PhysRevB.99.121111](https://doi.org/10.1103/PhysRevB.99.121111).

[31] Yang Gao and Di Xiao. “Nonreciprocal Directional Dichroism Induced by the Quantum Metric Dipole”. In: *Phys. Rev. Lett.* 122 (22 2019), p. 227402. DOI: [10.1103/PhysRevLett.122.227402](https://doi.org/10.1103/PhysRevLett.122.227402).

[32] Titus Neupert, Claudio Chamon, and Christopher Mudry. “Measuring the quantum geometry of Bloch bands with current noise”. In: *Phys. Rev. B* 87 (24 2013), p. 245103. DOI: [10.1103/PhysRevB.87.245103](https://doi.org/10.1103/PhysRevB.87.245103).

[33] Michael Kolodrubetz, Vladimir Gritsev, and Anatoli Polkovnikov. “Classifying and measuring geometry of a quantum ground state manifold”. In: *Physical Review B* 88.6 (2013). ISSN: 1550-235X. DOI: [10.1103/physrevb.88.064304](https://doi.org/10.1103/physrevb.88.064304).

[34] Lih-King Lim, Jean-Noël Fuchs, and Gilles Montambaux. “Geometry of Bloch states probed by Stückelberg interferometry”. In: *Physical Review A* 92.6 (2015). ISSN: 1094-1622. DOI: [10.1103/physreva.92.063627](https://doi.org/10.1103/physreva.92.063627).

[35] O. Bleu, D. D. Solnyshkov, and G. Malpuech. “Measuring the quantum geometric tensor in two-dimensional photonic and exciton-polariton systems”. In: *Phys. Rev. B* 97 (19 2018), p. 195422. DOI: [10.1103/PhysRevB.97.195422](https://doi.org/10.1103/PhysRevB.97.195422).

[36] Tomoki Ozawa and Nathan Goldman. “Extracting the quantum metric tensor through periodic driving”. In: *Phys. Rev. B* 97 (20 2018), p. 201117. DOI: [10.1103/PhysRevB.97.201117](https://doi.org/10.1103/PhysRevB.97.201117).

[37] Min Yu et al. “Experimental measurement of the quantum geometric tensor using coupled qubits in diamond”. In: *National Science Review* 7.2 (Nov. 2019), pp. 254–260. ISSN: 2095-5138. DOI: [10.1093/nsr/nwz193](https://doi.org/10.1093/nsr/nwz193).

[38] A. Gianfrate et al. “Measurement of the quantum geometric tensor and of the anomalous Hall drift”. In: *Nature* 578.7795 (2020), 381–385. ISSN: 1476-4687. DOI: [10.1038/s41586-020-1989-2](https://doi.org/10.1038/s41586-020-1989-2).

[39] Lih-King Lim et al. “Dirac points emerging from flat bands in Lieb-kagome lattices”. In: *Phys. Rev. B* 101 (4 2020), p. 045131. DOI: [10.1103/PhysRevB.101.045131](https://doi.org/10.1103/PhysRevB.101.045131).

[40] Ryan Barnett, G. R. Boyd, and Victor Galitski. “SU(3) Spin-Orbit Coupling in Systems of Ultracold Atoms”. In: *Phys. Rev. Lett.* 109 (23 2012), p. 235308. DOI: [10.1103/PhysRevLett.109.235308](https://doi.org/10.1103/PhysRevLett.109.235308).

[41] Soo-Yong Lee et al. “Arbitrary Chern Number Generation in the Three-Band Model from Momentum Space”. In: *Journal of the Physical Society of Japan* 84.6 (2015), p. 064005. DOI: [10.7566/JPSJ.84.064005](https://doi.org/10.7566/JPSJ.84.064005).

[42] David Bauer, T. S. Jackson, and Rahul Roy. “Quantum geometry and stability of the fractional quantum Hall effect in the Hofstadter model”. In: *Phys. Rev. B* 93 (23 2016), p. 235133. DOI: [10.1103/PhysRevB.93.235133](https://doi.org/10.1103/PhysRevB.93.235133).

[43] Oscar Pozo and Fernando de Juan. “Computing observables without eigenstates: Applications to Bloch Hamiltonians”. In: *Phys. Rev. B* 102 (11 2020), p. 115138. DOI: [10.1103/PhysRevB.102.115138](https://doi.org/10.1103/PhysRevB.102.115138).

[44] Ansgar Graf and Frédéric Piéchon. to be published.

[45] A. Raoux et al. “From Dia- to Paramagnetic Orbital Susceptibility of Massless Fermions”. In: *Phys. Rev. Lett.* 112 (2 2014), p. 026402. DOI: [10.1103/PhysRevLett.112.026402](https://doi.org/10.1103/PhysRevLett.112.026402).

[46] P.R. Halmos. *Finite-Dimensional Vector Spaces: Second Edition*. Dover Books on Mathematics. Dover Publications, 2017. ISBN: 9780486822266.

[47] Dimitri Kusnezov. “Exact matrix expansions for group elements of SU(N)”. In: *Journal of Mathematical Physics* 36.2 (1995), pp. 898–906. DOI: [10.1063/1.531165](https://doi.org/10.1063/1.531165).

[48] Arthur Cayley. “II. A memoir on the theory of matrices”. In: *Philosophical Transactions of the Royal Society of London* 148 (Jan. 1858), pp. 17–37. DOI: [10.1098/rstl.1858.0002](https://doi.org/10.1098/rstl.1858.0002).

[49] R.A. Horn and C.R. Johnson. *Matrix Analysis*. Matrix Analysis. Cambridge University Press, 2013. ISBN: 9780521839402.

[50] F. T. Hioe and J. H. Eberly. “N-Level Coherence Vector and Higher Conservation Laws in Quantum Optics and Quantum Mechanics”. In: *Phys. Rev. Lett.* 47 (12 1981), pp. 838–841. DOI: [10.1103/PhysRevLett.47.838](https://doi.org/10.1103/PhysRevLett.47.838).

[51] Walter Pfeifer. “The Lie algebras $su(N)$ ”. In: *The Lie Algebras $su(N)$: An Introduction*. Basel: Birkhäuser Basel, 2003, pp. 15–21. ISBN: 978-3-0348-8097-8. DOI: [10.1007/978-3-0348-8097-8_2](https://doi.org/10.1007/978-3-0348-8097-8_2).

[52] Gen Kimura. “The Bloch vector for N-level systems”. In: *Physics Letters A* 314.5 (2003), pp. 339 –349. ISSN: 0375-9601. DOI: [https://doi.org/10.1016/S0375-9601\(03\)00941-1](https://doi.org/10.1016/S0375-9601(03)00941-1).

[53] Mark S. Byrd and Navin Khaneja. “Characterization of the positivity of the density matrix in terms of the coherence vector representation”. In: *Phys. Rev. A* 68 (6 2003), p. 062322. DOI: [10.1103/PhysRevA.68.062322](https://doi.org/10.1103/PhysRevA.68.062322).

[54] Reinhold A Bertlmann and Philipp Krammer. “Bloch vectors for qudits”. In: *Journal of Physics A: Mathematical and Theoretical* 41.23 (2008), p. 235303. ISSN: 1751-8121. DOI: [10.1088/1751-8113/41/23/235303](https://doi.org/10.1088/1751-8113/41/23/235303).

[55] John E. Harriman. “Geometry of density matrices. I. Definitions, N matrices and 1 matrices”. In: *Phys. Rev. A* 17 (4 1978), pp. 1249–1256. DOI: [10.1103/PhysRevA.17.1249](https://doi.org/10.1103/PhysRevA.17.1249).

[56] L. Jakóbczyk and M. Siennicki. “Geometry of Bloch vectors in two-qubit system”. In: *Physics Letters A* 286.6 (Aug. 2001), pp. 383–390. ISSN: 0375-9601. DOI: [10.1016/S0375-9601\(01\)00455-8](https://doi.org/10.1016/S0375-9601(01)00455-8).

[57] Karol Zyczkowski and Hans-Jürgen Sommers. “Hilbert-Schmidt volume of the set of mixed quantum states”. In: *Journal of Physics A: Mathematical and General* 36.39 (Sept. 2003), pp. 10115–10130. ISSN: 1361-6447. DOI: [10.1088/0305-4470/36/39/310](https://doi.org/10.1088/0305-4470/36/39/310).

[58] Gen Kimura and Andrzej Kossakowski. “The Bloch-Vector Space for N-Level Systems: the Spherical-Coordinate Point of View”. In: *Open Syst. Inf. Dyn.* 12.03 (Sept. 2005), pp. 207–229. ISSN: 1230-1612. DOI: [10.1007/s11080-005-0919-y](https://doi.org/10.1007/s11080-005-0919-y).

[59] Istok P. Mendaš. “The classification of three-parameter density matrices for a qutrit”. In: *Journal of Physics A: Mathematical and General* 39.36 (Aug. 2006), pp. 11313–11324. ISSN: 1361-6447. DOI: [10.1088/0305-4470/39/36/012](https://doi.org/10.1088/0305-4470/39/36/012).

[60] Sandeep K Goyal et al. “Geometry of the generalized Bloch sphere for qutrits”. In: *Journal of Physics A: Mathematical and Theoretical* 49.16 (2016), p. 165203. DOI: [10.1088/1751-8113/49/16/165203](https://doi.org/10.1088/1751-8113/49/16/165203).

[61] L. M. Kaplan and M. Resnikoff. “Matrix Products and the Explicit 3, 6, 9, and 12-j Coefficients of the Regular Representation of $SU(n)$ ”. In: *Journal of Mathematical Physics* 8.11 (1967), pp. 2194–2205. DOI: [10.1063/1.1705141](https://doi.org/10.1063/1.1705141).

[62] Shi-Jian Gu. “Fidelity approach to quantum phase transitions”. In: *International Journal of Modern Physics B* 24.23 (2010), pp. 4371–4458. DOI: [10.1142/S0217979210056335](https://doi.org/10.1142/S0217979210056335).

[63] Andreas W W Ludwig. “Topological phases: classification of topological insulators and superconductors of non-interacting fermions, and beyond”. In: *Physica Scripta* T168 (2015), p. 014001. doi: [10.1088/0031-8949/2015/t168/014001](https://doi.org/10.1088/0031-8949/2015/t168/014001).

[64] J. Zak. “Berry’s phase for energy bands in solids”. In: *Phys. Rev. Lett.* 62 (23 1989), pp. 2747–2750. doi: [10.1103/PhysRevLett.62.2747](https://doi.org/10.1103/PhysRevLett.62.2747).

[65] Jean Dalibard et al. “Colloquium: Artificial gauge potentials for neutral atoms”. In: *Rev. Mod. Phys.* 83 (4 2011), pp. 1523–1543. doi: [10.1103/RevModPhys.83.1523](https://doi.org/10.1103/RevModPhys.83.1523).

[66] N. P. Armitage, E. J. Mele, and Ashvin Vishwanath. “Weyl and Dirac semimetals in three-dimensional solids”. In: *Rev. Mod. Phys.* 90 (1 2018), p. 015001. doi: [10.1103/RevModPhys.90.015001](https://doi.org/10.1103/RevModPhys.90.015001).

[67] N. R. Cooper, J. Dalibard, and I. B. Spielman. “Topological bands for ultracold atoms”. In: *Rev. Mod. Phys.* 91 (1 2019), p. 015005. doi: [10.1103/RevModPhys.91.015005](https://doi.org/10.1103/RevModPhys.91.015005).

[68] Tomoki Ozawa et al. “Topological photonics”. In: *Rev. Mod. Phys.* 91 (1 2019), p. 015006. doi: [10.1103/RevModPhys.91.015006](https://doi.org/10.1103/RevModPhys.91.015006).

[69] Dan-Wei Zhang et al. “Topological quantum matter with cold atoms”. In: *Advances in Physics* 67.4 (2018), pp. 253–402. doi: [10.1080/00018732.2019.1594094](https://doi.org/10.1080/00018732.2019.1594094).

[70] Giandomenico Palumbo and Nathan Goldman. “Revealing Tensor Monopoles through Quantum-Metric Measurements”. In: *Phys. Rev. Lett.* 121 (17 2018), p. 170401. doi: [10.1103/PhysRevLett.121.170401](https://doi.org/10.1103/PhysRevLett.121.170401).

[71] Yan-Qing Zhu, Nathan Goldman, and Giandomenico Palumbo. “Four-dimensional semimetals with tensor monopoles: From surface states to topological responses”. In: *Phys. Rev. B* 102 (8 2020), p. 081109. doi: [10.1103/PhysRevB.102.081109](https://doi.org/10.1103/PhysRevB.102.081109).

[72] Xinsheng Tan et al. “Experimental Observation of Tensor Monopoles with a Superconducting Qudit”. In: *Phys. Rev. Lett.* 126 (1 2021), p. 017702. doi: [10.1103/PhysRevLett.126.017702](https://doi.org/10.1103/PhysRevLett.126.017702).

[73] Z. Lan et al. “Dirac-Weyl fermions with arbitrary spin in two-dimensional optical superlattices”. In: *Physical Review B* 84.16 (2011). ISSN: 1550-235X. doi: [10.1103/physrevb.84.165115](https://doi.org/10.1103/physrevb.84.165115).

[74] Balázs Dóra, Janik Kailasvuori, and R. Moessner. “Lattice generalization of the Dirac equation to general spin and the role of the flat band”. In: *Phys. Rev. B* 84 (19 2011), p. 195422. doi: [10.1103/PhysRevB.84.195422](https://doi.org/10.1103/PhysRevB.84.195422).

[75] J. L. Mañes. “Existence of bulk chiral fermions and crystal symmetry”. In: *Phys. Rev. B* 85 (15 2012), p. 155118. doi: [10.1103/PhysRevB.85.155118](https://doi.org/10.1103/PhysRevB.85.155118).

[76] Hongming Weng et al. “Topological semimetals with triply degenerate nodal points in θ -phase tantalum nitride”. In: *Phys. Rev. B* 93 (24 2016), p. 241202. doi: [10.1103/PhysRevB.93.241202](https://doi.org/10.1103/PhysRevB.93.241202).

[77] Ziming Zhu et al. “Triple Point Topological Metals”. In: *Phys. Rev. X* 6 (3 2016), p. 031003. doi: [10.1103/PhysRevX.6.031003](https://doi.org/10.1103/PhysRevX.6.031003).

[78] Biao Lian and Shou-Cheng Zhang. “Five-dimensional generalization of the topological Weyl semimetal”. In: *Phys. Rev. B* 94 (4 2016), p. 041105. doi: [10.1103/PhysRevB.94.041105](https://doi.org/10.1103/PhysRevB.94.041105).

[79] Barry Bradlyn et al. “Beyond Dirac and Weyl fermions: Unconventional quasiparticles in conventional crystals”. In: *Science* 353.6299 (2016). ISSN: 0036-8075. doi: [10.1126/science.aaf5037](https://doi.org/10.1126/science.aaf5037).

[80] Motohiko Ezawa. “Pseudospin- $\frac{3}{2}$ fermions, type-II Weyl semimetals, and critical Weyl semimetals in tricolor cubic lattices”. In: *Phys. Rev. B* 94 (19 2016), p. 195205. DOI: [10.1103/PhysRevB.94.195205](https://doi.org/10.1103/PhysRevB.94.195205).

[81] B. Q. Lv et al. “Observation of three-component fermions in the topological semimetal molybdenum phosphide”. In: *Nature* 546.7660 (June 2017), pp. 627–631. ISSN: 1476-4687. DOI: [10.1038/nature22390](https://doi.org/10.1038/nature22390).

[82] Adrien Bouhon and Annica M. Black-Schaffer. “Global band topology of simple and double Dirac-point semimetals”. In: *Phys. Rev. B* 95 (24 2017), p. 241101. DOI: [10.1103/PhysRevB.95.241101](https://doi.org/10.1103/PhysRevB.95.241101).

[83] Guoqing Chang et al. “Unconventional Chiral Fermions and Large Topological Fermi Arcs in RhSi”. In: *Phys. Rev. Lett.* 119 (20 2017), p. 206401. DOI: [10.1103/PhysRevLett.119.206401](https://doi.org/10.1103/PhysRevLett.119.206401).

[84] Peizhe Tang, Quan Zhou, and Shou-Cheng Zhang. “Multiple Types of Topological Fermions in Transition Metal Silicides”. In: *Phys. Rev. Lett.* 119 (20 2017), p. 206402. DOI: [10.1103/PhysRevLett.119.206402](https://doi.org/10.1103/PhysRevLett.119.206402).

[85] I. C. Fulga, L. Fallani, and M. Burrello. “Geometrically protected triple-point crossings in an optical lattice”. In: *Phys. Rev. B* 97 (12 2018), p. 121402. DOI: [10.1103/PhysRevB.97.121402](https://doi.org/10.1103/PhysRevB.97.121402).

[86] Seiji Sugawa et al. “Second Chern number of a quantum-simulated non-Abelian Yang monopole”. In: *Science* 360.6396 (2018), pp. 1429–1434. ISSN: 0036-8075. DOI: [10.1126/science.aam9031](https://doi.org/10.1126/science.aam9031).

[87] Haiping Hu and Chuanwei Zhang. “Spin-1 topological monopoles in the parameter space of ultracold atoms”. In: *Phys. Rev. A* 98 (1 2018), p. 013627. DOI: [10.1103/PhysRevA.98.013627](https://doi.org/10.1103/PhysRevA.98.013627).

[88] Felix Flicker et al. “Chiral optical response of multifold fermions”. In: *Phys. Rev. B* 98 (15 2018), p. 155145. DOI: [10.1103/PhysRevB.98.155145](https://doi.org/10.1103/PhysRevB.98.155145).

[89] Guoqing Chang et al. “Topological quantum properties of chiral crystals”. In: *Nature Materials* 17.11 (Nov. 2018), pp. 978–985. ISSN: 1476-4660. DOI: [10.1038/s41563-018-0169-3](https://doi.org/10.1038/s41563-018-0169-3).

[90] Daichi Takane et al. “Observation of Chiral Fermions with a Large Topological Charge and Associated Fermi-Arc Surface States in CoSi”. In: *Phys. Rev. Lett.* 122 (7 2019), p. 076402. DOI: [10.1103/PhysRevLett.122.076402](https://doi.org/10.1103/PhysRevLett.122.076402).

[91] Miguel-Ángel Sánchez-Martínez, Fernando de Juan, and Adolfo G. Grushin. “Linear optical conductivity of chiral multifold fermions”. In: *Phys. Rev. B* 99 (15 2019), p. 155145. DOI: [10.1103/PhysRevB.99.155145](https://doi.org/10.1103/PhysRevB.99.155145).

[92] Yu-Ping Lin and Wei-Han Hsiao. “Dual Haldane sphere and quantized band geometry in chiral multifold fermions”. In: *Phys. Rev. B* 103 (8 2021), p. L081103. DOI: [10.1103/PhysRevB.103.L081103](https://doi.org/10.1103/PhysRevB.103.L081103).

[93] Malcolm P. Kennett et al. “Birefringent breakup of Dirac fermions on a square optical lattice”. In: *Phys. Rev. A* 83 (5 2011), p. 053636. DOI: [10.1103/PhysRevA.83.053636](https://doi.org/10.1103/PhysRevA.83.053636).

[94] Carl M Bender. “Making sense of non-Hermitian Hamiltonians”. In: *Reports on Progress in Physics* 70.6 (2007), 947–1018. ISSN: 1361-6633. DOI: [10.1088/0034-4885/70/6/r03](https://doi.org/10.1088/0034-4885/70/6/r03).

[95] Dorje C Brody. “Biorthogonal quantum mechanics”. In: *Journal of Physics A: Mathematical and Theoretical* 47.3 (2013), p. 035305. ISSN: 1751-8121. DOI: [10.1088/1751-8113/47/3/035305](https://doi.org/10.1088/1751-8113/47/3/035305).

[96] F. R. Gantmacher. *The Theory of Matrices*. Chelsea Publishing Company, 1980.

[97] E. T. Bell. “Exponential Polynomials”. In: *Annals of Mathematics* 35.2 (1934), pp. 258–277. ISSN: 0003486X. DOI: [10.2307/1968431](https://doi.org/10.2307/1968431).

[98] L. Comtet. *Advanced Combinatorics: The Art of Finite and Infinite Expansions*. Springer Netherlands, 1974. ISBN: 9789027704412.

[99] I. G. Macdonald. *Symmetric Functions and Hall Polynomials*. Oxford classic texts in the physical sciences. Clarendon Press, 1998. ISBN: 9780198504504.

[100] M. Abramowitz and I. A. Stegun. *Handbook of Mathematical Functions: With Formulas, Graphs, and Mathematical Tables*. Applied mathematics series. Dover Publications, 1965. ISBN: 9780486612720.

[101] Eric W. Weisstein. *Cubic Formula*. From MathWorld—A Wolfram Web Resource. <https://mathworld.wolfram.com/CubicFormula.html>. Last visited on 04/09/2020.

[102] S. P. Rosen. “Finite Transformations in Various Representations of $SU(3)$ ”. In: *Journal of Mathematical Physics* 12.4 (1971), pp. 673–681. DOI: [10.1063/1.1665634](https://doi.org/10.1063/1.1665634).

[103] Eric W. Weisstein. *Quartic Equation*. From MathWorld—A Wolfram Web Resource. <https://mathworld.wolfram.com/QuarticEquation.html>. Last visited on 04/09/2020.

[104] Van Kortryk. “Matrix exponentials, $SU(N)$ group elements, and real polynomial roots”. In: *Journal of Mathematical Physics* 57.2 (2016), p. 021701. DOI: [10.1063/1.4938418](https://doi.org/10.1063/1.4938418).

[105] Murray Gell-Mann. “Symmetries of Baryons and Mesons”. In: *Phys. Rev.* 125 (3 1962), pp. 1067–1084. DOI: [10.1103/PhysRev.125.1067](https://doi.org/10.1103/PhysRev.125.1067).

[106] A. J. Macfarlane, A. Sudbery, and P. H. Weisz. “On Gell-Mann’s λ -matrices, d- and f-tensors, octets, and parametrizations of $SU(3)$ ”. In: *Communications in Mathematical Physics* 11.1 (Mar. 1968), pp. 77–90. ISSN: 1432-0916. DOI: [10.1007/BF01654302](https://doi.org/10.1007/BF01654302).